

RP

TU Rheinland-Pfälzische
Technische Universität
Kaiserslautern
Landau

**Assembly and characterization of phycoerythrin-III from
Prochlorococcus marinus SS120**

vom Fachbereich Biologie

der Rheinland-Pfälzischen Technischen Universität Kaiserslautern-Landau

zur Verleihung des akademischen Grades „Doktor der Naturwissenschaften“ genehmigte

Dissertation

vorgelegt von

Bin Gu, M.Sc.

Wissenschaftliche Aussprache: 13.04.2023

Berichterstattende:

Prof. Dr. Nicole Frankenberg-Dinkel (Betreuerin)

Prof. Dr. Michael Schroda

Kaiserslautern im Jahr 2023

D 386

Table of contents

Abbreviations	VI
1 Introduction	1
1.1 Cyanobacteria	1
1.1.1 The photosynthetic machinery of cyanobacteria	2
1.1.2 The phycobilisome.....	3
1.1.3 Phycobiliproteins and chromophorylation	4
1.2 <i>Prochlorococcus marinus</i> SS120	7
1.2.1 Phycoerythrin in <i>Prochlorococcus</i>	10
1.2.2 Prochlorophyte chlorophyll-binding protein.....	12
1.2.3 Pigment biosynthesis	13
1.2.4 Phycobilinprotein lyases	16
1.3 Objectives of this work.....	20
2. Material and methods	21
2.1 Materials and chemicals	21
2.1.1 Equipment	21
2.1.2 Special chemicals, material, enzymes, kits and antibodies.....	22
2.1.3 Bacterial strains.....	24
2.1.4 Plasmids	25
2.1.5 Oligonucleotides	27
2.2 Microbiological methods.....	30
2.2.1 Preparation of chemically competent <i>E. coli</i> cells.....	30
2.2.2 Transformation of chemically competent <i>E. coli</i> cells	30

2.2.3 Culture media and supplements for <i>E. coli</i> cultures	30
2.2.4 Storage of <i>E. coli</i> cells	31
2.2.5 Cultivation of <i>E. coli</i> cells	31
2.2.6 Determination of <i>E. coli</i> cell density	31
2.2.7 Culture media and supplements for <i>Synechococcus</i> sp. PCC 7002 cultures	32
2.2.8 Storage of <i>Synechococcus</i> sp. PCC 7002 cultures	33
2.2.9 Transformation of <i>Synechococcus</i> sp. PCC 7002	33
2.2.10 Cultivation of <i>Synechococcus</i> sp. PCC 7002 cells.....	33
2.2.11 Determination of <i>Synechococcus</i> sp. PCC 7002 cell density.....	33
2.2.12 Cultivation of <i>Prochlorococcus marinus</i> SS120	34
2.3 Molecular biological techniques.....	34
2.3.1 Preparation of plasmid DNA.....	34
2.3.2 Preparation of genomic DNA from <i>P. marinus</i> SS120.....	34
2.3.3 Preparation of RNA from <i>E. coli</i>	34
2.3.4 Reverse Transcription	35
2.3.5 Determination of DNA and RNA concentration in aqueous solution	35
2.3.6 Agarose gel electrophoresis	36
2.3.7 Polymerase chain reaction	36
2.3.8 Purification of PCR products	37
2.3.9 Restriction of DNA	37
2.3.10 Gel extraction of DNA fragments.....	37

2.3.11 Ligation of DNA fragments	37
2.3.12 Sequencing of DNA	38
2.3.13 Site-directed mutagenesis	38
2.3.14 Gibson Assembly [®] of DNA molecules.....	39
2.3.15 AQUA cloning	40
2.4 Protein biochemical and biophysical methods	40
2.4.1 Production of recombinant proteins in <i>E. coli</i>	40
2.4.2 Cell disruption of <i>E. coli</i> cells.....	41
2.4.3 Affinity chromatography of His-tagged protein	41
2.4.4 Dialysis and concentration protein.....	42
2.4.5 Size exclusion chromatography	42
2.4.4 SDS-polyacrylamide gel electrophoresis (SDS-PAGE)	43
2.4.5 Immuno-staining of immobilized proteins (Western Blot).....	44
2.4.6 Zinc blot	45
2.4.7 Protein precipitation-trichloroacetic acid (TCA) precipitation.....	45
2.4.8 Determination of protein concentration	46
2.4.9 UV/Vis spectroscopy	47
2.4.10 Fluorescence spectroscopy.....	47
2.4.11 HPLC analyses.....	47
2.4.12 Production of recombinant proteins in <i>Synechococcus</i> sp. PCC 7002	49
2.4.13 Isolation of intact phycobilisomes from <i>Synechococcus</i> sp. PCC 7002	49

2.4.14 Preparation of protein samples from <i>Prochlorococcus marinus</i> SS120.....	50
2.4.15 Pull down assay for enrichment PE-III.....	50
2.4.16 AlphaFold	51
3. Results	52
3.1 What is the natural chromophorylation pattern of PE-III?	52
3.1.1 Pigment characterization of <i>Prochlorococcus marinus</i> SS120 by their spectroscopic properties and fluorescence emission spectroscopy.....	52
3.1.2 Protein analysis of <i>Prochlorococcus marinus</i> SS120.....	53
3.1.3 Identification of associated PE-III proteins from <i>Prochlorococcus marinus</i> SS120.....	56
3.1.4 Enrichment of PE-III from <i>Prochlorococcus marinus</i> SS120.....	58
3.2 Expression of the <i>P. marinus</i> SS120 PE cluster in a heterologous host using the TREX system	59
3.2.1 PE cluster transcription analysis in <i>E. coli</i>	61
3.2.2 PE cluster translation analysis in <i>E. coli</i>	62
3.3 <i>cpeBA</i> expression in <i>Synechococcus</i> sp. PCC 7002	64
3.3.1 Transformation of <i>Syn. 7002</i> pAQ1:: <i>GFP</i>	66
3.3.2 Construction of <i>Syn. 7002</i> pAQ1:: <i>cpeBA</i>	67
3.3.3 <i>cpeBA</i> transcription analysis in <i>Synechococcus</i> sp. PCC 7002.....	68
3.3.4 <i>cpeBA</i> translation analysis in <i>Synechococcus</i> sp. PCC 7002.....	69
3.3.5 Isolation of phycobiliprotein from <i>Synechococcus</i> sp. PCC 7002.....	71
3.4 <i>In vivo</i> characterization of different lyases involved in the chromophorylation of PE-III...75	
3.4.1 CpeS is a lyase specific for attachment of 3Z-PEB to Cys82 of CpeB.....	75
3.4.2 Analysis of recombinant T-type lyases on HT-CpeB	82

3.4.3 Analysis of recombinant E/F-type lyases on HT-CpeB and HT-CpeA	87
4 Discussion	92
4.1 Assembly of phycobiliprotein	92
4.1.1 Codon usage	92
4.1.2 Production condition	93
4.1.3 Regulation of gene expression	94
4.2 Function of lyases	95
4.2.1 CpeS is a PEB-specific phycobiliprotein lyase	95
4.2.2 T-type lyase	98
4.2.3 E/F type lyase	99
4.3 Phycoerythrin structure	101
4.3.1 Chromophorylation PE-III from <i>P. marinus</i> SS120	101
4.3.2 Predicted model of phycoerythrin from <i>Prochlorococcus</i>	102
5 Summary	106
6 Zusammenfassung	107
References	CIX
Appendix	CXXV
Acknowledgement	CXXXII
Curriculum Vitae	CXXXIV
Publication	CXXXV
Eidesstattliche Erklärung	CXXXVI

Abbreviations

A	absorption
Amp	ampicillin
AP	alkaline phosphatase
APC	allophycocyanin
APS	ammonium peroxydisulfate
Aqua dist.	distilled water
BCIP	5-bromo-4-chloro-3-indolyl phosphate
BSA	bovine serum albumin
BV	biliverdin
CA	chromatic acclimation
Chl	chlorophyll
Cmp	chloramphenicol
CV	column volume
Cys (C)	cysteine
Da	Dalton
DF	dilution factor
DHBV	dihydrobiliverdin
et al.	and others
FDBR	ferredoxin-dependent bilin reductase
FPLC	fast protein liquid chromatography
Gln (Q)	glutamine
Glu (E)	glutamic acid
HL	high light
HO	heme oxygenase
HPLC	high performance liquid chromatography
IPTG	isopropyl-1-thio- β -D-galactoside
Km	kanamycin
LB	lysogeny broth
Leu (L)	leucine
LHC	light harvesting complex
LL	low light
Lys (K)	lysine
M	marker
ML	maximum likelihood
MSA	multiple sequence alignment
MW	molecular weight
MWCO	molecular weight cut off
NBT	nitro blue tetrazolium chloride
OD578	optical density at 578 nm
PBP	phycobiliprotein
PBS	phycobilisome

PBS-T	phosphate buffered saline - tween
PC	phycocyanin
PCB	phycocyanobilin
Pcbs	prochlorophyte chlorophyll-binding proteins
PCR	polymerase chain reaction
PDB	protein data bank
PE	phycoerythrin
PEB	phycoerythrobilin
PEC	phycoerythrocyanin
pLDDT	predicted local distance difference test
PS	photosystem
pTM	predicted template modeling score
PUB	phycourobilin
PVB	phycoviolobilin
PVDF	polyvinylidene fluoride
RMSD	root-mean-square deviation
rpm	rounds per minute
RT	room temperature
RT-HPLC	reversed phase high performance liquid chromatography
SDS-PAGE	sodium dodecyl sulfate polyacrylamide gel electrophoresis
TEMED	N,N,N',N'-tetramethylethane-1,2-diamine
TFA	trifluoroacetic acid
UV/Vis	Ultra violet/Visible
v/v	volume per volume
w/v	weight per volume
WT	wild type

1 Introduction

1.1 Cyanobacteria

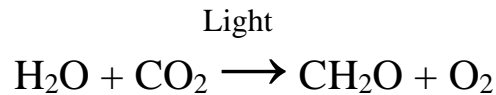
Cyanobacteria are oxygenic photosynthetic prokaryotes with a diameter between 0.2 and 40 μm that can be found in numerous ecological habitats. They are distributed all over the Earth in various niches across drastic changes of salinity and temperature, including marine, aquatic (lakes, ponds, streams, saline marshes, hot springs, and rice paddies), terrestrial environments (microbial mats, rocks, sand, soils, and deserts), and can also be found in symbiosis with plants, mosses and fungi (Rippka *et al.* (1979), Flombaum *et al.* (2013)). They are known to be the world's oldest oxygen-evolving organisms and are found in fossils dating back more than 3.5 billion years (Blank (2004)). These oxygenic photosynthetic organisms created an oxygen-rich atmosphere that we can breathe in today. However, cyanobacteria differ from other photosynthetic microorganisms, such as purple bacteria and archaea, in their presence of chlorophyll *a* (Chl *a*), phycobiliproteins and their ability to conduct oxygenic photosynthesis. In addition, another essential ecological feature is the ability of some cyanobacteria species to fix atmospheric nitrogen but not all cyanobacteria. A number of cyanobacteria have physiological strategies which allow them to fix N_2 under well-oxygenated conditions even without a heterocyst and this becomes more widespread under low oxygenic conditions (Whitton & Potts (2012)).

In 1967, Lynn Sagan formulated the modern theory of endosymbiosis. People started to recognize the similarity between cyanobacteria and chloroplasts of higher plants and red algae (Sagan (1967)). Recent phylogenomic studies suggest that the first cyanobacteria occurred in terrestrial or freshwater environments and that the marine environment was colonized only later (Blank & Sanchez - Baracaldo (2010)). Marine *Synechococcus* and *Prochlorococcus* both could be responsible for more than 25 % of the ocean's primary production. (Flombaum *et al.* (2013)).

Moreover, the cyanobacteria that have been documented so far exhibit a range of beneficial properties, including antibacterial, antifungal, anti-cancer, immunosuppressive, anti-inflammatory, and anti-tuberculosis activities. These properties hold promise for their application in various fields, such as pharmacology, cosmetology, agriculture, the food industry and as biofuel (Singh *et al.* (2017)).

1.1.1 The photosynthetic machinery of cyanobacteria

Among the organisms that use light as an energy source, phototrophic cyanobacteria are the only prokaryotes that are capable to perform oxygenic photosynthesis. This process, which appeared 3.5 billion years ago, allows the fixation of inorganic carbon thanks to the conversion of light energy to chemical energy (Awramik (1992)). It is based on the use of a water molecule as an electron donor which determines the release of oxygen according to the following reaction:



Photosynthetic reactions are classically divided into "light" and "dark" reactions. The photosynthetic machinery is embedded in the thylakoid membranes, with phycobilisomes acting as light-harvesting antennae associated to the membrane. The complete photosynthetic reaction in cyanobacteria are executed by four major protein supercomplexes including photosystem I (PSI), photosystem II (PSII), cytochrome b_6f and ATP synthase (Fig. 1). The supercomplexes of both PSI and PSII utilize chlorophyll molecules to sense varying spectrums and intensities of light. The photoreactions of the light phase of photosynthesis are possible thanks to the presence of light-collecting antennae, which transfer their energy to a reaction center (RC) and initiate electron transport. The light-collecting antennae exist in different forms in cyanobacteria and are called Phycobilisomes (PBSs).

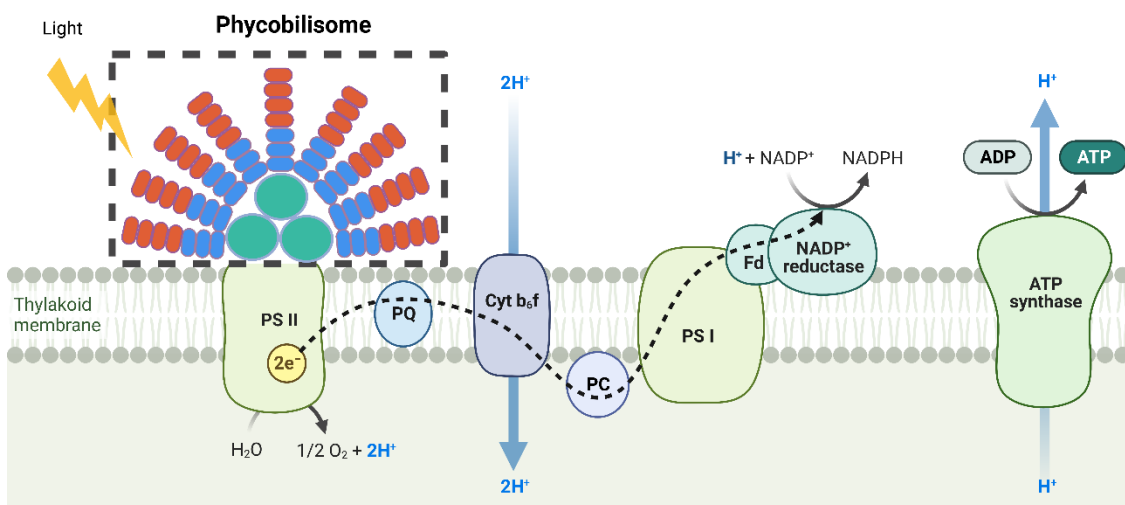


Figure 1. Thylakoid photosynthetic complexes in cyanobacteria. The four complexes of the photosynthetic reactions are present in the thylakoid membrane, in the form of circular membrane sacs in the cytosol. Phycobilisomes as photosynthetic light-harvesting antennas associated to the thylakoid membrane:

1.1.2 The phycobilisome

Most cyanobacteria and red algae possess complete phycobilisomes (PBSs) as photosynthetic light-harvesting antennas with a molecular mass in the range from 7 to 15 MDa. Unlike photosynthetic reaction centers and other light-harvesting antennas, the phycobilisome chromophores are linear tetrapyrroles (phycobilins) rather than chlorophylls (Chls). The PBS is located in the cytoplasmic side of thylakoid membranes, filling up most of the gap between individual thylakoids (Adir *et al.* (2020)). Phycobilisomes absorb light and transfer the energy to chlorophylls in PSII and PSI, where charge separation occurs (Liu *et al.* (2013)).

Cyanobacterial phycobilisomes are typically hemidisoidal in form, with a diameter usually in the range of 32-70 nm. These water-soluble complexes are constituted of a conserved central core surrounded by six to eight rods (Arteni *et al.* (2009)). The rods are made of a special class of proteins called phycobiliproteins (PBPs). The cyanobacterial phycobilisome model has a core of three short rods of allophycocyanin (APC). Attached to this core are several rods, each made up of one or more phycocyanin (PC) hexamers. In some marine *Synechococcus* strains, these rods are extended by the addition of phycoerythrin (PE) hexamers. Assembly rods rely on a variety of linker proteins. PC, APC, and PE rods each require their own specific linker proteins, while other proteins serve to connect different types of rods. Moreover, PBS association to the thylakoid membrane depends on a specific APC unit called core-membrane linker protein (L_{CM}). Phycobilisomes can be excited very specifically by light in the region from 550 to 650 nm, depending on the phycobilin content. The distal region of the phycobilisome absorbs shorter wavelengths compared to the proximal region and performs an efficient unidirectional energy transfer to the final acceptors (Fig. 2B; Acuña *et al.* (2018)). Phycobilisomes are mainly associated with PSII, however, in *Synechocystis* PCC6803 PBS was found to be associated with both PSII and PSI in a “megacomplex” (Fig. 2A; Liu *et al.* (2013)).

Different ocean depths are characterized by different light intensities. As the intensity of light declines with the depth, cyanobacteria have the capacity to adjust by enlarging their phycobilisome (PBS) structures that consist of more phycobiliprotein (PE) rods. Additionally, they can enhance the size and quantity of their photosynthetic units, which refers to the ratio of light-harvesting chromophores to chlorophyll in the reaction center. (Perry *et al.* (1981) Mauzerall & Greenbaum (1989) Kolodny *et al.* (2022)). The relationship between PBS and nitrogen condition has already

been proved, under N deprivation in both cyanobacteria and red algae, the PBS is highly prone to disassembling. (Grossman *et al.* (1993)).

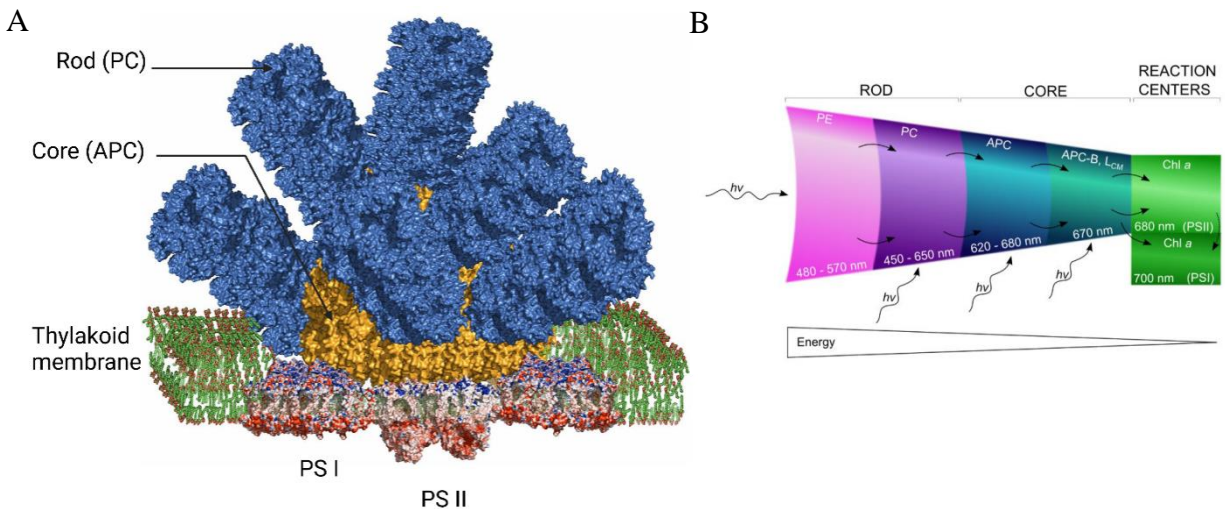


Figure 2. Model of phycobilisome associated to the thylakoid membrane and energy transfer in phycobilisomes. **A.** The complex is made of one phycobilisome attached to a dimer of PSII. Two trimeric PSI surround the PSII dimer. Figure adapted from (Blankenship (2015)). **B.** Excitation energy transfer from the distal to the proximal end of the rod, then to the core and to the photosystem II or I. Figure reproduced from (Pittera (2015)).

1.1.3 Phycobiliproteins and chromophorylation

Four phycobiliproteins (PBPs) have been described in cyanobacteria: phycocyanin, phycoerythrocyanin (PEC), phycoerythrin and allophycocyanin. PBPs generally constitute about 20-30 % of cells dry weight, however, their content may increase to 40-50 % in low-light conditions (Muramatsu & Hihara (2012)). They are usually made of two basic heterodimers (α and β subunits) with molecular weights of 15-22 kDa, each can bind one to three chromophores on conserved cysteine residues. Chromophore attachment onto phycobiliprotein subunits is necessary for the initial formation of a stable complex of ($\alpha\beta$) heterodimer. Three ($\alpha\beta$) monomers are arranged about a threefold axis and form a trimer ($(\alpha\beta)_3$). Two such trimers are associated face-to-face to form a hexamer ($[(\alpha\beta)_3]_2$) (Fig. 3; Adir (2005) Zhang *et al.* (2017) Grébert *et al.* (2022)).

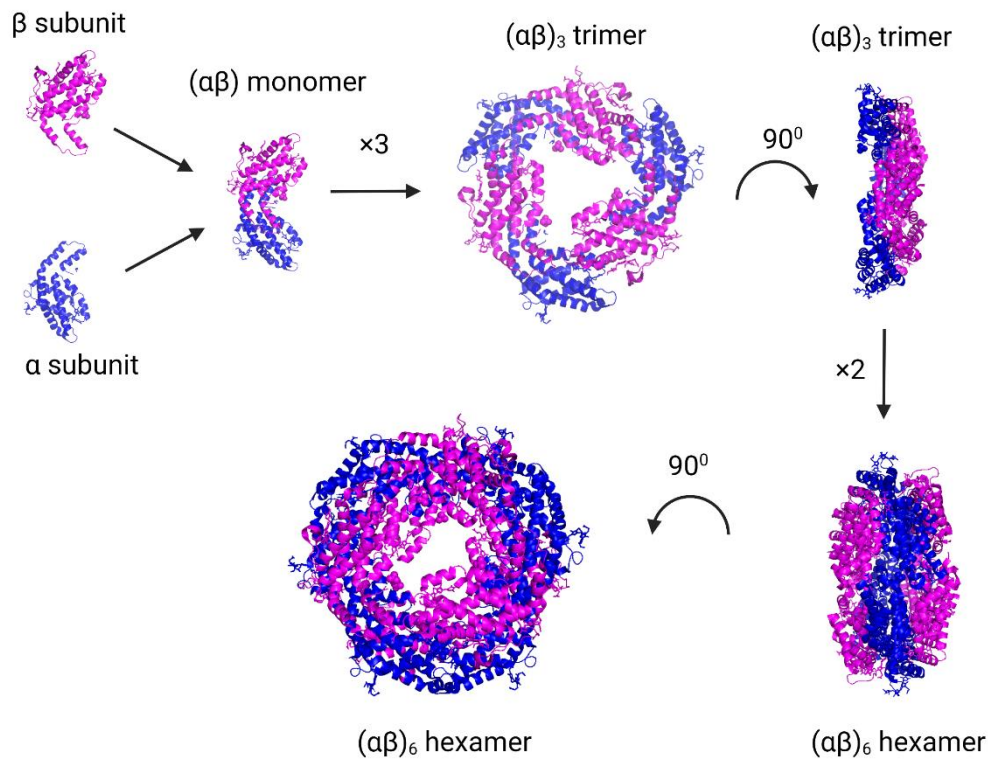


Figure 3. Assembly of phycobiliproteins into hexamers. The protein backbone of an α -subunit is displayed as blue ribbons, and in pink for a β -subunit. Phycoerythrobilins located on α -Cys82, α -Cys139, β -Cys48/59, β -Cys80 and β -Cys165. The assembly into monomer and trimers is spontaneous and stable, but the hexamers are only stable when associated with linker protein (not shown here). The structure used is a modified version of phycoerythrin crystal structure from cyanobacterium *Phormidium* sp. A09DM (PDB: 5AQD).

Although structurally very similar, the different PBPs display very bright and diverse colors due to the chromophores associated with them. These chromophores, named phycobilins, are linear tetrapyrrolic molecules, covalently attached to cysteine residues of the apoprotein by thioether linkages. The different bilins are isomeric to each other. They are various in the number and location of double bonds, which are sufficient to give them different spectroscopic properties (Fig. 4; Glazer (1989)). In cyanobacteria, four phycobilins can be associated with PBPs: the blue pigment, phycocyanobilin (PCB, $A_{\max} = 620$ nm), the red phycoerythrobilin (PEB, $A_{\max} = 540$ nm), the orange phycourobilin (PUB, $A_{\max} = 495$ nm), and the violet pigment, phycoviolobilin ($A_{\max} = 590$ nm) (Fig. 4). While, only PEB, PCB and PUB have been observed in marine picocyanobacteria. In principle, phycobilins are bound to the A-ring of the four-pyrrole ring system (A-D). In PBPs, the chromophore is usually bound to the C3¹ atom of the A-ring of the phycobilin via a single bond. The two chromophores PEB and PUB can also be doubly bound. The additional binding occurs via the C18¹ atom on the D-ring of the PBP (Scheer & Zhao (2008)).

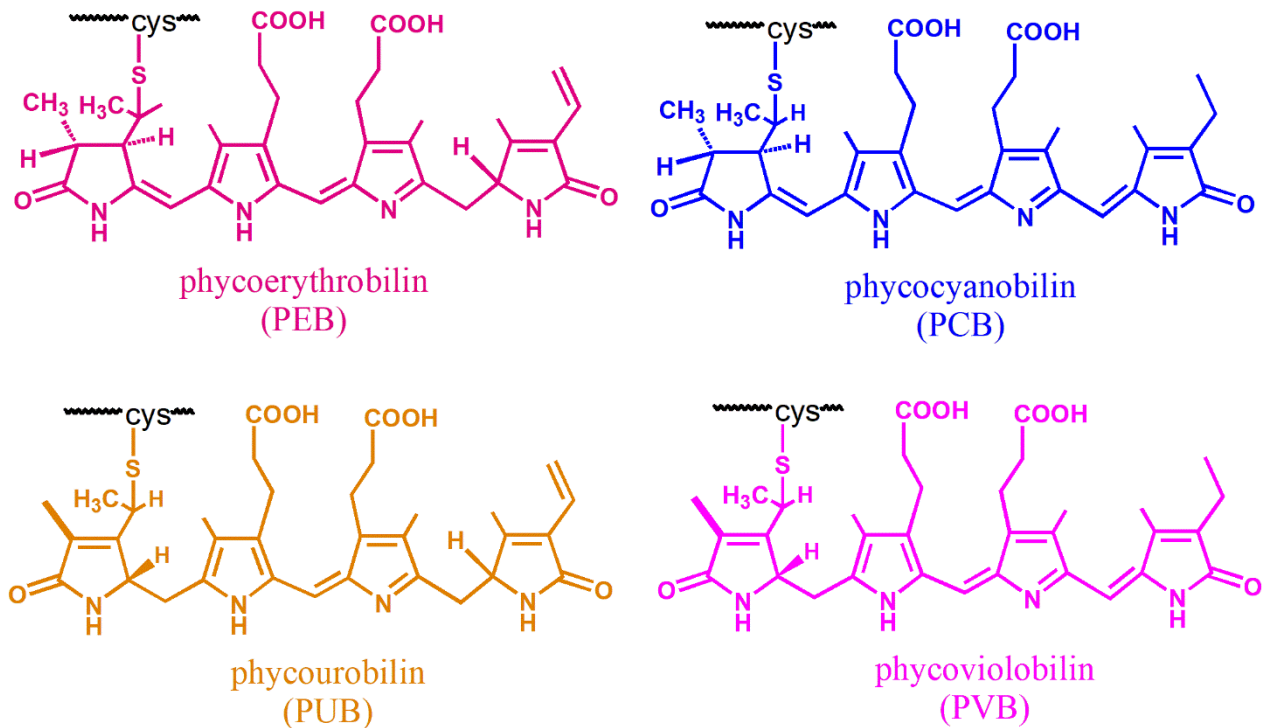


Figure 4. Structure of the phycobilins in cyanobacteria. Shown in pink is phycoerythrobilin (PEB), phycoviolobilin (PVB) in purple, phycocyanobilin (PCB) in blue, and phycourobilin (PUB) in yellow.

Allophycocyanin, which makes the core of the PBS, presents a single-bound PCB on Cys 82. Although only a few strains have phycocyanin alone, most *Synechococcus* species have rods with both PC and PE, and the majority of these possess PC as well as two forms of PE called phycoerythrin-I (PE-I) and phycoerythrin-II (PE-II) (Stal (2022) Bar-Eyal *et al.* (2018) Six *et al.* (2007) Sanfilippo *et al.* (2019)). PE-I and PE-II are related both at the structural and amino acid sequence levels, but they bind different chromophores and are encoded by different genes. PE-I α and β subunits, called CpeA and CpeB, are encoded by the *cpeBA* operon. There are five cysteine residues capable of binding phycobilins for PE-I (α -84, α -143, β -84, β -155 and the doubly linked β -50, 61), while PE-II presents an addition at α -75 for PE-II. PE-II α and β subunits, called MpeA and MpeB, are encoded in the *mpeBA* operon (Everroad *et al.* (2006) Humily *et al.* (2013)).

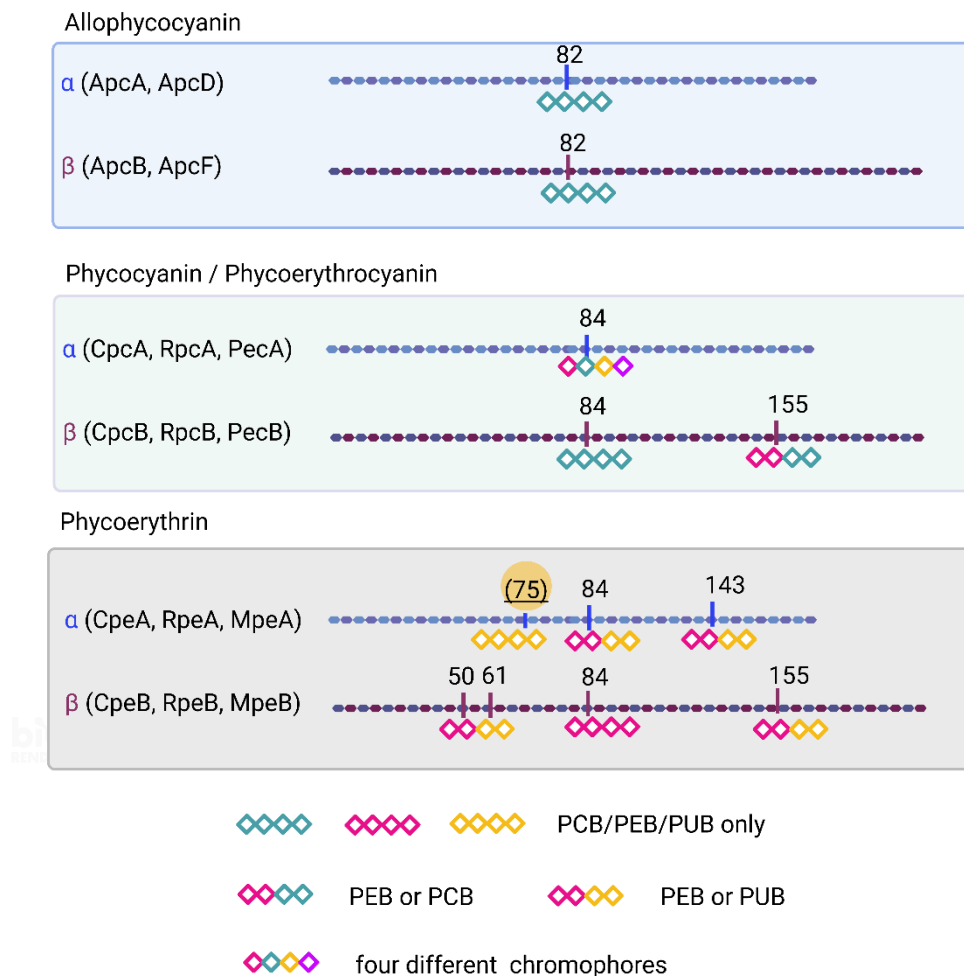


Figure 5. Chromophorylation of phycobiliproteins in cyanobacteria. The chromophore binding sites (cysteine residues) are indicated in the figure. The four chromophores that can bind to phycobiliproteins are shown in blue (phycocyanobilin), purple (phycoviolobilin), red (phycoerythrobin) and orange (phycourobilin). The most variable site is Cys- α 84, to which the attachment of all four chromophores has been reported. The name of each protein subunit is indicated in brackets protein subunit: Apc, allophycocyanin subunit; Cpc, phycocyanin subunit when it binds only phycocyanobilin. Rpc when phycoerythrin is present, and Pec when phycocyanin is associated with phycoviolobilin; Cpe when the chromophorylated bilin at position α -84 is a phycoerythrobin, Rpe when it is a phycourobilin. Mpe, additional phycourobilin at α -75 (only present in some marine *Synechococcus* strains).

1.2 *Prochlorococcus marinus* SS120

Prochlorococcus is one of the most abundant unicellular marine photosynthetic cyanobacterium. It contributes 30-80 % of the total photosynthesis in the low- to mid-latitude oceans and plays a significant role in the global carbon cycling and climate regulation on the earth (Bryant (2003), Paul *et al.* (2010)). Because of its small size of 0.5 to 0.7 μm in diameter and weak fluorescence, *Prochlorococcus* has been overlooked for a long time. Johnson and Sieburth first revealed the

typical ultrastructure of *Prochlorococcus* (Fig. 6; Morel *et al.* (1993)). It possesses a typical prokaryotic Gram-negative cell wall and peripheral thylakoids that are closely appressed to one another (Johnson & Sieburth (1979), Chisholm (2017)).

Prochlorococcus is incapable of dinitrogen gas (N₂) fixation, and none of the isolated strains are able to utilize nitrate as a source of nitrogen (N). However, all strains can use ammonium, the form incorporated biosynthetically by glutamine synthetase and generated through recycling (Coleman & Chisholm (2007)). Compared with marine *Synechococcus* cyanobacteria, characterized by a high G+C content (47.4 to 69.5 %), *Prochlorococcus* strains have a low G+C content. Why *Prochlorococcus* has a low G+C content is not known, but might be related to the higher sensitivity of AT-rich DNA sequences to UV light-induced oxidative DNA damage or high mutant rates (Wikner & Hagström (1988)). In contrast to other cyanobacteria, *Prochlorococcus* lacks PBS but uses divinyl-chlorophyll (DV-Chl) *a/b*-Pcb (prochlorophyte chlorophyll-binding protein) protein complex as its major light-harvesting antenna complex (Partensky *et al.* (1999)). These chlorophylls present red-shifted absorption peaks compared to typical Chl *a* and *b*, allowing them to absorb blue-light more efficiently. During evolution, large parts of the phycobiliprotein genes coding for other structural components of the phycobilisome e.g. allophycocyanin, phycocyanin, and linkers were lost.

Based on their physiological characteristics, ecological distribution, and phylogeny, *Prochlorococcus* strains can be grouped into high-light-adapted (HL) clades and low-light-adapted (LL) clades (Rocap *et al.* (2002), Johnson *et al.* (2006)). The HL ecotype dominates in the upper part of the water column, whereas the LL ecotype dominates below 100 meters (Fig. 7B). At the intensity at which the HL ecotype achieves maximum growth, the LL ecotype is photo-inhibited (Fig. 7A) (Biller *et al.* (2015)). As they are present at different depths, HL and LL strains exhibit different pigment ratios and sizes of their Pcb antennas (Coleman & Chisholm (2007), Garczarek *et al.* (2007)). In the LL SS120 strain, more DV-Chl *b* is present if compared to the HL MED4 (Moore *et al.* (1995)). While HL strains possess one to two *pcb* associated genes involved in PS, LL strains have more. For the LL SS120 strain, there are eight Pcb copies, two are associated to PSI, and the remaining six to PSII (Bibby *et al.* (2001), Coleman & Chisholm (2007), Grébert (2017)). LL ecotypes were shown to synthesize a seemingly functional though divergent PE (called PE-III) and HL ecotypes a β -PE remnant (Hess *et al.* (1996)).

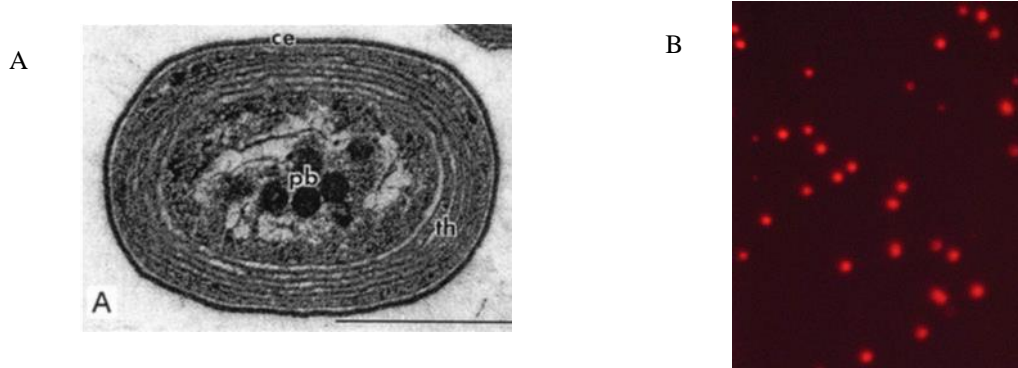


Figure 6. *Prochlorococcus*. **A.** Electron microscope photograph of a *Prochlorococcus* cell from the North Atlantic Ocean. (pb) polyhedral bodies; (th) thylakoid membranes; (ce) cell envelope, scale bar, 0.5 μm (Johnson & Sieburth (1979)). **B.** *Prochlorococcus* cells as they appear under an epifluorescence microscope when excited by blue light. The red fluorescence is from their chlorophyll. Each cell is about 0.6 μm in diameter (pictures took from Chisholm (2017)).

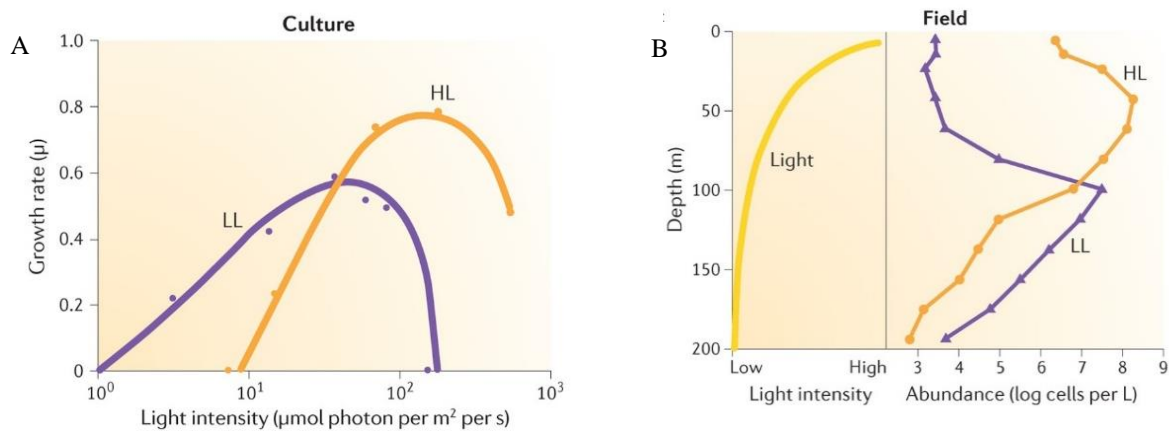


Figure 7. Light ecotypes in *Prochlorococcus*. **A.** Light physiology of the HL and LL ecotypes. The LL ecotype grows well at light intensities below the HL ecotype compensation point. **B.** Typical distribution of both light ecotypes in the environment. The HL ecotype dominates in the upper part of the water column, whereas the LL ecotype dominates below 100 m (pictures took from Biller *et al.* (2015)).

The first cultivated strain, *Prochlorococcus marinus* SS120, was isolated in 1988 from the bottom of the euphotic zone in the Sargasso Sea at 120 m depth (Chisholm *et al.* (1992)). The genome of *P. marinus* SS120 is composed of a single circular chromosome of 1,751,080 bp with an average G+C content of 36.4 %. It contains 1,884 predicted protein-coding genes with an average size of 825 bp, a single rRNA operon, and 40 tRNA genes (Dufresne *et al.* (2003)). *P. marinus* SS120 and MED4 possess four genes involved in the biosynthesis of phycobilins. Three genes for the biosynthesis of PEB (*ho1*, *pebA* and *pebB*), as well as *pcyA* coding PCB (Frankenberg *et al.* (2001),

Steglich *et al.* (2005)). No phycobiliproteins were detected to bind PCB in *Prochlorococcus*. Thus, the functional relevance of PcyA remains to be proven. Most of the required genes for PE-III synthesis and assembly are encoded in a 10 kb gene cluster (Fig. 8) (Hess *et al.* (1996)). This cluster not only contains genes for the α - and β -subunit of PE (*cpeA* and *cpeB*) but also five putative phycobiliprotein lyase genes which are likely involved in the posttranslational attachment of the light-harvesting pigments to the PBP subunits (*cpeS*, *cpeT*, *cpeY*, *cpeZ*, and *mpeX*). Furthermore, it contains a gene encoding a γ -linker protein (*ppeC*), likely involved in anchoring the PE to the thylakoid membrane (Hess *et al.*, 1996) and an open reading frame (orf 62) of unknown function possibly encoding a micro protein (Staudt & Wenkel (2011)). In the HL *Prochlorococcus*, most of PBP genes were lost during the evolution, and only *cpeB* and *cpeS* have been retained.

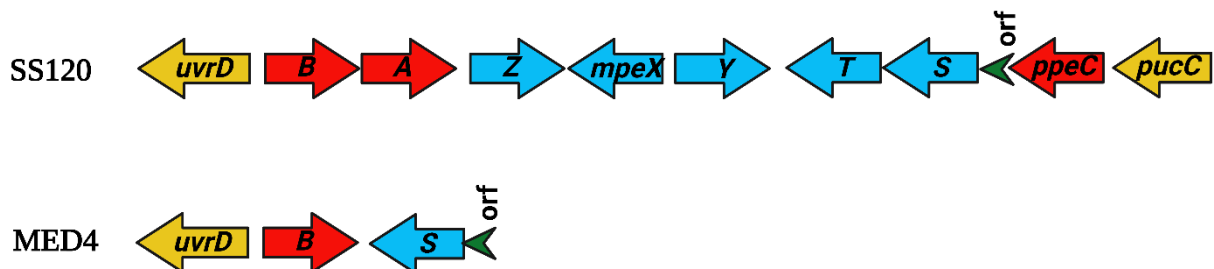


Figure 8. PE gene cluster in *P. marinus*. Red arrows correspond to genes encoding apo- or linker proteins (*cpeA*, *cpeB*, and *ppeC*), blue arrows correspond to genes encoding putative PBP lyases (*cpeZ*, *mpeX*, *cpeY*, *cpeT* and *cpeS*). Green arrow depicts an open reading frame of unknown function. Orange arrows mark the flanking genes *uvrD*, DNA helicase, and *pucC*, bacteriochlorophyll synthase.

1.2.1 Phycoerythrin in *Prochlorococcus*

In addition to the Pcb, *Prochlorococcus* ecotypes only possess a single phycobiliprotein, phycoerythrin (PE). The structure of PE in *Prochlorococcus* spp. is distinguished by PE demonstrated in *Synechococcus*. Phycoerythrin-III (PE-III) is the phycoerythrin found in LL *Prochlorococcus* strains. The PE-III of *P. marinus* SS120 consists of an α - and β -subunit encoded by the genes *cpeA* and *cpeB*, respectively. While the α -subunit possesses one conserved cysteine residue at position 73, four cysteine residues are located at positions 50, 61, 82 and 155 in the β -subunit (Fig. 9). Although previous *in vivo* physiological studies revealed a pigment composition of phycourobilin (PUB) and phycoerythrobilin (PEB) at a 3:1 ratio, the exact chromophorylation of PE-III is still unknown (Steglich *et al.* (2003)). Interestingly, HL-adapted strains like MED4 carry an even more degenerated form of PE-III, consisting of a single β -subunit with only one conserved cysteine residue at position 82 (Fig. 8; Steglich *et al.* (2005) Wiethaus *et al.* (2010)).

Linker proteins are not only essential for PBS assembly, but also for energy transmission, and are functionally classified as rod linkers, core linkers, rod-core linkers and core-membrane linkers. CpcG is a rod-core linker protein that is required for attachment of peripheral rods to the PBS core. Rod linkers are further divided into PC-associated linkers (CpcC, CpcD), PE-I associated linkers (CpeC, CpeD and MpeD) and PE-II associated linkers (MpeC, MpeE, MpeF, MpeG and MpeH) (Six *et al.* (2007) Liu *et al.* (2005) Watanabe & Ikeuchi (2013) Sidler (1994)). A putative linker protein, PpeC which is phylogenetically connected with MpeC family was found in all LL *Prochlorococcus* spp., with the exception of MIT9303 and MIT9313 (Hess *et al.* (1999)). In addition, none of the HL *Prochlorococcus* have the *ppeC* gene. PpeC is thought to act as a helper for the PE complex coupling to the thylakoid membrane (Roache-Johnson (2013)).

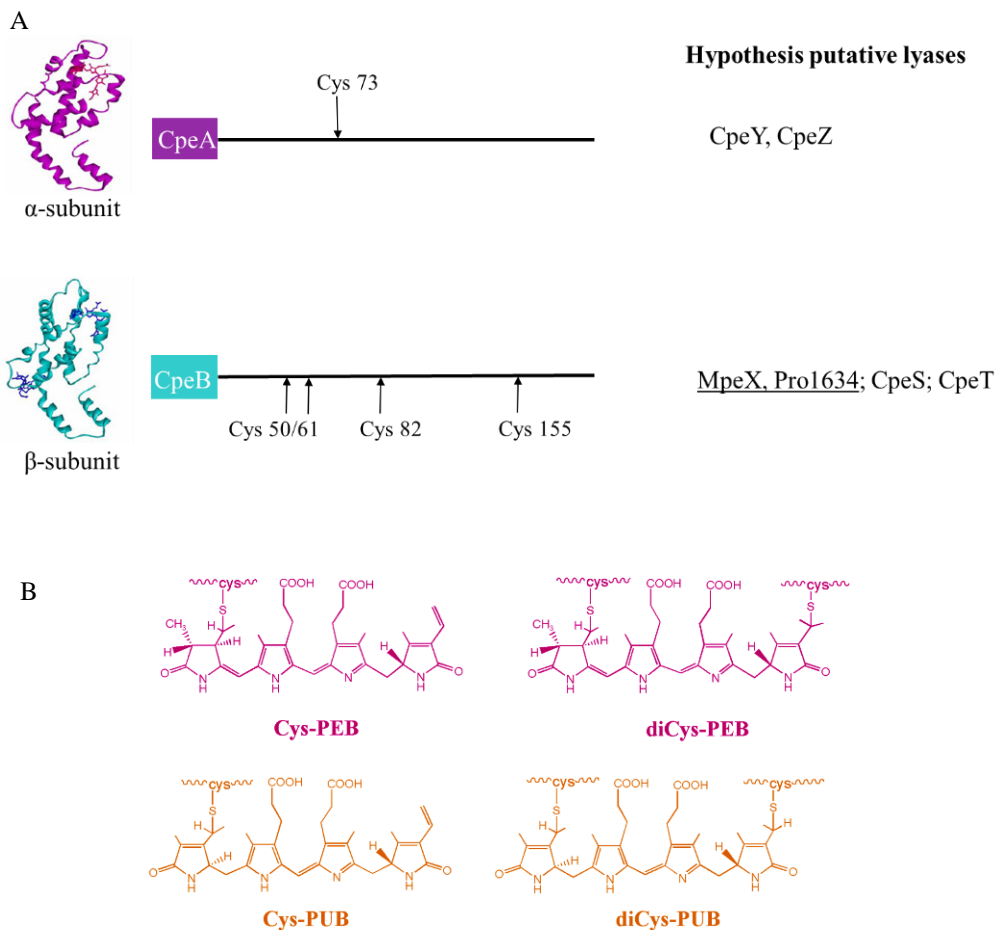


Figure 9. Structure of PE-III. **A.** Schematic representation of α - and β -subunit of PE-III from *P. marinus* SS120 indicating the conserved cysteine residues and hypothesis putative lyases. CpeA carries one, CpeB three of such binding sites. **B.** Structure of single and double linked phycobilins PEB and PUB depicted as they might occur bound to PE-III in *P. marinus* SS120.

1.2.2 Prochlorophyte chlorophyll-binding protein

Compared with other typical cyanobacteria, *Prochlorococcus* does not have phycobilisomes, but an original light-harvesting antenna intrinsic to the thylakoid membrane and made of “prochlorophyte chlorophyll binding” proteins (Pcb). The Pcb-based light-harvesting antenna requires less nutrition in terms of nitrogen and iron, and the replacement of sulfolipids with phospholipids to adapt to its oligotrophic lifestyle (Partensky *et al.* (1999), Ting *et al.* (2002), Biller *et al.* (2015)). In most prochlorophytes, *Prochlorothrix*, *Prochloron* and *Acaryochloris* included, Pcb bind Chl *a/b* (d). On the other hand, in *Prochlorococcus*, Pcb bind specific chlorophyll derivatives, such as DV-Chl *a* and *b*. In *Prochlorococcus*, a chlorophyll-binding protein of the iron-stress-induced (IsiA) type, which is typical of marine *Synechococcus* and is phylogenetically connected with the *Prochlorococcus* Pcb family (Garczarek *et al.* (2000), Ulloa *et al.* (2021)). Moreover, this protein family bears sequence similarity to the CP43 protein (encoded by the *psbC* gene) of PSII in cyanobacteria (Leonhardt & Straus (1994), Roche *et al.* (1996)). The DV-Chl *a/b*-Pcb protein complex is encoded by a variable number of *pcb* genes. HL-adapted ecotypes MED4 and TAK9803-2 only carry a single *pcb* gene (*pcbA*). Conversely, in LL MIT 9313 strain two *pcb* genes (*pcbA* and *pcbB*) exist. Another LL strain SS120 which grows at the lowest light intensity of these three has eight copies (Garczarek *et al.* (2000), Garczarek *et al.* (2001), Coleman & Chisholm (2007)). Thus, the multiplication of *pcb* genes appears as a key factor in the capacity of deep *Prochlorococcus* populations to survive at extremely low photon fluxes (Garczarek *et al.* (2000)). There is currently no high-resolution structure for the Pcb antenna. A projection map of this antenna has revealed that it organizes itself into an integral membrane multimeric complex that surrounds the trimeric photosystem I and photosystem II core complexes of these cyanobacteria (Bibby *et al.* (2001), Bibby *et al.* (2003), Saer & Blankenship (2017)). In LL-adapted *Prochlorococcus* ecotypes, the organization of the Pcb antennas with PSI and PSII is different. PcbG is the most abundant Pcb protein in SS120. The Pcb-PSI supercomplex comprises the surrounding PSI reaction center trimer with an 18-membered PcbG ring (PcbG₁₈PSI₃), which is similar to the IsiA-PSI structure found in iron-limited *Synechocystis* sp. PCC 6803 (Bibby *et al.* (2001)). Studies on MIT9313 revealed that the Pcb-PSI supercomplex was only observed in iron deficient cells, whereas PSI complexes were almost exclusively organized into a pseudo-hexagonal lattice (Bibby *et al.* (2003)). In SS120 and MIT9313 PSII dimers are flanked by eight Pcb subunits (Pcb₈PSII₂). In the prochlorophyte cyanobacteria *Prochlorothrix* and *Acaryochloris* electron microscopy revealed a similar Pcb-PSI supercomplex model (PcbC₁₈PSI₃) (Bumba *et al.* (2005), Chen *et al.* (2005), Durchan *et al.* (2010)).

The HL-adapted ecotype MED4 does not possess any Pcb-PSI supercomplex in iron-rich or -depleted conditions, although it does appear to assemble a Pcb-PSII supercomplex (MacGregor-Chatwin *et al.* (2019)). Until now, only a Pcb-PSII supercomplex from *Prochloron didemni* was structurally characterized. The model shows that 10-Pcb subunits associate with the PSII dimeric reaction center core and are adjacent to CP47 and CP43. Furthermore, it was demonstrated that the energy migration occurs between Pcb's first, then moving to PSII (Bibby *et al.* (2003)). In *Prochlorococcus*, it is clear that Pcb proteins act as peripheral antenna complexes for PSII, but how these supercomplexes associate in the membrane environment and what kind of role they are playing in energy transmission are still unknown.

1.2.3 Pigment biosynthesis

P. marinus grows by photosynthesis, and necessarily contains chlorophyll and carotenoids, whose main functions are light harvesting and photoprotection. Chlorophylls are essential molecules in oxygenic photosynthesis. In cyanobacteria, algae and terrestrial plants, chlorophyll (Chl) *a* (monovinyl Chl *a*, MV-Chl *a*) is the major chlorophyll (Averina *et al.* (2019)). *Prochloron*, *Prochlorothrix*, and *Prochlorococcus* are unique among cyanobacteria because they contain both Chl *a*- and Chl *b*-type Chls. Furthermore, *Prochlorococcus* is a unique photosynthetic genus since it uses divinyl chlorophyll (DV-Chl) instead of monovinyl chlorophyll (MV-Chl). The only exception among the *Prochlorococcus* species is represented by *Prochlorococcus* sp. NIES-2086, which possesses MV-Chl *b* as well as DV-Chl *b* as its major chlorophylls light harvesting (Komatsu *et al.* (2016)). Compared to normal MV-Chl, DV-Chl is characterized by an 8-10 nm red shift. The ability of DV-Chl to harvest blue light more efficiently than MV-Chl allows *Prochlorococcus* to photosynthesize and grow under the deep-sea water column, where blue light predominates.

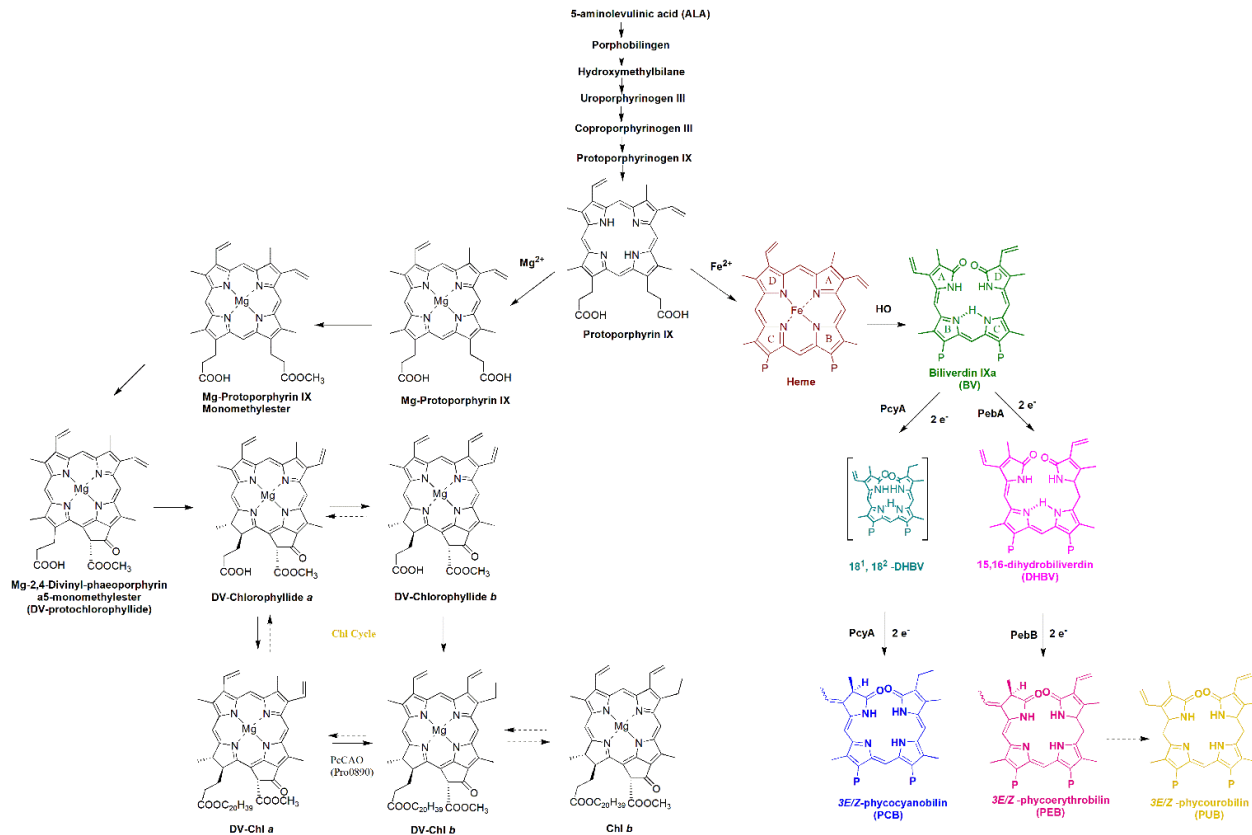


Figure 10. Bilin pigment PEB, PCB and Chl biosynthesis pathway in *Prochlorococcus marinus* SS120. All phycobilins originate from biliverdin (BV) IX α , the first open chain tetrapyrrole and product of the heme oxygenase reaction. BV IX α is subsequently reduced by ferredoxin-dependent bilin reductases (FDBR). PcyA, PebA and PebB catalyze the four-electron reduction of BV IX α to phycocyanobilin (PCB) and phycoerythrobilin (PEB), respectively. However, no PUB biosynthesis enzyme has been identified yet and it is hypothesized that it is produced during the attachment process to the phycobiliprotein by an isomerase/lyase. As for Chl biosynthesis, it was shown on the left side of the figure. The chlorophyll biosynthesis pathway in *Prochlorococcus* is similar to other photosynthetic organisms.

The biosynthesis of chlorophylls involves multiple steps, starting with the precursor molecule 5-aminolevulinic acid (ALA). In *Prochlorococcus*, ALA is synthesized by the action of glutamate-1-semialdehyde aminotransferase. ALA is then converted to protoporphyrin IX through a series of enzymatic reactions. The first step in the synthesis of chlorophyll from protoporphyrin IX is the insertion of magnesium into the tetrapyrrole macrocycle to make magnesium protoporphyrin IX. Later several additional steps are required to convert magnesium protoporphyrin IX into DV-Chl *a* including the addition of a phytol side chain and the removal of a carboxymethyl group. Genomic analyses of marine *Synechococcus* and *Prochlorococcus* revealed that *Prochlorococcus* lost the 3,8-divinyl protochlorophyllide 8-vinyl reductase (DVR) and chlorophyllide an oxygenase (CAO)

that catalyzes the conversion of Chl *a* to Chl *b* genes (Hess *et al.* (2001), Satoh & Tanaka (2006)). Interestingly, the CAO family has been found to convert DV-Chl *a* to DV-Chl *b* in *Prochlorococcus* named PcCao (Fig. 10 left; Satoh & Tanaka (2006)). Overall, the biosynthesis of chlorophylls in *Prochlorococcus* involves a complex pathway that requires multiple enzymes, but ultimately results in the production of essential pigments for photosynthesis.

Phycobilins are linear tetrapyrroles derived from heme. They are especially efficient at absorbing particular light, that is not well absorbed by chlorophyll *a*. Their synthesis first requires the opening of the heme ring in an oxygen-dependent step, which is catalyzed by a heme oxygenase encoded by *hol* resulting in biliverdin IX_α (BV IX_α). BV IX_α is then reduced by different ferredoxin-dependent bilin reductases (FDBR) to phycobilins (Grébert (2017); Dammeyer & Frankenberg-Dinkel (2006)). In *Prochlorococcus*, there are three genes (*hol*, *pebA*; *pebB*) that encode for the pink pigment PEB biosynthetic enzyme and one gene (*pcyA*) encoding for the PCB biosynthesis enzyme. Additionally, another member of the FBDR family, named phycoerythrobilin synthase (PebS), found in the *Prochlorococcus* infecting cyanophage P-SSM2 has a novel activity replacing the functions of two separate enzymes in the host cell, *PebA* and *PebB*, by directly synthesizing PEB (Dammeyer *et al.* (2008)). Interestingly, the only FDBR found capable of reducing reduce BV to PUB, is phycourobilin synthase (PUBS), which was recently discovered in the moss *Physcomitrella patens*. It appears to be involved in light sensing and photomorphogenesis. PUBS is a four-electron reducing FDBR and converts BV via 15,16-dihydrobiliverdin (15,16-DHBV) to PUB (Chen *et al.* (2012)). Although, until today, no PUBS homolog was detected in cyanobacteria. A large amount of PUB has been detected in many *Prochlorococcus* spp. *in vivo*. However, it is still unknown how they are synthesized. Most likely they are produced during the covalent attachment to phycobiliprotein by bi-functional enzymes called phycobilin lyase-isomerases that concomitantly attach and isomerize bilins.

Carotenoids are lipid-soluble pigments which are essential for all oxygenic photosynthetic organisms including cyanobacteria They may be divided into two groups: xanthophylls and carotenes (Erdoğan *et al.* (2016)). *Prochlorococcus marinus* also contains β-carotene and zeaxanthin as well as α-carotene and related carotenoids(Takaichi & Mochimaru, 2007). These pigments are not considered to have a light-harvesting function, but their role still remains unknown. Although lacking ketocarotenoids, CrtO-like and CrtW-like proteins, the HL MED4 strain contains two lycopene cyclases (CrtL-b and CrtL-e) which are essentially involved in

carotenoids biosynthesis (Stickforth *et al.* (2003)). Recently, it was demonstrated that the amount of zeaxanthin in the SS120 strain is dependent on light type and intensity. In particular, zeaxanthin production increased under higher light intensity or red LED light (Hamada *et al.* (2017)).

1.2.4 Phycobilinprotein lyases

Phycobiliproteins not only possess very similar chromophores but also use the same mechanism of covalent binding and similar interactions with their apoproteins. In heterologous expression, the attachment of phycobilin to phycobiliproteins can occur spontaneously. However, those spontaneous interactions have low fidelity, especially showing oxidations, and can not ensure the correct stereochemistry. Since in cyanobacteria, phycobiliprotein synthesis is the major metabolic pathway, the chromophores are reactive and the concentrations are low, spontaneous chromophore binding *in vivo* is not likely (Scheer & Zhao (2008)). In *in vitro* experiments, phycobilin lyases catalyze the covalent attachment of the specific phycobilin to conserved cysteine residues distinguished from autocatalytic reactions (Adir *et al.* (2020)). For the attachment of bilins to the different conserved cysteine residues, three classes of lyases have been characterized, the S/U-type lyases, T-type lyases and the E/F-type lyases (Table 1) (Ledermann *et al.* (2017)).

S/U-type lyases have rather broad apoprotein as well as chromophore substrate specificity. Generally, these proteins can be classified into two groups. One is involved in the PE biosynthesis or assembly, playing a role in PEB attachment to PE subunits. CpeS from *Fremyella diplosiphon* and *Prochlorococcus marinus* MED4 are responsible for the attachment of PEB to the β -subunit of PE (CpeB) at β -Cys 82, respectively (Wiethaus *et al.* (2010), Biswas *et al.* (2011)). The second group is involved in PC synthesis and can be further divided into three subfamilies (CpcS-I, CpcS-II, CpcS-III), CpcS-II/CpcU-II only exist in marine *Synechococcus* /Cyanobium and have not been formally characterized yet, but likely some of them produce PC and PE (Bretaudeau *et al.* (2012)). The crystal structure of CpcS-III from *T. elongatus* BP1 (TeCpcS) revealed that it belongs to the lipocalin structural family, exhibiting a β -barrel structure with an additional α -helix (Fig. 11; Kuzin *et al.* (2007), Schluchter *et al.* (2010)). TeCpcS forms homodimers in solution and can transfer bilins, PCB, PEB as well as phytochromobilin (P Φ B) to Cys82 of several different PBP substrates (Kronfel *et al.* (2013)). The S/U family of lyases were found to function as monomers, homodimers, or heterodimers. S-type lyase are present in all *Prochlorococcus* sp., being the only lyase found in the HL *Prochlorococcus* ecotype.

T-type lyases are distantly related to the S/U-type lyases and have not been reported to form heterodimers. CpcT forms a homodimer and adopts a calyx-shaped β -barrel fold (Fig. 11; Shen *et al.* (2006), Zhao *et al.* (2007), Zhou *et al.* (2014)). The CpcT lyase from *Nostoc* sp. PCC7120 contributes to the attachment of PCB to β -Cys155 of PC and PEC. On the other hand, the CpcT from *Synechococcus* sp. PCC 7002 has been only detected to attach PCB at PC β -153. Furthermore, T-type group member CpeT from *Fremyella diplosiphon* was recently found by Schluchter's lab. They demonstrated that CpeT alone can bind PEB, but CpeZ, a chaperone-like protein, is needed to correctly and efficiently attach PEB to PE at β -Cys 165 (Nguyen *et al.* (2020)). Similarly, the CpeT found in cyanophage P-HM1 (P-HM1CpeT), can stably bind PEB, but did not show any direct lyase-transferase activity (Gasper *et al.* (2017)). When changing the β -PE subunit to low-light *Prochlorococcus* (SS120CpeB), P-HM1CpeT still could not assist PEB binding to β -155 (unpublished data). It has been suggested that P-HM1CpeT contributes to the *Prochlorococcus* host lyase CpeS in binding PEB to β -Cys 82, but it needs "potential assistance" to perform the holo-PE assembly. When S and T-type lyases activity were evaluated together, only a specific sequential attachment, first at Cys-155 (CpcT working site) and then at Cys-84 (CpcS working site), resulted in the correct product and prior chromophorylation at Cys-84 interfering with the subsequent attachment to Cys-155 (Zhao *et al.* (2007)). Thus, the order in which the lyases work is essential when more than one binding site is present.

Compared with the other two lyase groups, **E/F-type lyases** demonstrate the common feature of forming HEAT-repeat domains, which may be involved in protein-protein interactions. Some homologs of the E/F-type lyase, such as Nb1B, do not have lyase activity, but are rather involved in PBS degradation (Neuwald & Hirano (2000)). According to several E/F-type lyases that have been characterized in the last five years, the E/F family can be divided into two subgroups. One only possesses phycobiliprotein lyase activity, such as the heterodimeric lyase CpcE/F which is required for correct binding of PCB to α -Cys 84 in *Synechococcus* PCC 7002 (Zhou *et al.* (1992), Zhao *et al.* (2017)). Two E/F-type lyases have been confirmed in *Fremyella diplosiphon*, CpeY and CpeZ, forming a heterodimer that attaches PEB at α -82. CpeF was recently seen to perform the attachment of PEB to Cys-48/Cys-59 of CpeB, but only in the presence of the chaperone-like protein CpeZ (Biswas *et al.* (2011) Kronfel *et al.* (2019)). Separated from the above group of lyase, E/F-type lyase isomerase possesses a much more complicated role in the ocean system. They are not only helping the chromophore PCB or PEB to be correctly attached to specific cysteine residues

but also act as an isomerase to PVB or PUB. This could explain why some cyanobacteria strains have the large amount of PUB detected. The first lyase-isomerases catalyzing the attachment of PCB at α -84 of PEC and isomerizing into PVB were PecE and PecF, both found in *Mastigocladus laminosus* (Zhao *et al.* (2000), Zhao *et al.* (2017), Kumarapperuma *et al.* (2022)). MpeU is a phycobilin lyase-isomerase which is present in all *Synechococcus* strains adapted to blue light (Mahmoud *et al.* (2017)), but, as of now it still remains to be biochemically characterized. MpeV and MpeQ were newly detected as lyase-isomerases. MpeV is the only one that can complete the double linkage required for PUB attachment to Cys-50/61 (Carrigee *et al.* (2021)). As for MpeQ, the crystal structure showed two protein molecules in an asymmetric unit (E and F domains), which compound with 23 α -helices that are supercoiled in a right-handed manner (Fig. 11; Kumarapperuma *et al.* (2022)). In the SS120 strain, there are several potential lyases (CpeY, CpeZ, MpeX, Pro1634) belonging to this group. We strongly suspect that they do not only possess lyase functions, but are also involved in the isomerase reaction from PEB or PCB to PUB *in vivo*. Until now, no E/F type lyase was detected in any HL *Prochlorococcus* strains.

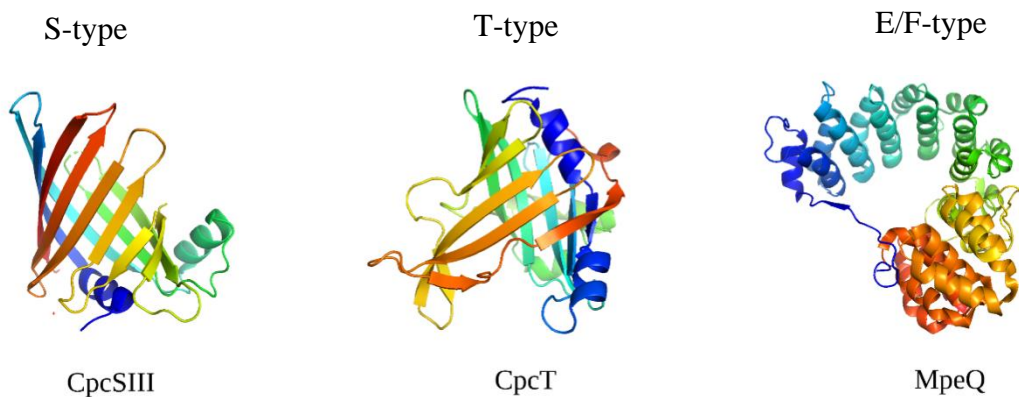


Figure 11. 3D structure of three type of lyases. CpcSIII from *Thermosynechococcus elongatus* (PDB: 3BDR); CpcT from *Nostoc* sp. PCC 7120 (PDB: 4O4O); MpeQ from *Synechococcus* sp. A15-62 (PDB: 7MCH).

Table 1 Summary of phycobiliprotein lyase types

Types	Group	Protein	Organism	Chromophore	Apoprotein specificity
S/U	Group1	CpeS	<i>Fremyella diplosiphon</i>	PEB	Low
		CpeS	<i>Prochlorococcus marinus</i> MED4	PEB	?
		CpeS	<i>Guillardia theta</i>	DHBV and PEB	?
	Group2	CpcS-I/CpcU	<i>Synechococcus</i> sp. PCC 7002	PCB	Low
		CpcS-I	<i>Nostoc</i> sp. PCC7120	PCB	Low
		CpcS-I/CpcU	<i>Arthrospira platensis</i> FACHB314	PCB	?
		CpcS-III	<i>Thermosynechococcus vestitus</i> BP-1	PCB, PEB and PΦB	Low
T		CpcT	<i>Synechococcus</i> sp. PCC7002	PCB	High
		CpcT	<i>Nostoc</i> sp. PCC7120	PCB	Low
		CpeT	<i>Fremyella diplosiphon</i>	PEB	?
		CpeT	Cyanophagen P-HM1	PEB	?
E/F	Lyase	CpcE/CpcF	<i>Synechococcus</i> sp. PCC 7002	PCB	High
		CpeY/CpeZ	<i>Fremyella diplosiphon</i>	PEB	High
		CpeF	<i>Fremyella diplosiphon</i>	PEB	?
		CpeY	<i>Synechococcus</i> sp. RS9916	PEB	High
	Lyase-isomerase	PecE/PecF	<i>Mastigocladus laminosus</i>	PVB	High
		RpcG	<i>Synechococcus</i> sp. WH8102	PUB	High
		MpeZ	<i>Synechococcus</i> sp. RS9916	PUB	High
		MpeV	<i>Synechococcus</i> sp. RS9916	PUB	Low
		MpeQ	<i>Synechococcus</i> sp. A1562	PUB	?

1.3 Objectives of this work

The primary objective of this work is to determine the natural chromophorylation state of PE-III and to investigate how this state is achieved. Since *Prochlorococcus* sp. is not (yet) genetically accessible and large-scale production of biomass for classical biochemical experiments is hard to achieve, we employed a synthetic biology approach to address this problem. The first approach is based on TREX system (transfer and expression of biosynthetic pathways) and the expression of the whole PE cluster including the chromophore biosynthetic genes in *E. coli*. Additionally, we utilized the pDuet™ vector system (Novagen-Merck) to determine the PBP lyases necessary for the chromophorylation of PE-III in parallel. However, we encountered difficulties in conducting *in vitro* experiments with purified proteins, as many PBP lyases were insoluble. Hence, in an *E. coli* expression system, proteins of the PE cluster and biosynthesis proteins were co-produced with multiple lyase candidates to investigate potential covalently binding to bilins.

Another part of this project involved exploring alternative cyanobacteria for the assembly of PE-III. To achieve this, we utilized *Synechococcus* sp. PCC 7002 as the host and biochemically characterized the recombinant product to gain further insights into the system's mechanism.

2. Material and methods

2.1 Materials and chemicals

All chemicals and reagents used in this work were ACS grade or better unless stated otherwise. They were purchased from Sigma-Aldrich (Munich), AppliChem (Darmstadt), Merck (Darmstadt), Carl Roth (Karlsruhe), Fluka (USA) and New England Biolabs (Frankfurt am Main) unless stated otherwise. Solutions for microbial cultivation were autoclaved or filter sterilized prior to use. The glassware was sterilized by dry heat at 180 °C for 3 h.

2.1.1 Equipment

Table 2. Instruments.

Type of instrument	Name	Manufacturer
Autoclave	VX 150	Systec
Blotting system	Semidry Blot Trans-Blot@SD	BioRad
Cell disruption	LM10	Microfluidics
Centrifuges and rotors	Centrifuge 5415D	Eppendorf
	Rotor F-45-24-11	Eppendorf
	5810R	Eppendorf
	Rotor A-4-62	Hermle
	Z32HK	Hermle
	Rotor 12/002	Hermle
Circular dichroism spectrometer	Sorvall LYNX 6000	ThermoFisher
	Rotors T29, F9	ThermoFisher
	Chirscan Plus Spectropolarimeter	Applied Photophysics, Leatherland, UK
Gel documentation	Gel iX20 Imager	Intas
Gel electrophoresis	EasyPhor Mini/Midi	Biozym
Incubator	Innova 44 Incubator Shaker	New Brunswick Scientific
	Innova 2300 Shaker	New Brunswick Scientific
NanoTemper	Nano Temper Tycho NT.6	NanoTemper Technologies
pH meter	Basic pH Meter P-11	Sartorius
SDS-page documentation	HP Scanjet 300	HP
FPLC	Äkta Explorer	GE Healthcare
FPLC columns	UNICORN™ control system	GE Healthcare
	Superdex™ 75 Increase 10/300 GL	Cytiva™
	Superdex™ 200 Increase 10/300 GL	Cytiva™

Freeze dryer	ALPHA 2-4 LSC <i>plus</i>	Christ
HPLC	1100 Series Degasser G1370A Quat pump G1311A DAD	Agilent Technologies
HPLC column	Jupiter® 5 µm C4 300 Å	Phenomenex
HPLC software	Agilent Chem Station	Agilent Technologies
Gel documentation	GeliX20 Imager	Intas
Thermocycler	T1 Thermocycler peqSTAR 2	Biometra VWR
Thermoblock	HB-202 Thermocell ThermoStat plus	Bioer Eppendorf
Ultrasonic homogenizer	UW 2200 with tip KE 76	Bandelin
Ultra-pure water system	MilliQ® Integral Water Purification System	Merck Millipore
Power supply	PowerPac 300	Bio-Rad
Pipettes	Abimed Discovery Comfort Pipetman Eppendorf Research® plus ErgoOne®	HTL Lab Solutions HTL Lab Solutions Gilson Eppendorf Starlab
Scales	AccuLab Research	Sartorius Sartorius
SDS-PAGE electrophoresis	Mini-Protean® Tetra cell System Mini-PROTEAN® 3 Cell	Bio-Rad Bio-Rad
Photometers	Novaspec III NanoDrop™ Lite	Amersham Biosciences Thermo Fisher
Sterile bench	Antares	Biohit
UV-Vis-Spectrometer	8453 UV-Visible System	Agilent
Fluorescence Spectrometer	FP-8300	Jasco
Vacuum pump	Laboport®	KNF
Vortex	Vortex-Schüttler	VWR

2.1.2 Special chemicals, material, enzymes, kits and antibodies

Table 3. Special chemicals and materials.

Type of material	Name	Manufacturer
Centrifugal concentrators	Amicon Ultra 15-50K	Merck Millipore

Chromatography columns	<i>Strep</i> -tactin® Sepharose® TALON® Superflow™ Superdex™ 75 10/300 GL	IBA VWR GE Healthcare
Dialysis tubing	Visking MWCO 14000	Carl Roth
DNA loading dye	DNA Gel Loading Dye Purple (6x)	NEB
DNA size standard	GeneRuler™ DNA Ladder Mix 1kb plus Low molecular weight DNA Ladder	Thermo Fisher NEB
Filter	PTFE 0.2 µm/0.45 µm ø 4 mm	Phenex
Protein size standard	PageRuler™ prestained protein ladder Unstained Protein Standard Blue Prestained Protein Standard	Thermo Fisher NEB NEB
PVDF membrane	Roti®-PVDF-Membrane	Carl Roth
Protein Standards for SEC	lysozyme Albumin Ovalbumin Blue Dextran Carbonic anhydrase	Sigma Aldrich Sigma Aldrich Sigma Aldrich Sigma Aldrich Sigma Aldrich
Sterile filter	Rotilabo® RC, 0.2 µm Rotilabo® RC, 0.45 µm	Carl Roth Carl Roth

Table 4. Enzymes and kits.

Type of material	Name	Manufacturer
cDNA synthesis kit	ProtoScript® II first strand cDNA synthesis kit	New England Biolabs
Alkaline phosphatase	Shrimp Alkaline Phosphatase (rSAP)	New England Biolabs
DNase I	DNase I (RNase-free)	New England Biolabs
DNA ligase	T4 DNA Ligase	Thermo Fisher
DNA Polymerase	Phusion High-Fidelity DNA Pfu DNA polymerase Q5 High-Fidelity DNA polymerase	Thermo Scientific homemade New England Biolabs
Restriction endonucleases	Restriction endonucleases or high fidelity endonucleases (HF®-line)	New England Biolabs
gDNA isolation kit	NucleoSpin® Microbial DNA Mini kit	Macherey-Nagel
Lysozyme	Lysozyme	Carl Roth
PCR clean-up kit	NucleoSpin® Gel and PCR Clean-up	Macherey-Nagel
Plasmid miniprep kit	NucleoSpin® Plasmid EasyPure	Macherey-Nagel
Restriction endonucleases	FastDigest restriction nucleases	Thermo Scientific

RNase inhibitor	RNase Inhibitor (Human Placenta)	New England Biolabs
RNA isolation kit	Quick-RNA Miniprep kit	Zymo Research

Table 5. Antibodies for Western Blot analyses.

Antibody	Dilution	Antigen	Manufacturer
Anti-6xHis-tag antibody (mouse)	1:3000	His ₆ -tag (1.AK)	Thermo Scientific
Anti-Mouse IgG AP conjugate	1:10000	His ₆ -tag (2.AK)	Sigma Aldrich
Anti Streptacin-AP conjugate	1:4000	<i>StrepII</i> -tag	IBA Lifesciences GmbH
β-PE rabbit IgG, against whole protein	1:1000	β-PE (<i>Prochlorococcus</i>)	(Hess and Partensky, 1999)
Anti-Rabbit IgG Ap conjugate	1:30000	β-PE (2.AK)	Sigma Aldrich
Anti-beta-PE rabbit IgG	1:20000	Native holo-CpeB (<i>Fremyella diplosiphon</i>)	(Kronfel <i>et al.</i> , 2019)

2.1.3 Bacterial strains

Table 6. *E. coli* strains.

Strain	Genotype	Reference
<i>E. coli</i> DH5α	F ⁺ <i>supE44D(argF-lac) U169 j80dlacZ ΔM15 hsdR17 recA1 endA1 gyrA96 thi-1 relA1</i>	Sambrook <i>et al.</i> , 1989
<i>E. coli</i> BL21 (DE3)	F ⁺ <i>ompT gal dcm lon hsdS_B(r_B⁻m_B⁻) λ(DE3 [lacI lacUV5-T7p07 ind1 sam7 nin5]) [malB⁺]_{K-12}(λ^S)</i>	Studier and Moffatt, 1986

Table 7. *Synechococcus* strains.

Strain	Features	Reference
<i>Synechococcus</i> sp. PCC 7002	Growth in medium A ⁺	Donation of Gen Enomoto, Albert-Ludwigs-Universität Freiburg
<i>Synechococcus</i> sp. PCC 7002 glycerol tolerant	Growth in medium A ⁺ with 10 mM glycerol	This study
<i>Synechococcus</i> sp. PCC 7002 pAQ1::GFP	pAQ1GFP plasmid insert, Growth in medium A ⁺	This study
<i>Synechococcus</i> sp. PCC 7002 pAQ1::cpeBA	<i>cpeBA</i> fragment inserted from <i>P. marinus</i> SS120, Growth in medium A ⁺	This study
<i>Synechococcus</i> sp. PCC 7002 pAQ1::cpeBA glycerol tolerant	<i>cpeBA</i> fragment inserted from <i>P. marinus</i> SS120, Growth in medium A ⁺ with 10 mM glycerol	This study

2.1.4 Plasmids

Table 8. Used plasmids.

Plasmid	Features	Affinity-tag	Reference
pIC20H-RL	Expression cluster empty vector, Amp ^R	No tag	Loeschcke <i>et al.</i> , 2013
pTREX- <i>PE</i>	pIC20H-RL derivate carrying PE cluster with RBS from <i>P. marinus</i> SS120, Amp ^R	No tag	This study
pTREX- no rbs <i>PE</i>	pIC20H-RL derivate carrying PE cluster from <i>P. marinus</i> SS120, Amp ^R	No tag	This study
pSAQSTflag- <i>sfgfpt</i>	Modified pAQ1 plasmid from <i>Synechrococcus</i> 7002, GFP insert, Sm ^R	N-term FLAG tag	Donation of Gen Enomoto, Albert-Ludwigs-Universität Freiburg
pAQ1- <i>cpeBA</i>	<i>cpeBA</i> fragment modified from <i>P. marinus</i> SS120, Sm ^R	N-term FLAG tag CpeB; C-term His tag CpeA	This study
pAQ1-rbs- <i>cpeBA</i>	<i>cpeBA</i> fragment modified from <i>P. marinus</i> SS120, Sm ^R	N-term FLAG tag CpeB; C-term His tag CpeA	This study
pTDho1 <i>pebS</i>	pACYCDuet1 vector; <i>pebS</i> and <i>ho1</i> modified from Cyanophage P-SSM2, Cm ^R	N-term His-tag <i>PebS</i> ; C-term S-Tag <i>Ho1</i>	T. Dammeyer, 2008
pTDho1 <i>pebS</i> (no His)	pACYCDuet1 vector; <i>pebS</i> and <i>ho1</i> modified from Cyanophage P-SSM2, Cm ^R	C-term S-Tag <i>Ho1</i>	This study
pTDho1 <i>pcyA</i>	pACYCDuet1 vector; <i>pcyA</i> modified from P-SSM4; <i>ho1</i> modified from Cyanophage P-SSM2, Cm ^R	N-term His-tag <i>PcyA</i> ; C-term S-Tag <i>Ho1</i>	T. Dammeyer, 2008
pTDho1 <i>pcyA</i> (no His)	pACYCDuet1 vector; <i>pcyA</i> modified from P-SSM4; <i>ho1</i> modified from Cyanophage P-SSM2, Cm ^R	C-term S-Tag <i>Ho1</i>	This study
pTDho1 <i>pubS</i> (no tag)	pACYCDuet1 vector; <i>Physcomitrella patens</i> phycourobilin synthase (PUBS) mRNA; <i>ho1</i> modified from Cyanophage P-SSM2, Cm ^R	C-term S-Tag <i>Ho1</i>	This study
pETDuet1- <i>cpeA</i>	pETDuet1 vector; <i>cpeA</i> modified from <i>P. marinus</i> SS120, Amp ^R	N-term His-tag	C. Scholte, 2008
pETDuet1- <i>cpeA</i> (L102 Q)	pETDuet1 vector; <i>cpeA</i> modified from <i>P. marinus</i> SS120, Amp ^R	N-term His-tag	This study
pETDuet1- <i>cpeB</i>	pETDuet1 vector; <i>cpeB</i> modified from <i>P. marinus</i> SS120, Amp ^R	N-term His-tag	C. Scholte, 2008

pETDuet-1- <i>cpeB</i> (L109 F)	pETDuet1 vector; <i>cpeB</i> modified from <i>P. marinus</i> SS120, Amp ^R	N-term His-tag	This study
pETDuet-1- <i>cpeB</i> (L109 F)- <i>cpeZ</i>	pETDuet1 vector; MCS1 <i>cpeB</i> and MCS2 <i>cpeZ</i> modified from <i>P. marinus</i> SS120, Amp ^R	N-term His-tag CpeB	This study
pETDuet-1- <i>cpeA</i> (L102 Q)- <i>cpeB</i> (L109 F)	pETDuet1 vector; MCS1 <i>cpeA</i> and MCS2 <i>cpeB</i> modified from <i>P. marinus</i> SS120, Amp ^R	N-term His-tag CpeA N-term His-tag CpeB	This study
pCDFDuet-1- <i>cpeS</i>	pCDFDuet1 vector; MCS1 <i>cpeS</i> modified from <i>P. marinus</i> SS120, Sm ^R	No tag	This study
pCDFDuet-1- 1 <i>cpeT</i> _{SS120}	pCDFDuet1 vector; MCS1 <i>cpeT</i> modified from <i>P. marinus</i> SS120, Sm ^R	No tag	This study
pCDFDuet-1- 2 <i>cpeT</i> _{SS120}	pCDFDuet1 vector; MCS2 <i>cpeT</i> modified from <i>P. marinus</i> SS120, Sm ^R	No tag	This study
pCDFDuet-1- 2 <i>ScpeT</i> _{SS120}	pCDFDuet1 vector; MCS2 <i>cpeT</i> modified from <i>P. marinus</i> SS120, Sm ^R	C-term S-tag	This study
pCDFDuet-1-2 <i>cpeT</i> _{P-HM1}	pCDFDuet1 vector; MCS2 <i>cpeT</i> modified from Cyanophagen P-HM1, Sm ^R	No tag	This study
pCDFDuet-1- <i>cpeS</i> - <i>cpeT</i> _{SS120}	pCDFDuet1 vector; MCS1 <i>cpeS</i> and MCS2 <i>cpeT</i> modified from <i>P. marinus</i> SS120, Sm ^R	CpeT, C-term S-tag	This study
pCDFDuet-1- <i>cpeS</i> - <i>cpeT</i> _{P-HM1}	pCDFDuet1 vector; MCS1 <i>cpeS</i> modified from <i>P. marinus</i> SS120 and MCS2 <i>cpeT</i> modified from Cyanophagen P-HM1, Sm ^R	No tag	This study
pCold TF- <i>cpeT</i>	pCold TF vector; <i>cpeT</i> modified from <i>P. marinus</i> SS120, Amp ^R	N-term His-tag	This study
pRSFDuet-1- <i>mpeX</i>	pRSFDuet1 vector; MCS1 <i>mpeX</i> from <i>P. marinus</i> SS120, Kan ^R	C-term Strep-Tag II	J. Hackh, 2022
pRSFDuet-1- <i>pro1634</i>	pRSFDuet1 vector; MCS2 <i>pro1634</i> from <i>P. marinus</i> SS120, Kan ^R	No tag	This study
pRSFDuet-1- <i>pro1634S</i>	pRSFDuet1 vector; MCS2 <i>pro1634</i> from <i>P. marinus</i> SS120, Kan ^R	C-term S-Tag	J. Hackh, 2022
pRSFDuet-1- <i>mpeX</i> - <i>pro1634S</i>	pRSFDuet1 vector; MCS1 <i>mpeX</i> from <i>P. marinus</i> SS120; MCS2 <i>pro1634</i> from <i>P. marinus</i> SS120, Kan ^R	C-term Strep-Tag II MpeX, C-term S-Tag Pro1634	J. Hackh, 2022

pCOLADuet-1- <i>cpeZ</i>	pCOLADuet1 vector; MCS2 <i>cpeZ</i> from <i>P. marinus</i> SS120, Kan ^R	N-term Strep-Tag II	This study
pCOLADuet-1- <i>cpeY</i>	pCOLADuet1 vector; MCS1 <i>cpeY</i> from <i>P. marinus</i> SS120, Kan ^R	N-term Strep-Tag II	This study
pCOLADuet-1- <i>cpeY</i> - <i>cpeZ</i>	pCOLADuet1 vector; MCS1 <i>cpeY</i> from <i>P. marinus</i> SS120; MCS2 <i>cpeZ</i> from <i>P. marinus</i> SS120, Kan ^R	N-term Strep-Tag II CpeY N-term Strep-Tag II CpeZ	This study

2.1.5 Oligonucleotides

Oligonucleotides for PE cluster

Table 9. Oligonucleotides for the PE cluster.

No.	Name	Sequence 5' – 3'	Construction of plasmid
1	APE1fw	GTCGACTCTAGAATGCTTGATGCATTCTCAAG	pTREX- <i>PE</i>
2	APE1rv	CAAGTCTTCCCAGGACCTCTATAGCCTTTC	pTREX- <i>PE</i>
3	APE2fw	CTGGGAAGACTTGGCTGTAAAAAAGCAATCAC	pTREX- <i>PE</i>
4	APE2rv	GTGGGGATCCTCTAGTATGAAGACTAGCAAAG	pTREX- <i>PE</i>
5	pAQ1fw	GATTATAAAGATGATGATGATAAAATGCTTGATGCA TTCTCAAGAGCAG	pAQcpe <i>BA</i>
6	pAQ1rv	CGTCAGTGGTGATGATGGTGATGAGCCAAGGCATTA ATAA	pAQcpe <i>BA</i>
7	pAQ2fw	CTCATCACCATCATCACCCTGACGCAGAAGCG	pAQcpe <i>BA</i>
8	pAQ2rv	CTTCCTGTTTTTGCTCACCCAGAAACGCTGGTGAAA GTAAA	pAQcpe <i>BA</i>
9	pAQ3fw	GTTTCTGGGTGAGCAAAAACAGGAAGGCAAAAATG	pAQcpe <i>BA</i>
10	pAQ3rv	GAATGCATCAAGCATTTTATCATCATCATCTTTATAA TCAATATCATG	pAQcpe <i>BA</i>
11	PE RBSfw	ATGCCTGCAGGTCGACTAAGGAGGCTTCATCATGCTTGA TGC	pTREX-rbs <i>PE</i>
12	PE RBSrv	ATAGGAGTGGGGATCCTAGGAGGCTTCATCATGAAGAC TAGC	pTREX-rbs <i>PE</i>
13	pAQSQfw	AGAAGAAGATCGCTTGGC	sequencing
14	pAQSQrv	CCCATCTGTGCATAAGAG	sequencing

Oligonucleotides for RNA

Table 10. Oligonucleotides for RNA isolation.

No.	Name	Sequence 5' – 3'
1	rpeBfw	CCACTAGAAGGATGGCAGCT
2	rpeB rv	AGCTCCTGACCCTGAATTGA
3	rpeAfw	AGGGGTCTTTTGATAGGGCT
4	rpeArv	CCAGCTTGCTGACCCATATC
5	rpeZfw	TCAGCGCTTGTTGATGAATCT
6	rpeZrv	TGGCTTGTATTGCAGCATCC
7	rpeYfw	CCTGGGAAGACTTGGCTGTA
8	rpeYrv	AGCAGCTCCTTTAACTCCTGA
9	rpecfw	TCCAATGGAAAGCGAACGTC
10	rpecrv	AGGGTGAATTCCAGTGCCTT
11	rpeSfw	TGGGGATTGAGGAGTTTGTC
12	rpeSrv	TCCAGTTTACTCCCCAGAC
13	rpeTfw	ACAGGCAAGCGGTACATAGA
14	rpeTrv	TCATCTTCTTCAGACTGCCTCT
15	rpeFfw	TGGGCCAGCATCTATACCTG
16	rpeFrv	ATTCAATCGCATGTTCGCCA
17	rmpeUfw	TGGCTTCAATTTGCACCTCA
18	rmpeUrv	TCGGAGATGCAATGTGGTCT
19	rblafw	GGTCGCCGCATACACTATTC
20	rblarv	CTGCAACTTTATCCGCCTCC

Oligonucleotides for cloning

Table 11. Oligonucleotides for Duet system cloning.

No.	Name	Sequence 5' – 3'	Construction of plasmid
1	cpeBfw	GATATACATATGCATCACCATCATCAC	pET <i>cpeB</i>
2	cpeBrv	CTCGAGGGTACCTCAATTTAAAG	pET <i>cpeB</i>
3	pro1634fw	GGAGATATACATATGAAAGAAGATCGC	pRSFDuet-1- <i>pro1634</i>
4	pro1634rv	GTGGGGATCCTCTAGTATGAAGACTAGCAA AG	pRSFDuet-1- <i>pro1634</i>
5	cpeYfw	GAGATATACCATGGATGGCTAGCTGG	pCOLADuet-1- <i>cpeY</i>
6	cpeY1rv	TTATGCGGCCGCAAGCTTTTATATCA	pCOLADuet-1- <i>cpeY</i>
7	cpeZfw	GCAGATCTCAATTGTATGGCTAGCTGGA	pCOLADuet-1- <i>cpeZ</i>
8	cpeZrv	GTACCGACGTCTAATCAAGGATATTAGTT TCC	pCOLADuet-1- <i>cpeZ</i>

9	cpeSfw	GAGATATAACCATGGGGATTGAGG	pCDFDuet-1- <i>cpeS</i>
10	cpeSrv	GCCGCAAGCTTTTATTCTCTATAG	pCDFDuet-1- <i>cpeS</i>
11	cpeTfw	GGAGATATACATATGAGCTTTAAAGAAAGT C	pCDFDuet-1- <i>cpeT_{SS120}</i>
12	cpeTrv	ACCAGACTCGAGTTATTTGG	pCDFDuet-1- <i>cpeT_{SS120}</i>
13	PHM1cpeTfw	GAAGGAGATATACATATGATAGATAAATTT TG	pCDFDuet-1- <i>cpeT_{P-HM1}</i>
14	PHM1cpeTrv	CAGACTCGAGTTATACATTCTTTTTG	pCDFDuet-1- <i>cpeT_{P-HM1}</i>
15	pebSfw	GAGATATAACCATGGGCATGACTAAAAAC	pTD <i>holpebS</i> (no His-tag)
16	pebSrv	CATTATGCGGCCGCTCATTTG	pTD <i>holpebS</i> (no His-tag)
17	QCcpeBfw	GTAAGTTATGCATTGTTTCGCAGGTGACCCA TC	pETDuet-1- <i>cpeB</i> (L109 F)
18	QCcpeBrv	GATGGGTCACCTGCGAACAATGCATAACTT AC	pETDuet-1- <i>cpeB</i> (L109 F)
19	QCcpeAfw	GATAAACTATTGCCAGGTTACTGGAGGCAC	pETDuet-1- <i>cpeA</i> (L102 A)
20	QCcpeArv	GTGCCTCCAGTAACCTGGCAATAGTTTATC	pETDuet-1- <i>cpeA</i> (L102 A)
21	QCcpeTfw	GAAGAAGCCAAAGAACTCGAGTCTG	pCDFDuet-1- <i>ScpeT_{SS120}</i>
22	QCcpeTrv	CAGACTCGAGTTCTTTGGCTTCTTC	pCDFDuet-1- <i>ScpeT_{SS120}</i>
23	QCpubSfw	GATATAACCATGGCTTCCATTGTGTC	pTD <i>holpubS</i> (no His-tag)
24	QCpubSRV	GACACAATGGAAGCCATGGTATATC	pTD <i>holpubS</i> (no His-tag)
25	QCpcyAfw	GGAGATATAACCATGGGCATGATTGTTGATG	pTD <i>holpcyA</i> (no tag)
26	QCpcyArv	CATTATGCGGCCGCTCACAGGTTG	pTD <i>holpcyA</i> (no tag)

2.2 Microbiological methods

2.2.1 Preparation of chemically competent *E. coli* cells

Competent bacterial cells can incorporate external DNA molecules. The ability to transform *E. coli* strains with extrinsic DNA is a powerful molecular tool to achieve specific features. Usually, *E. coli* cells are not competent, therefore they were treated chemically to become competent.

E. coli cells were made chemically competent with CaCl₂. 100 ml LB medium with appropriate antibiotics and supplements was inoculated 1:100 with an overnight pre-culture. Cells were incubated at 37 °C around 2-2.5h and 180 rpm to an OD₅₇₈ of 0.5. The culture was centrifuged at 4000 rpm for 10 min at 4 °C (Centrifuge 5810 R, Eppendorf, rotor A-4-6). The supernatant was discarded, and the cell pellet was resuspended in 50 ml cold 50 mM CaCl₂ in H₂O_{dest.} Afterwards, the cells were incubated on ice for at least 45 min, followed by a further centrifugation step at 4000 rpm for 10 min at 4 °C (Centrifuge 5810 R, Eppendorf, rotor A-4-6). The pellet was resuspended in 5 ml 50 mM CaCl₂ with 15 % (v/v) glycerol. The competent cells were aliquoted to 200 µl, frozen with liquid nitrogen and stored at -80 °C.

2.2.2 Transformation of chemically competent *E. coli* cells

To transfer DNA into chemically competent cells an aliquot of 200 µl competent cells was thawed on ice and 50-100 ng of plasmid DNA or 10 µl of a ligation reaction was added. The cell-plasmid-mix was gently inverted and further incubated on ice for 30 min. A heat shock was performed incubating the mix at 42 °C for 1 min. Afterwards, the mix was kept on ice for 1 min and 700 µl LB was added before incubation at 37 °C, 160 rpm (Innova 2300 Shaker) for at least 1 h. Subsequently, cells were plated on selective agar plates and incubated at 37 °C overnight. To generate *E. coli* strains that carry two or more plasmids, the cells were first transformed with one plasmid and chemically competent cells were prepared using the transformed cells. Then, the second plasmid was transferred into the cells by transformation.

2.2.3 Culture media and supplements for *E. coli* cultures

For the cultivation of *E. coli* Luria Bertani (LB) medium was used with appropriate antibiotics and supplements. To produce cultivation plates 1.5 % (w/v) Agar-Agar was added before autoclavation. The cultivation media were autoclaved for 20 min at 121 °C with a pressure of 2 bar. All supplements were filtrated (pore size 0.2 µM) and added after autoclaving to the respective cooled-down media.

LB-medium (Lennox)
 LB-Medium 20 g/l
 (Lennox), Braun
 In Aqua dest.

LB-Agar
 LB-Medium
 Agar-Agar 15 g/l

Table 12. Media supplements.

Supplement	Dissolve in	Stock concentration	Final concentration
Ampicillin (Amp)	Aqua dest.	100 mg/ml	50-100 µg/ml
Kanamycin (Km)	Aqua dest.	50 mg/ml	25-50 µg/ml
Spectinomycin (Spc)	Aqua dest.	50 mg/ml	25-50 µg/ml
Chloramphenicol (Cmp)	70 % EtOH	34 mg/ml	17-34 µg/ml
Gentamycin (Gm)	Aqua dest.	10 mg/ml	10 µg/ml
Tetracycline	70 % EtOH	10 mg/ml	10 µg/ml
Isopropyl-β-D-	Aqua dest.	1 M	0.1-0.5 mM
Anhydrotetracyclin (AHT)	70 % EtOH	2 mg/ml	200 ng/ml

2.2.4 Storage of *E. coli* cells

For short-term storage (not longer than one week), *E. coli* cells were streaked out on LB agar plates and kept at 4 °C. For long-term storage, an *E. coli* overnight culture was diluted with sterile 86 % (v/v) glycerol to a final glycerol concentration of 40 % (v/v) and stored at -80 °C.

2.2.5 Cultivation of *E. coli* cells

E. coli pre-cultures were grown overnight at 37 °C, 160 rpm (Innova 2300 Incubator Shaker) in LB media containing flasks with specific antibiotics (1:1000). The following day the pre-culture was used to inoculate the main growing culture in a ratio of 1:100. The cultures were incubated at 37 °C and 100 rpm (Innova 44 Incubator Shaker) to an OD_{578nm} of ~ 0.4-0.6. Gene expression was induced after a construct specific reduction of the temperature.

For cultivation on agar-plates, 100-200 µl of pre-culture were spread on a solid agar-plate with respective antibiotics (1:1000 dilution) and incubated at 37 °C.

2.2.6 Determination of *E. coli* cell density

E. coli cell densities in liquid cultures were determined by measuring the optical density at 578 nm using the cultivation medium as reference.

2.2.7 Culture media and supplements for *Synechococcus* sp. PCC 7002 cultures

Medium A⁺ was prepared starting from five different stock solutions (Table 13-17). All solutions were kept at 4 °C. Stock Solution 1 (Table 13) need to be diluted of two-folds before refrigerating to avoid precipitation. The final media was made mixing 2 ml of 2xdil stock solution 1, 10 ml of stock solution 2, 100 ml of stock solution 3, 10 ml of stock solution 4, 10 ml of stock solution 5 and filled with H₂O_{dest} to 1 liter. 0.4 mg/ml Vitamin B12 (Cyanocobalamin), previously filter-sterilized and stored at -20 °C, was added to the media before usage (10 µl per liter medium). Growth on agar plate was obtained by mixing in a 1:1 to ratio 2x Medium A⁺ and 1.5 % Bacto agar in the sterile bench. If necessary, proper antibiotics were added before pouring around 30 ml of the media per Petri dish.

Table 13. Stock 1 for Medium A⁺.

Chemical	Amount (g)	Remarks
FeCl ₃ 6H ₂ O	3.89	deliquescent
H ₃ BO ₃	34.3	Boric acid
MnCl ₂ 4H ₂ O	4.3	
ZnCl ₂	0.315	toxic
MoO ₃	0.03	H ₂ MoO ₄
CuSO ₄ 5H ₂ O	0.003	toxic
CoCl ₂ 6H ₂ O	0.0122	
Milli Q		to 1 L

Table 14. Stock 2 for Medium A⁺.

Chemical	Amount (g)	Remarks
Tris	100	deliquescent
Hcl	0.0122	to pH8.2
Milli Q		to 1 L

Table 15. Stock 3 for Medium A⁺.

Chemical	Amount (g)	Remarks
kH ₂ PO ₄	0.5	
NaNO ₃	10	
MgSO ₄	24.4	heptahydrate: 50
NaCl	180	
KCl	6	
Milli Q		to 1 L

Table 16. Stock 4 for Medium A⁺.

Chemical	Amount (g)	Remarks
Na ₂ EDTA	0.3	
Milli Q		to 100 mL

Table 17. Stock 5 for Medium A⁺.

Chemical	Amount (g)	Remarks
CaCl ₂	2.8	dihydrate: 3.7 g
Milli Q		to 100 mL

2.2.8 Storage of *Synechococcus* sp. PCC 7002 cultures

Cultures maintained on agar plates were re-streaked every month to maintain the culture, and DMSO (5 %) stocks were stored at -80 °C.

2.2.9 Transformation of *Synechococcus* sp. PCC 7002

An exponentially growing culture (OD₇₃₀ = 1.0-1.5) of *Synechococcus* sp. PCC 7002 was obtained at 37 °C in liquid medium A⁺ after about 1 to 3 days. 1 µg linearized transformation cassette DNA was mixed with 1.5 ml of the fresh liquid culture in 2 ml sterile fraction and shaking overnight at 37 °C. Negative control was prepared without the addition of linearized DNA. After the overnight incubation, the cells were concentrated by centrifugation for 1 min at 1,500 × g. Most of the cleared medium was removed and the remaining cell suspension was spread over a A⁺ media plate containing the appropriate antibiotic. The plate was sealed with parafilm and incubated at 30 °C for about 15-20 days, until colonies appeared.

2.2.10 Cultivation of *Synechococcus* sp. PCC 7002 cells

Synechococcus sp. PCC 7002 cultures were grown in medium A⁺, with the appropriate antibiotics if needed, in an Innova 2300 shaking incubator equipped with photosynthetic light bank. *Synechococcus* sp. PCC 7002 was incubated at 30 °C, shaken at 150 rpm and an average of 60 µmol photons m⁻² s⁻¹ of continuous light intensity.

2.2.11 Determination of *Synechococcus* sp. PCC 7002 cell density

Synechococcus sp. PCC 7002 cell densities in liquid cultures were determined by measuring the optical density at 730 nm using the cultivation medium as reference.

2.2.12 Cultivation of *Prochlorococcus marinus* SS120

For laboratory cultivation of *Prochlorococcus*, media PCRS11-Red sea was designed by Station Biologique de Roscoff. The cultivation of *P. marinus* is extremely demanding and requires the utmost care, a high degree of purity of the chemicals used and the avoidance of any contamination. All glass stock solution bottles used in the preparation of the medium were previously soaked in 1 M hydrochloric acid and sterilized. Cultures were grown at 22-24 °C in plastic bottles under 16 h light/ 8 h dark cycle with white light intensities around 10 $\mu\text{mol quanta m}^{-2} \text{s}^{-1}$. Cultures were diluted with 5 parts of fresh media every three weeks.

2.3 Molecular biological techniques

2.3.1 Preparation of plasmid DNA

Preparation of plasmid DNA was performed using the NucleoSpin® Plasmid EasyPure kit (Macherey Nagel). 5 ml of LB-medium with corresponding antibiotics were inoculated with a single colony and incubated overnight at 37 °C and 180 rpm (Innova 2300 Platform Shaker, New Brunswick Scientific). To harvest the cells, 4 ml of the culture was centrifuged at 13,000 rpm for 3 min (Centrifuge 5415D, rotor: F45-24-11, Eppendorf). The plasmid DNA was isolated according to the manufacturer's instructions. Prepared plasmids were controlled by agarose gel electrophoresis and stored at -20 °C.

2.3.2 Preparation of genomic DNA from *P. marinus* SS120

For isolation of genomic DNA from *P. marinus* SS120 50 ml of culture (donation from Dr. Claudia Steglich, University of Freiburg) was centrifuged for 10 min at 10000 x g. The supernatant was discarded and the pellet was dissolved in 150 μl 50 mM Tris/HCl buffer, pH 7.0. Further DNA preparation was performed according to the manufacturer's instructions of the NucleoSpin® Microbial DNA Mini kit for DNA from microorganisms (Macherey-Nagel). Extracted genomic DNA was then used as a template for PCR.

2.3.3 Preparation of RNA from *E. coli*

In order to isolate total RNA from *E. coli* for expression analysis, 50 ml cultures were incubated at 37 °C and 180 rpm (Innova 2300 Platform Shaker, New Brunswick Scientific) until $\text{OD}_{578} = 0.5-0.6$, then cooled down to 25 °C before adding 0.5 mM IPTG and shaking for 3 h. The growth was stopped by adding 5 ml of ice-cold RNA stop solution (5 % buffered phenol in EtOH) to the culture.

Cells were pelleted at 4000 rpm for 10 min and 4 °C (Centrifuge 5810 R, rotor: A-4-6, Eppendorf) in 50 ml falcon tubes. After discarding the supernatant, the pellet was immediately frozen with liquid nitrogen and stored at -80 °C. For RNA isolation, the Quick-RNA™ Miniprep kit (Zymo Research) with an on-column DNase I digestion was used according to the manufacturer's instructions. The pellet was lysed in 600 µl lysis buffer and vortexed twice. The elution was performed with 50 µl nuclease-free water to enhance the final RNA concentration. RNA isolation was tested via agarose gel electrophoresis and PCR to verify the absence of DNA. For the test PCR, primer amplifying the 400 bp *bla* gene was used. In this reaction, genomic DNA (gDNA) served as a positive control. RNA concentration was measured using NanoDrop™ Lite Spectrophotometer (Thermo Fisher).

2.3.4 Reverse Transcription

During a reverse transcription reaction, a RNA-dependent DNA polymerase (reverse transcriptase) synthesises DNA copies of an RNA molecule (complementary DNA, cDNA). Extracted RNA (see 2.3.3) was reverse transcribed into first-strand cDNA with the help of the NEB Standard Protocol #M0368 (New England BioLabs) and its components. First 1000 ng of the RNA sample was mixed with 2 µl Random Primer Mix (60 µM), 2 µl dNTPs (10 mM) in a total volume of 20 µl in nuclease-free H₂O. The RNA-primer mix was then denatured for 5 min at 65 °C to get rid of secondary structures and put promptly on ice. Then, the following components were added: 8 µl 5x ProtoScript II Buffer, 4 µl dithiothreitol (DTT) (0.1 M), 1 µl ProtoScript II RT (200 U/ µl), 0.4 µl RNase inhibitor (40 U/ µl) and 6.6 µl nuclease-free H₂O. This 40 µl cDNA-synthesis reaction was incubated first at 25 °C for 5 min (recommended for Radom Primer Mix usage), followed by the incubation at 42 °C for 1 h. After that, the enzymes were inactivated at 65 °C for 20 min. The samples were cleaned up using the NucleoSpin® PCR Clean-up kit according to manufacturer's instructions (Macherey and Nagel) and the concentration was measured using the NanoDrop™ Lite photometer (Thermo Fisher). Purified cDNA was used as a template for fragment amplification.

2.3.5 Determination of DNA and RNA concentration in aqueous solution

The concentration of double-stranded DNA (dsDNA), single-stranded DNA (ssDNA) and RNA were determined by the NanoDrop™ Lite photometer (Thermo Fisher). The absorbance was measured at 260 nm. The purity of the samples was determined by the comparison of the absorbance at 260 nm (A₂₆₀) and 280 nm (A₂₈₀). For DNA an A₂₆₀/A₂₈₀ ratio of ~1.8 and for RNA an A₂₆₀/A₂₈₀ ratio of ~2.0 was accepted as sufficiently pure.

2.3.6 Agarose gel electrophoresis

Agarose gel electrophoresis was performed to separate DNA fragments according to their size. Negatively charged DNA migrates in the electric field from the cathode to the anode. The migrated distance correlates with the size of the DNA. Agarose (1 % w/v) was dissolved in 1x TAE buffer and heated until clearance of the solution. Gels were poured and sample spacers were added until the gel polymerized. Samples were mixed with 6x loading dye and separated in an electrophoresis chamber (100 V) and stained using an ethidium bromide bath (0.05 % (v/v)). Ethidium bromide intercalates with double-stranded DNA and enhances the intensity of DNA fluorescence. Visualization of the samples was achieved via fluorescence excitation with UV light and documented via a GelDoc (Intas).

50x TAE buffer

Tris/acetate pH 8.0	2 M
EDTA	50 mM

2.3.7 Polymerase chain reaction

The amplification of DNA was conducted via the polymerase chain reaction (PCR). Respective complementary oligonucleotides (primers) to the template DNA were used to start the reaction and to define the range of amplification. A thermocycler was used for the respective heat-regulated reaction steps. First, the double-stranded DNA was denatured at 95°C (denaturation step) allowing the annealing of the primers at 50-65°C (annealing step). This results in the hybridization of the primer with the complementary template DNA. The extension of the hybridized primer-DNA was performed with a thermostable DNA polymerase (elongation step). Specificity of the PCR was achieved by the choice of the primers in combination with the annealing temperature. The PCRs in this work were performed using the *Phusion*®-HF polymerase.

PCR-reaction

Template	10 ng
5x Phusion HF Buffer	10 µl
dNTPs	0.2 mM each
Forward Primer	0.5 µM
Reverse Primer	0.5 µM
Phusion HF DNA Polymerase	1 U
H ₂ O	ad 50 µl

Table 18. PCR thermal-cycling program.

Cycle step	Temperature	Duration	
Initial Denaturation	98°C	30 s	
Denaturation	98°C	10 s	} 30 cycles
Annealing	Primer specific	20 s	
Elongation	72°C	30 s/kb	
Final Elongation	72°C	420 s	

2.3.8 Purification of PCR products

PCR products were purified by using the NucleoSpin® Gel and PCR Clean-up kit (Macherey-Nagel) according to manufacturer's instructions.

2.3.9 Restriction of DNA

Restriction of DNA was carried out using FastDigest enzymes (Thermo Fisher) according to manufacturer's instructions. Plasmid digestion was achieved using the 10x FD White Buffer in an approach with a total volume of 20 µl, whereas test restriction were performed using 10x Green buffer in a total volume up to 10 µl. The reactions were incubated for 20 min at 37 °C. Inactivation of the restriction enzymes was achieved by incubating the samples at 65 °C for 10-25 min depending on the restriction enzyme used.

2.3.10 Gel extraction of DNA fragments

Digested DNA was subjected to an agarose gel electrophoresis and the corresponding band was cut out from the gel. The DNA was extracted using the NucleoSpin® Gel and PCR Clean-up Kit (Macherey Nagel) according to manufacturer's instructions.

2.3.11 Ligation of DNA fragments

The ligation of DNA fragments was carried out by using T4 DNA Ligase (Thermo Fisher). For the ligation reaction, 100 ng of vector DNA was incubated with a 3-fold molar excess of insert DNA. The reaction was performed in a total volume of 20 µl for 1 h at room temperature. The T4 DNA Ligase was inactivated for 5 min at 70 °C. Later, the mixture was transformed in *E. coli* DH5α cells.

Ligation reaction

Vector DNA	100 ng
Insert DNA	3-fold molar excess to vector
10x T4 DNA Ligase buffer	2 μ l
T4 DNA Ligase	5 U
H ₂ O	ad 20 μ l

2.3.12 Sequencing of DNA

For sequencing 2 μ l 50-100 ng/ μ l plasmid-DNA was mixed with 5 μ l of the appropriate primer (5 μ M). Sequencing was conducted by Eurofins Genomics (Ebersberg).

2.3.13 Site-directed mutagenesis

Site-directed mutagenesis was performed to substitute amino acids by generating point mutations in the coding DNA sequence via the use of specific primers. Primers were designed containing the respective bases that should be substituted. Upon the amplification via PCR this results in an in-frame point mutation that changes the base triplet encoding a specific amino acid to an alternate amino acid. First, to gain a higher amount of amplified DNA, two separate PCRs were performed employing the *Phusion*[®]-HF polymerase: one reaction mix only contained the forward and the other only the reverse primer (Table 19-20). Afterwards the two separate amplifications were mixed with 1 U polymerase, and a second PCR was performed (Table 21).

Table 19. Reaction mix for the first PCR.

Components	Mix A	Mix B
H ₂ O	35 μ l	35 μ l
5x buffer HF	10 μ l	10 μ l
Template	1 μ l	1 μ l
Primer forward	2.5 μ l	-
Primer reverse	-	2.5 μ l
dNTPs (2.5 mM each)	1 μ l	1 μ l
Phusion [®] polymerase (2 U/ μ l)	0.5 μ l	0.5 μ l
Total volume	50 μ l	50 μ l

Table 20 PCR program for the first PCR.

Cycle step	Temperature	Duration	
Initial Denaturation	98°C	30 s	
Denaturation	98°C	15 s	} 8 cycles
Annealing	Primer specific	30 s	
Elongation	72°C	180 s	
Keep	4°C	hold	

Table 21. PCR program for the second PCR.

Cycle step	Temperature	Duration	
Initial Denaturation	98°C	30 s	
Denaturation	98°C	10 s	} 18 cycles
Annealing	Primer specific	30 s	
Elongation	72°C	180 s	
Final Elongation	72°C	600 s	
Keep	4°C	hold	

PCR products constructed by site-directed mutagenesis contain the template plasmid DNA and the new DNA product with substituted bases. To exclude the template DNA, the PCR product was treated with a restriction endonuclease (RE). REs cleave the DNA at specific binding sites due to their binding properties. The endonuclease used for the restriction (1 h, 37 °C) of the template plasmid DNA was with *DpnI* (New England BioLabs). *DpnI* only cleaves methylated restriction sites which makes the enzyme suitable for the degradation of the methylated template DNA. The new constructed DNA plasmid is not methylated. *DpnI* restriction mixture was then used to transform to *E. coli* DH5 α cells.

DpnI restriction mix

PCR product (plasmid)	8.5 μ l
10x restriction buffer	1 μ l
<i>DpnI</i>	0.5 μ l

2.3.14 Gibson Assembly[®] of DNA molecules

As an alternative to the conventional cloning technique, the Gibson Assembly[®] was designed for enhancing cloning efficiency. This new technique employs a 5'-exonuclease, a 3'-extension and a DNA-ligase activity in a single tube reaction. For primers design, the NEBuilder[®] Assembly Tool (<http://nebuilder.neb.com>) was used. Target genes were amplified using the generated primers and the designated vector was digested with the appropriate restriction enzyme. Both vector DNA and PCR product were prepared as described in chapter 2.3.11 and 10-100 ng of each fragment was added in a total volume of 5 μ l autoclaved MilliQ water. This was mixed with 15 μ l of the assembly master mix. The reaction was incubated in a heating block at 50 °C for 1 h. Afterwards, the whole assembly mix was transformed in *E. coli* DH5 α .

5x isothermal reaction buffer

1 M Tris-HCl	3 mL
1 M MgCl ₂	300 μL
100 mM dATP	60 μL
100 mM dCTP	60 μL
100 mM dGTP	60 μL
100 mM dTTP	60 μL
1 M DTT	300 μL
PEG-8000	1.5 g
10 mM NAD	300 μL

Gibson assembly master mix

5x isothermal reaction buffer	320 μL
10 U/μL T5 exonuclease	0.64 μL
2 U/μL Phusion DNA Polymerase	20 μL
40000 U/ μL Taq DNA Ligase	0.16 μL
Aqua dist.	860 μL

2.3.15 AQUA cloning

AQUA (advanced quick assembly) is a simple and versatile seamless assembly cloning approach. AQUA cloning harnesses intrinsic *in vivo* processing of linear DNA fragments with short regions of homology of 16 to 32 bp mediated by *Escherichia coli*. It does not require any kits, enzymes or preparations of reagents and is the simplest assembly cloning protocol to date. For AQUA cloning, all DNA fragments were mixed in a total volume of 10 μL with molar ratios of 3:1 (insert: vector) and 12 ng of linearized vector per 1 kb vector size (Beyer *et al.* (2015)). DNA mixtures were incubated for 1 h at room temperature. Afterwards, the whole assembly mix was transformed in *E. coli* DH5α.

2.4 Protein biochemical and biophysical methods**2.4.1 Production of recombinant proteins in *E. coli***

Heterologous protein expression was performed under dark conditions using *E. coli* BL21(λDE3). Culture media were complemented with appropriate antibiotics and supplements (Tab. 10), except for main cultures for protein production, for which the antibiotic concentration was halved. A starter culture of *E. coli* cells containing recombinant plasmids was grown at 37 °C overnight, then added to 4 L of LB growth media in a 1:100 ratio and incubated at 37 °C and 100 rpm until OD₆₀₀ = 0.5-0.6. Before starting the expression with 0.4 mM IPTG, the cultures were cooled down for 20-30 min. The protein production took place at 17 °C and 100 rpm for 20-22 h. Cells were

collected by centrifugation at $17.600 \times g$ and 4°C for 15 min (9000 rpm; Sorvall, F9-6x1000 LEX Rotor) and pellets obtained from 2 L cultures were merged and stored at -20°C .

2.4.2 Cell disruption of *E. coli* cells

Prior to cell disruption, the cells were thawed overnight on ice. After 12-16 h, they were resuspended in ice-cold lysis buffer. After addition of a spatula tip of lysozyme, DNase I, and 0.5 mM phenylmethylsulfonyl fluoride (PMSF) the cells were incubated on ice for 30 min. The cells were disrupted by sonication in intervals of 5 sec of sonication and 10 sec breaks, in total for 15 min (60 rounds) on ice in the dark (cycle 5/10, 40 % power output, Bandelin UW 2200 with tip KE 76). To separate the soluble parts from the debris, the lysate was centrifuged for 1 h at $45000 \times g$ (Sorvall™ LYNX™ 6000 centrifuge, rotor T29). The supernatant with soluble protein was filtered with a membrane filter unit (0.45 μm pore size, Starlab).

Lysis Buffer pH 7.4

Na ₂ HPO ₄	50 mM
NaCl	100 mM
MgCl ₂	5 mM
Triton 100	0.05 % (v/v)

2.4.3 Affinity chromatography of His-tagged protein

Recombinantly produced His₆-tagged proteins were purified by affinity chromatography. The TALON® Superflow™ (VWR) column was equilibrated with 10 column volumes (CV) of buffer A. The filtered lysate was incubated with column material under continuous rolling agitation at 4°C for 2 h. After adding the mix to the column, unbound fraction was let flow through. Unwanted proteins were washed off with 40 CV of ice-cold buffer A first, then 40 CV of ice-cold buffer B. In the next step, tagged proteins were eluted with 7 CV of buffer E. The column material was regenerated with 10 CV MilliQ H₂O and stored on 20 % EtOH at 4°C .

Buffer A pH 7.4

Na ₂ HPO ₄	50 mM
NaCl	300 mM

Buffer E pH 7.4

Na ₂ HPO ₄	50 mM
NaCl	300 mM
Imidazole	250 mM

Buffer B pH 7.4

Na ₂ HPO ₄	50 mM
NaCl	300 mM
Imidazole	10 mM

2.4.4 Dialysis and concentration protein

After the success of the purification had been verified by SDS-PAGE, the protein-containing fractions were collected, transferred to a dialysis tube (14 kDa molecular cut-off) and incubated in the new buffer system under constant stirring overnight. Subsequently, the dialyzed protein solution was concentrated with centrifugal concentrators (Amicon Ultra 10K, Merck Millipore) to the desired concentration at 4000 rpm, 4 °C and several 2 min centrifugation steps (Centrifuge 5810 R, Eppendorf, rotor A-4-6).

Dialysis Buffer pH 7.4

Na ₂ HPO ₄	50 mM
NaCl	300 mM
Glycerol	10 % (v/v)

2.4.5 Size exclusion chromatography

To determine the oligomerization state of affinity-purified proteins, they were analyzed by size exclusion chromatography (Moore (1964)). SEC is a method that separates the analytes based on their hydrodynamic radius. For globular proteins, the hydrodynamic radius is directly related to their size. This allows a size determination by comparison of the elution volume of the protein of interest with the elution volumes of standard proteins. The SEC experiments were performed using an Äkta Explorer system equipped with a SuperdexTM 75 10/300 GL column (GL Healthcare or Merck, Darmstadt). The column was equilibrated with 1.5 CV (CV = 24 ml) of dialysis buffer prior to use and the flow rate was set to 0.1 ml/min. After equilibration, the 500 µl sample loop was washed three times with water and three times with dialysis buffer. The protein sample was filtered through a 0.2 µm syringe filter (Rotilabo® RC, Roth) before transferring the sample onto the column. The elution profile was determined by measuring the absorbance at 280 nm for proteins and 560 nm for PEB bound to CpeB. For elution 1.5 CV of buffer was used employing a flow rate of 0.1 ml/min and collecting 250 µl elution fractions. Desired fractions were combined (~ 1 ml) and stored at -20 °C. The SEC served as purifying method for further studies of proteins via UV/Vis- and Fluorescence spectroscopy and HPLC.

The calibration curve for the size determination was created by plotting the log of the MW of standard proteins against the quotient of the elution volume (V_e) and the void volume (V₀). The calibration curve was calculated using a linear regression in Origin. The standards used for the calibration were: albumin (MW = 66 kDa), ovalbumin (MW = 44 kDa), carbonic anhydrase (MW

= 29 kDa) and lysozyme (MW = 14.3 kDa). The void volume of the column was determined by the elution volume of Blue Dextran 2000 (MW~ 2000 kDa). All standards were obtained from Sigma-Aldrich.

2.4.4 SDS-polyacrylamide gel electrophoresis (SDS-PAGE)

Proteins were separated and analyzed according to their molecular weight by SDS-polyacrylamide gel electrophoresis (SDS-PAGE). The separation of the proteins was conducted in a discontinuous system which consisted of a stacking gel (pH 6.8) with an acrylamide concentration of 5.25 % and a separation gel (pH 8.8) with an acrylamide concentration of 12.5 % or 15 %. SDS is a negatively charged detergent, which binds proteins in a ratio nearly one molecule SDS per two amino acid side chains, thereby denaturing the protein. The acrylamide concentration determines the resolution of the separation. Larger proteins migrate slower through the acrylamide matrix than smaller proteins. The samples were prepared by the addition of 5x loading dye and incubation for 10 min at 95 °C, centrifugation (1 min, 13200 rpm, 5415D, Rotor F-45-24-11) prior to loading onto the gel. The electrophoresis was performed by applying a constant current of 200 V until the tracking dye reached the bottom of the gel. Afterwards, the gel was transferred to the Coomassie Brilliant Blue G250 containing staining solution and shaken for 10 min. The gel was then destained with destaining solution until protein bands were visible. The protein marker mix Page Ruler™ Prestained Protein Ladder or PageRuler™ Unstained Protein Ladder (ThermoScientific™) was used to determine the size of the proteins.

4x Stacking gel buffer

Tris-HCl pH 6.8	1.5 M
SDS	4 % (w/v)

4x Separation gel buffer

Tris-HCl pH 6.8	1.5 M
SDS	0.4 % (w/v)

10x SDS-running buffer

Tris-HCl pH 8.8	0.25 M
Glycine	1.92 M
SDS	1 % (w/v)

Stop gel (4 mini gels)

Aqua dest.	330 µl
Separation buffer	250 µl
Acrylamide 30 %	420 µl
10 % APS	10 µl
TEMED	2 µl

Separation gel 15 % (4 gels)

Aqua dest.	4 ml
Separation buffer	4 ml
Acrylamide 30 %	8 ml
10 % APS	80 µl
TEMED	8 µl

Sample staining solution

Tris-HCl pH 6.8	100 mM
SDS	8 % (v/v)
Glycerol	40 % (v/v)
β -mercaptoethanol	10 % (v/v)
Bromophenol Blue	0.08 % (w/v)

Stacking gel (4 gels)

Aqua dest.	4.6 ml
Stacking gel buffer	2 ml
Acrylamide 30 %	1.4 ml
10 % APS	30 μ l
TEMED	20 μ l

Staining solution

Acetic acid	10 % (v/v)
Ethanol	30 % (v/v)
Coomassie Brilliant Blue	0.25 % (w/v)

Unstaining solution

Acetic acid	10 % (v/v)
Ethanol	30 % (v/v)

2.4.5 Immuno-staining of immobilized proteins (Western Blot)

For detection of a specific protein in the sample, the western blotting method was performed. The protein samples were first separated according to their molecular weight by SDS-PAGE (see chapter 2.4.4) and subsequently transferred to a PVDF membrane using a semi-dry blotting system for 18 min at 15 V. The PVDF membrane was activated in 100 % methanol and afterwards equilibrated in Towbin buffer together with the gel and two blotting papers (Whatman; 3 mm) for 5-10 min. The blotting construction was set up as follows: the equilibrated gel and the membrane were placed between the two blotting papers and the sandwich was placed between the anode and the cathode of the blotting machine. After blotting, the membrane was either blocked at RT for 1 h or overnight at 4 °C using Bovine serum albumin (BSA). Incubation with the first antibody (Table 5) in 10 ml blocking solution followed upon gently for 1 h at RT. After three times of 5 min washing steps with PBS-T buffer, the membrane was incubated with the second antibody (Table 5) in 10 ml blocking solution, also kept shaking gently for 1 h at RT. The membrane was washed three times with PBS-T buffer and twice with PBS buffer. For detection 33 μ l nitro blue tetrazolium chloride (NBT, 100 mg/ml) and 66 μ l 5-bromo-4-chloro-3-indolyl phosphate (BCIP, 50 mg/ml) were added in 10 ml of AP buffer. The reaction was stopped by removing the buffer and by addition of A. dest.

For the detection of Strep-tagged proteins, the membrane was washed with PBS-T buffer three times for 5 min and then incubated with 2 μ g/ml avidin dissolved in PBS-T for 10 min. Avidin prevents the detection of endogenous biotin-carboxyl containing proteins from *E. coli* cells. The membrane was washed again three times (5 min) with PBS-T before it was incubated with the anti-Strep-Tactin®-AP conjugate (1:4000, IBA GmbH) for 1 h.

Towbin buffer pH 8.3

Tris-HCl	25 mM
Glycine	192 mM

PBS buffer pH 7.4

Na ₂ HPO ₄	100 mM
KH ₂ PO ₄	18 mM
NaCl	137 mM
KCl	2.7 mM

AP-buffer pH 9.5

Tris-HCl	100 mM
NaCl	100 mM
MgCl ₂	5 mM

Blocking solution

1x PBS-T buffer	
Albumin fraction V	3 % (w/v)

PBS-T buffer

1x PBS	
Tween-20	0.1 % (v/v)

Detection solution

AP buffer	10 ml
NBT solution	33 µl
BCIP solution	66 µl

2.4.6 Zinc blot

Covalent linkage of a linear tetrapyrrole to a protein was analyzed using zinc blot analysis (adapted from Berkelman and Lagarias 1986). The zinc ions form fluorescent complexes with the bilin-linked polypeptides, which are then visualized under UV-light. After SDS-PAGE, the samples were transferred to PVDF membrane (see chapter 2.4.5). The membrane was then incubated for 1 h at 4 °C in a freshly prepared 1.3 M zinc acetate solution. Detection was done under UV-light illumination.

2.4.7 Protein precipitation-trichloroacetic acid (TCA) precipitation

Trichloroacetic acid (TCA) is a relatively weak acid so it cannot hydrolyze the peptide bonds of proteins, but it does maintain an acidic pH in water. The addition of TCA to proteins in an aqueous solution disrupts the hydrogen-bonded water molecules (hydration sphere) surrounding a protein. These protein no longer remain soluble and can be recovered by centrifugation. However, because TCA disrupts hydrogen bonds, the proteins will also lose their secondary structure and become denatured (Koontz (2014)). After adding half the sample volume of 30 % TCA to the protein sample, the mixture was vortexed. The protein were stored on ice for 30 min to allow precipitation and the mixture was then centrifuged at 10,000 ×g at 4 °C for 5-10 min. The supernatant was carefully aspirated and the pellet was resuspended using 40 µl of A. dest and 10 ul of 5x SDS

loading buffer. The mixture was incubated for 10 min at 95 °C and centrifuged (1 min, 13,200 rpm, 5415D, Rotor F-45-24-11) prior to loading onto the gel.

2.4.8 Determination of protein concentration

The concentration of proteins purified by affinity chromatography or size exclusion chromatography (SEC) was determined by their absorbance at 280 nm. The amino acids that contribute to the absorption at 280 nm are cysteine, tryptophan and tyrosine and therefore, the molar extinction coefficients of proteins can be calculated depending on the content of these amino acids as described by Gill and von Hippel according to the following formula (Gill & Von Hippel (1989)).

$$\epsilon_{280} = (n_{\text{Trp}} \cdot 5690 + n_{\text{Tyr}} \cdot 1280 + n_{\text{Cys}} \cdot 120) \text{ M}^{-1} \text{ cm}^{-1}$$

n_x = number of the amino acid per molecule of protein

The concentration of the protein is then calculated in accordance to Lambert-Beer's law:

$$c = \frac{A_{280}}{\epsilon_{280}} \cdot d$$

c = concentration in $\frac{\text{mol}}{\text{l}}$

A_{280} = absorption at 280 nm

ϵ_{280} = molar extinction coefficient at 280 nm

d = light path in the cuvette in cm

To convert the concentration based on the weight the molar concentration was multiplied with the calculated relative molecular weight (M_r)

$$c \left[\frac{\text{g}}{\text{l}} \right] = M_r \left[\frac{\text{g}}{\text{mol}} \right] \times c \left[\frac{\text{mol}}{\text{l}} \right]$$

c = concentration in $\frac{\text{mol}}{\text{l}}$ or $\frac{\text{g}}{\text{l}}$

M_r = relative molecular weight of a protein in $\frac{\text{g}}{\text{mol}}$

Table 22. Molar extinction coefficient of the proteins examined in this study. Calculated from amino acid sequence with Protein Calculator v3.4

Protein	Extinction coefficient ϵ_{280} ($M^{-1} \text{ cm}^{-1}$)	calculated relative molecular weight (kDa)
His-CpeB	8940	20.89
Flag-CpeB	13410	22.08
His-CpeA	17420	18.92

For determination of protein mixture concentration, the difference in the absorbance between 235 and 280 nm was used. Diluted sample into proper absorbance reading region around 0.1 to 1.2 (Whitaker & Granum (1980)). Protein concentration(mg/ml) = (A235 - A280)/2.51*dilution times

2.4.9 UV/Vis spectroscopy

The use of UV/Vis spectroscopy allows the recording of spectra in the ultraviolet and visible wavelength ranges of light. While proteins only absorb at 280 nm, phycobilins are characterised by very pronounced absorption in both wavelength ranges. The absorption of the substances to be investigated was always recorded in a range between 300 and 800 nm (8453 UV-Visible system, Agilent Technologies).

2.4.10 Fluorescence spectroscopy

Purified PBP are highly fluorescent and show specific emission spectra when excited with suitable wavelengths for their bound phycobilins. For the recording, purified PBPs by SEC were diluted in dialysis buffer. Emission spectra were measured between 510-700 nm after excitation at 490 nm for PEB with the fluorescence spectrometer FP-8300 of Jasco.

2.4.11 HPLC analyses

High performance liquid chromatography (HPLC) is a technique that separates analytes in a mixture depending on their polarity. A HPLC system comprises a stationary and a mobile phase with different polarities. This causes a different partitioning of each analyte between the two phases. As a result, each compound of a mixture has a specific retention time on the stationary phase, leading to a separation.

HPLC analyses of different bilins

To analyses lyase bound bilins, a solid phase extraction with Sep-Pak[®] C18 light cartridges was performed. After the samples had been loaded, the cartridges were washed with 5 ml of 0.1 % TFA, 5 ml 20 % MeOH in 0.1 % TFA and 5 ml 20 % acetonitrile in 0.1 % TFA. The bilins were eluted

with 1 ml acetonitrile and subsequently frozen at -80°C . In the next step, the samples were desiccated by lyophilization (Alpha 2-4 LSC plus, Martin Christ GmbH) for approximately 24 h. After the samples had been dried, they were dissolved in 15 μl of DMSO and mixed with 200 μl of the mobile phase. After a filtration through a 0.2 μm PTFE filter the samples were ready for the application to the HPLC system. For the analyses an Agilent 1100 series HPLC system with a reversed-phase column (Phenomenex - Luna 5 μm C18 (2) 100 \AA) as stationary phase was used. The mobile phase consisted of a mixture of 50 % (v/v) 20 mM formic acid and 50 % (v/v) acetone. The samples were applied to the system using a 200 μl sample loop. The elution was isocratic with a constant flow rate of 0.6 ml/min. The analytes were monitored using an UV-Vis detector at 380, 560 and 680 nm, as most bilins possess absorbance maxima at ~ 380 nm and in a range between 540 and 680 nm. To further characterize the separated compounds, peak absorbance spectra were recorded between 350 nm and 800 nm. Compounds designated for further examinations were collected directly after the outlet of the UV-Vis detector, immediately frozen at -80°C , freeze-dried and stored at -80°C prior to use.

HPLC mobile phase

Acetone	50 %
Formic acid (20 mM)	50 %

HPLC analyses of different chromophore peptides

Purified protein (1 ml) was dialyzed over night against digestion buffer using a reusable dialysis system for small sample volumes (QuixSep[®] 1.0 ml Roth & MWCO 12000 - 14000 Da, Servapor[®] dialysis tube, SERVA). For digestion a ratio of 1:5 for trypsin:peptide (w/w) was used. The enzyme was added from a 200 $\mu\text{g}/\text{ml}$ stock (Trypsin from bovine pancreas, TPCK treated, $\geq 10,000$ BAEE units/mg protein, T1426, Sigma-Aldrich) to the denatured protein mixture and incubated at 30°C for 3 h in the dark. The reaction was quenched by adding 30 % (v/v) glacial acetic acid (Carrigee *et al.* (2021)). For preparing the sample for HPLC, digested peptides were passed through a pre-equilibrated Sep-Pak[®] Vac 3cc (200 mg) C18 cartridge (Waters Corporation, Milford, MA). For equilibration, the cartridge was washed with 4 ml of methanol and 4 ml 0.1 % TFA. After adding the sample, three washing steps with 4 ml of 0.1 % TFA each time took place. For elution 20 ml methanol were used, whereas the desired proteins eluted within the first 2 ml. Thereafter the eluted samples were vacuum dried and stored at -80°C before HPLC.

Digestion buffer pH 7.0

Na ₂ HPO ₄	2 mM
β-mercaptoethanol	1 mM

HPLC was used to determine and identify recombinant produced PBPs. The trypsin digested and desalted PBPs (CpeB, PEB and /or PUB) samples were analysed on a Jupiter[®] 5 μm C4 300 Å column (Phenomenex) equipped on the Agilent 1100 series HPLC. Before analysis, the column was equilibrated overnight with the mobile phase consisting of degassed and filtered 85 % (v/v) 0.1 % formic acid and 15 % (v/v) acetonitrile with a constant flow rate of 0.01 ml/ min. The samples were prepared under dim-light to prevent photo-damage of the pigments. The lyophilized samples were dissolved in 300 μl of 0.1 % formic acid and filtered through a 0.2 μm Phenex (Phenomenex[®]) syringe filter. An amount of 0.15 mg of peptide was sufficient for analysis. Before loading the sample, the loop was washed five times with 200 μl 0.1 % formic acid. The sample injection was carried out manually with a Hamilton syringe into a 200 μl sample loop. The flow rate was kept constantly at 1 ml/min over a measurement period of 30 min. A gradient elution was applied, starting with 15 % acetonitrile and 85 % of 0.1 % formic acid, increasing acetonitrile over 30 min. The eluted fractions were detected by absorption at 280, 380, 560 and 650 nm. The column was stored on 65 % acetonitrile and 35 % water.

HPLC mobile phase gradient

Acetonitrile	15 % – 99.9 %
0.1 % Formic acid	85 % – 0.1 %

2.4.12 Production of recombinant proteins in *Synechococcus* sp. PCC 7002

A culture (A⁺ medium containing proper antibiotics) of *Synechococcus* sp. PCC 7002 was grown harboring pAQ1Ex-insert gene to late exponential phase. Cells were harvested by centrifugation at 5000 x g (Sorvall SLC- 4000 rotor). Pelleted cells were resuspended in lysis buffer (50 mM Na₂HPO₄, 300 mM NaCl, pH 7.5) with protein inhibitor. Cells were disrupted by two passages through a chilled French press operated at 138 MPa. The extract was clarified by centrifugation at 4 °C, 21000 x g for 1h.

2.4.13 Isolation of intact phycobilisomes from *Synechococcus* sp. PCC 7002

Isolation of PBS was conducted with a culture of *Synechococcus* sp. PCC 7002 in the state of exponential growth. 100 ml of cell culture was transferred to centrifugation tubes and spun down

for 10 min at 1480 x g at room temperature. The pellet was transferred in 2 ml tube and resuspended in 0.5 ml of 0.75 M Potassium-Phosphate Buffer pH 7.0. Afterwards, the sample was centrifuged for 5 min at 3000 x g, and the supernatant was discarded. The pellet was resuspended in 0.75 ml of Potassium-Phosphate Buffer and mixed with glass beads (ϕ 0.25-0.5 mm) in a 1:1 ratio, The cells were disrupted in a homogenizer for 10 min and then centrifuged for 5 min at 25000 x g. The supernatant was transferred in a new tube and spun down for 15 min at 25000 x g. The newly collected supernatant was mixed with 20 % Triton X-100 to achieve a final concentration of 2 % Triton X-100 and centrifuged at 25000 x g for 10 min. The bottom phase was loaded on top of a prepared discontinuous sucrose gradient in an ultracentrifuge tube (sucrose layer dissolved in 1.5 M, 1 M, 0.75 M, 0.5 M Potassium-Phosphate Buffer). The subsequent ultracentrifugation step was performed for 15 h in a swing-out rotor, set at 18 °C (acceleration = 7; deceleration = 0) and 120000 x g (L8-M ultracentrifuge, Beckman Coulter swing-out rotor SW 40). The intact PBSs are found in the layer with the highest density. The coloured layers containing phycobiliproteins (500 μ l) were transferred into reaction tubes and further analysed using UV/Vis spectroscopy (scanning absorptions from 200 nm to 900 nm), and zinc blot.

2.4.14 Preparation of protein samples from *Prochlorococcus marinus* SS120

4 L of a *Prochlorococcus marinus* SS120 cell culture was harvested by centrifugation at 10000 x g for 10 min at 4 °C. The obtained ~2.1 g of cells were resuspended in 10 mL of “extraction buffer” containing 5 mM EDTA and 0.5 mM PMSF. Cells were disrupted on ice by sonication in intervals of 5 seconds pulse and 10 seconds pause during 4 min (cycle 5/10, 40 % power output, Bandelin UW 2200 with tip KE 76). By 15 min centrifugation at 8000 x g at 4 °C, cell debris (P1) were separated and the supernatant (S1) was once more centrifuged in a L8-70M Beckman ultracentrifuge at 100000 x g for 30 min at 4 °C. After centrifugation, 14 mg pellet (P2) was separated from the supernatant (S2) and resuspended in 1 mL of 2 % n-Decyl- β -D-maltopyranoside (DM) detergent buffer. Membrane protein solubilization was performed under continuous rolling agitation at 4 °C. After 2 h, the solubilized material (So) was ultracentrifuged at 100000 x g for 30 min at 4 °C. Pellet (P3) and supernatant (S3) were collected to be analyzed via SDS-PAGE and Western Blot (Fig. 14A):

2.4.15 Pull down assay for enrichment PE-III

Cells from *Prochlorococcus* were collected by centrifugation and then lysed into extraction buffer (5 mM MgCl₂, 100 mM NaCl, 50 mM Na₂HPO₄ (pH 7.4), 0.05 % Triton X-100 (v/v)). After two

chilled cycles of French press operated at 6.5 bar and centrifugation at 4 °C, 21,000 g for 1 h, the supernatants were collected and concentrated to 3 mL to be used for immunoprecipitation. The supernatants were prepared and mixed with 18 µL β-PE rabbit IgG antibody for immunoprecipitation (at 4 °C for overnight). After incubation with the antibody, 25 µL of protein A-agarose SC-2001 beads (pre-blocked overnight with 10 % BSA in PBS) were added for 4 h. The beads were washed three times with PBS buffer and resuspended in 50 µl of SDS sample buffer with β-Mercaptoethanol.

2.4.16 AlphaFold

AlphaFold is an artificial intelligence method for predicting protein structures that has been highly successful in recent years (Jumper *et al.* (2021)). AlphaFold2_advanced was run with ColabFold, a software for use as a Jupyter Notebook inside Google Colaboratory. Offering a MMseqs2 (Many-against-Many sequence searching)-based homology search server to build diverse MSAs and to find templates. Calculated structures are sorted by AlphaFold2 confidence measures. Single chain predictions are ranked by pLDDT (predicted local distance difference test; a per-residue confidence metric) between 0 and 100 and complexes by pTM-score (predicted template modeling score, between 0 and 1). Default settings were used, except 24 max. recycles were chosen for sampling options. Results and scores can be downloaded, offering 5 predicted structures for each run as PDB file (Mirdita *et al.* (2022)).

3. Results

3.1 What is the natural chromophorylation pattern of PE-III?

This chapter aimed to reveal the chromophorylation pattern of natural PE-III of *P. marinus* SS120. Several approaches were undertaken to isolate enrich and identify the protein. Based on preliminary data, PE-III is hypothesized to carry four bilin chromophores: one at position α -Cys73, one at β -Cys82, one at β -Cys163 and one doubly linked to β -Cys50 and 61 (Steglich *et al.* (2003)). Phycoerythrins of cyanobacteria often contain two types of phycobilins, phycourobilin (PUB) and phycoerythrobilin (PEB). Although previous *in vivo* physiological studies revealed a pigment composition of PUB and PEB at a 3:1 ratio, we still do not know which phycobilins are attached to which cysteine residue (Steglich *et al.* (2003)).

3.1.1 Pigment characterization of *Prochlorococcus marinus* SS120 by their spectroscopic properties and fluorescence emission spectroscopy

Absorption spectra of *Prochlorococcus marinus* SS120 showed a pronounced peak at 483 nm that can be attributed mainly to DV-Chl *b* but also to zeaxanthin and α -carotene, the major carotenoids in *Prochlorococcus*. It also shows two DV-Chl *a* peaks at 452 nm and 672 nm (Fig. 12). No peak was detected for PE-III. This may be due to the low concentration of the phycoerythrin accumulated within the cells or the overlapping of PE-III absorption with the Soret-band of DV-Chl *b* and carotenoids.

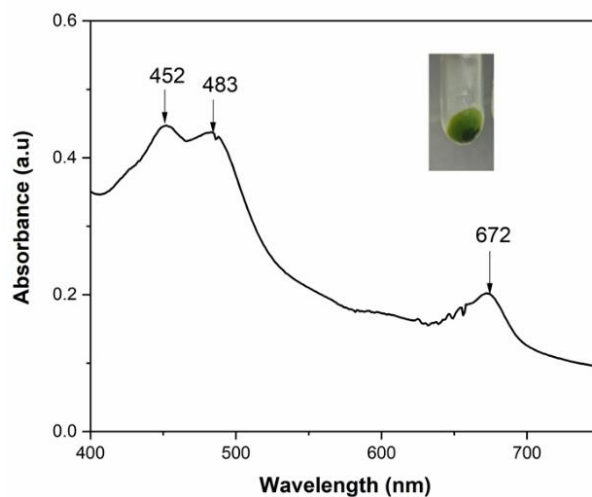


Figure 12. UV Absorption spectrum of *Prochlorococcus marinus* SS120 pigments. Inserted into the graph a picture of the cell pellet is shown. DV-Chl *a* maxima at 452 nm and 672 nm. The peak at 483 nm corresponds to the carotenoids or DV-Chl *b*. Spectra were normalized to the DV-Chls maxima.

However, PE-III can be detected by fluorescence spectroscopy using glycerol as “signal enhancer” (Wyman *et al.* (1985), Lokstein *et al.* (1999)). The addition of glycerol uncouples PE-III from the thylakoid membrane, thereby enhancing the PE-III emission signal with a concurrent decrease in chlorophyll emission. The excitation wavelength was set at the PUB maxima of 495 nm and showed two main emission spectra peaks (Fig. 13).

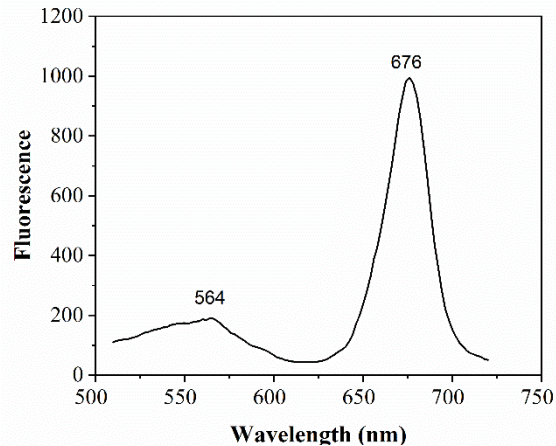


Figure 13. Fluorescence emission spectra at 495 nm excitation (PUB absorption maximum) of *P. marinus* SS120 cells in the presence of 50 % glycerol. The first peak with absorbance at 564 nm corresponds to PE-III emission, and the other at 676 nm corresponds to chlorophyll *a* emission, the terminal energy acceptor.

3.1.2 Protein analysis of *Prochlorococcus marinus* SS120

Due to the absence of visible PE-III in cellular absorbance, the protein extraction protocol was established. Several centrifugation steps were described in the chapter 2.4.14 (Fig. 14A). Western Blot experiments revealed a significant signal at around 10 kDa, which was suspected to be β -PE-III or PE-III. To identify the proteins present in each fraction, S2 and S3 were concentrated using a 3 kDa MWCO filter and subjected to mass spectrometry (MS) analysis. The concentrated samples were also analyzed by SDS-PAGE and zinc-blot with a signal appearing at approximately 15 kDa in the zinc-blot corresponding to the concentrated S3 fraction (S3c) (Fig. 15). Protein identification results for samples S2 and S3 are presented in Tables 23 and 24, respectively.

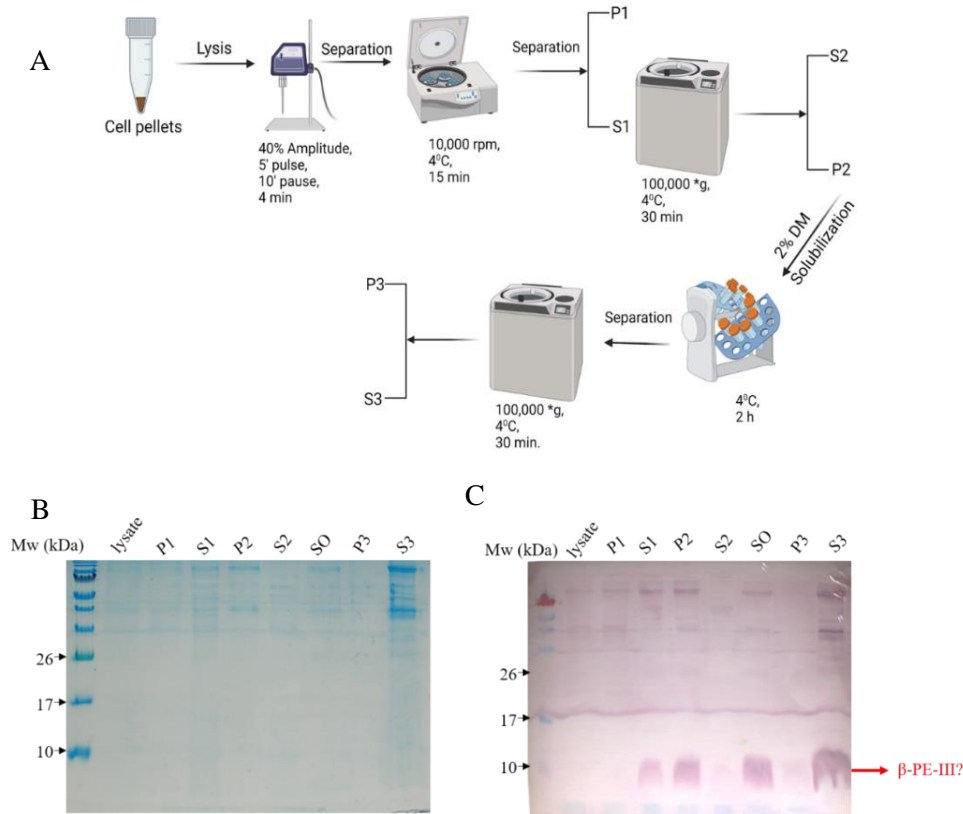


Figure 14. Analysis of proteins from *P. marinus* SS120 **A.** Scheme showing the isolation of proteins from *P. marinus* SS120. **B.** SDS-PAGE containing the following samples: lysate, P1, S1, P2; So, P3 and S3. **C.** Corresponding western blot using the specific *P. marinus* SS120 CpeB antibody.

The photosynthetic apparatus in *P. marinus* SS120 is organized in two supercomplexes: a naked PSI-trimer and a PSII-dimer. The peripheral antennae in the photosynthetic membranes are of two types: either associated with the photosystems (fixed antenna) forming supercomplexes or as mobile antenna subjected to light regulation. PSII is a supercomplex formed by a dimeric PSII with 8 Pcb subunits (Pcb_8PSII_2). In *Prochlorococcus marinus* SS120, the Pcb-PSI supercomplex comprises the surrounding PSI reaction center trimer with an 18-membered PcbG ring ($PcbG_{18}PSI_3$), which is similar to the IsiA-PSI structure found in iron-limited *Synechocystis* sp. PCC 6803 (Bibby *et al.* (2001)). After the solubilization using 2 % of DM, seven different Pcb family proteins were identified in the S3 sample as well as PsbB and PsbL, two essential proteins for PSII were also detected. Moreover, PetH a ferredoxin-NADP⁺ reductase, which catalyzes the electron transfer from photochemically reduced ferredoxin to NADP, was detected. PetH has an

N-terminal domain with a predicted transmembrane helix that could anchor the protein to the thylakoid membrane. This is in contrast with PetH from freshwater cyanobacteria (Table 23). However, no proteins associated with PE-III were detected in the MS analysis.

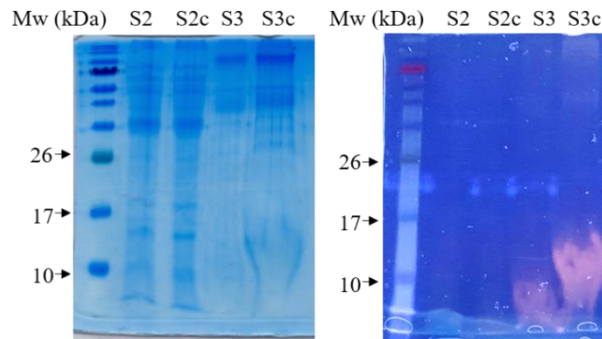


Figure 15. SDS-PAGE and Zinc-blot of concentrated samples for mass spectrum. S2: S2 step fraction; S2c: concentrated S2 step fraction; S3: S3 step fraction; S3c: concentrated S3 step fraction. Zinc-blot detected under 380nm.

Table 23. Protein identification of sample S3

ID	Function	Gene
Q7VCF7	Divinyl chlorophyll a/b light-harvesting protein PcbA	<i>pcbA</i>
Q9L8M5	Divinyl chlorophyll a/b light-harvesting protein PcbB	<i>pcbB</i>
Q7VBC8	Divinyl chlorophyll a/b light-harvesting protein PcbD	<i>pcbD</i>
Q9L8M2	Divinyl chlorophyll a/b light-harvesting protein PcbE	<i>pcbE</i>
Q9L8M1	Divinyl chlorophyll a/b light-harvesting protein PcbF	<i>pcbF</i>
Q7VC50	Divinyl chlorophyll a/b light-harvesting protein PcbG	<i>pcbG</i>
Q7VBC2	Divinyl chlorophyll a/b light-harvesting protein PcbH	<i>pcbH</i>
Q7VDM2	Photosystem II CP47 reaction center protein	<i>psbB</i>
Q7VDN8	Photosystem II reaction center protein	<i>psbL</i>
Q7VB31	Porin homolog	<i>pro1269</i>
Q7VCK3	Porin homolog	<i>pro0737</i>
Q7VAA1	Adhesin-like protein	<i>pro1563</i>
Q7VD33	Ribulose biphosphate carboxylase large chain	<i>cbbL</i>
Q7VBH1	Ferredoxin-NADP reductase	<i>petH</i>
Q7V9I0	CTP synthase	<i>pyrG</i>
Q7VBQ4	Glutamine synthetase	<i>glnA</i>
Q7VAD1	Phosphate-binding protein	<i>pstS</i>
Q7VC60	Ferritin	<i>ftn</i>
Q7VA76	ATP synthase subunit beta	<i>atpD</i>
Q7V9X2	50S ribosomal protein L14	<i>rplN</i>
Q7VDA2	Membrane protease subunits	<i>hflC</i>

Table 24. Protein identification of sample S2

ID	Function	Gene
Q7VB31	Porin homolog	<i>pro1269</i>
Q7VCT2	Uncharacterized protein	<i>pro0658</i>
Q7VBH1	Ferredoxin-NADP reductase	<i>petH</i>
Q7VC60	Ferritin	<i>ftn</i>
Q7VCF0	Lycopene epsilon cyclase	<i>lcyE</i>
Q7VBI7	Diaminopimelate decarboxylase	<i>lysA</i>
P0A328	Carboxysome shell protein CsoS1	<i>csoS1</i>
Q7V9G2	Chaperone protein dnaK2	<i>dnaK2</i>
Q7V9M7	6,7-dimethyl-8-ribityllumazine synthase	<i>ribH</i>
Q7VAU5	30S ribosomal protein S16	<i>rpsP</i>
Q7VBY9	DIM6/NTAB family protein	<i>pro0953</i>
Q7VDY8	50S ribosomal protein L7/L12	<i>rplL</i>
Q7VEI6	Biotin carboxyl carrier protein of acetyl-CoA carboxylase	<i>accB</i>

3.1.3 Identification of associated PE-III proteins from *Prochlorococcus marinus* SS120

Using a similar approach as previously described, our objective was to determine the composition of the chromophore in PE-III. While previous *in vivo* studies had shown that the pigment composition of phycourobilin (PUB) and phycoerythrobilin (PEB) occurred at a 3:1 ratio, the specific chromophorylation pattern of PE-III remained unknown (Steglich *et al.* (2003)). This experiment aimed to validate Steglich *et al.*'s proposed effect and determine which phycobilin is bound to which Cys position, with particular interest in the question of which phycobilin is doubly attached via β -Cys50/61. We obtained *P. marinus* SS120 cells from an 8 L culture, which we treated with sonication, and the soluble fraction was obtained via centrifugation. However, neither SDS-PAGE nor zinc-blot gels showed any significant signals indicating the presence of PE (Fig. 16). We also did not observe additional pink staining of the PE subunits on the zinc-blot. We subsequently digested the proteins in the gel using trypsin and identified further proteins through mass spectrometry.

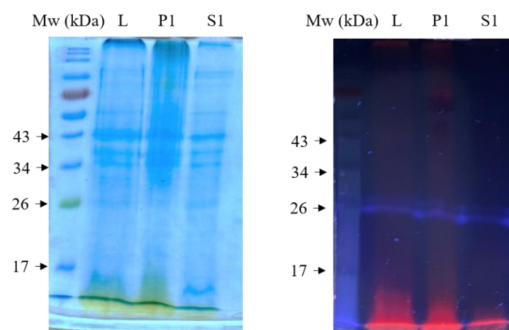


Figure 16. SDS-PAGE and zinc-blot of each step samples. L: Lysate; P1: Insoluble fraction; S1: Soluble fraction. Zinc-blot detected under 380nm

Table 25. Identified peptides of CpeA

CpeA peptides	Mass	Cleavage
AKDRLEAAEK	1129.6	34-43
FTSQALDYVYGTENYEQANK	2340.1	51-70

Table 26. Identified peptides of CpeB

CpeB peptides	Mass	Cleavage
AIEIMK	703.4	129-135
AVVSADSK	775.4	8-15
GATIGSAELSSLR (K)	1260.7 (1388.8)	16-28 (29)
DGEILR	814.5	85-91
DIASEAASYFDR	1343.6	165-176
ETYIALGVPLSNAIR	1615.9	115-129
IATVAIMTETNSGR (K)	1462.7 (1590.8)	136-149
(K) YVADANKR	1063.6 (935.5)	(29) 30-37
MLDAFSR	838.4	1-7
YVSYALLAGDPSVLDDR	1852.9	92-108

Table 27 Identified peptides of CpeS

CpeS peptides	Mass	Cleavage
AILQTSFASEIK (R)	1306.7 (1462.8)	162-173 (174)
GIEEFVNK	934.5	2-9
QEGILR	827.5	97-104
SSVILSLESK	1061.6	152-161

Table 28 Identified peptides of Pro1634

Pro1634 peptides	Mass	Cleavage
IALEQIQSPDVLK (R)	1452.8 (1608.9)	245-257
IDQEPLVR	968.5	194-201
LKTLVEDGLLL	1212.7	258-269
LYGNLPQSLK	1131.6	211-220
MSAVYALGR	966.5	101-109
NPSPLAVDTLLQLLENDNAYVR	2541.3	110-132
SLHTDVAAVR	1067.6	154-163

We aimed to identify all the proteins involved in PE-III assembly. A summary of the identified peptides for CpeA, CpeB, CpeS, and Pro1634 can be found in Table 25-28. CpeB, CpeA, and CpeS were identified in both the lysate and soluble fractions. However, Pro1634 was only detected in the lysate. Unfortunately, we were unable to detect chromophorylated peptides for either CpeA or

CpeB. Due to the large amount of material required and the minimal difference in quality between the PEB and PUB chromophores, this strategy was not pursued further.

3.1.4 Enrichment of PE-III from *Prochlorococcus marinus* SS120

As the quantity of PE-III per cell is extremely limited, a pull-down assay was implemented to enrich it from *P. marinus* SS120 (chapter 2.4.15). Prior to conducting the experiment, a preliminary test was carried out to confirm whether the available antibodies (anti *F. diplosiphon* β -PE rabbit IgG and anti *P. marinus* CpeB rabbit IgG) could extract either β -PE or the entire PE-III. The test was performed on a sample obtained from the soluble lysate mixture of *E. coli*. The findings revealed that both antibodies were able to extract the CpeB: PEB complex *in vitro*. (Fig. 17).

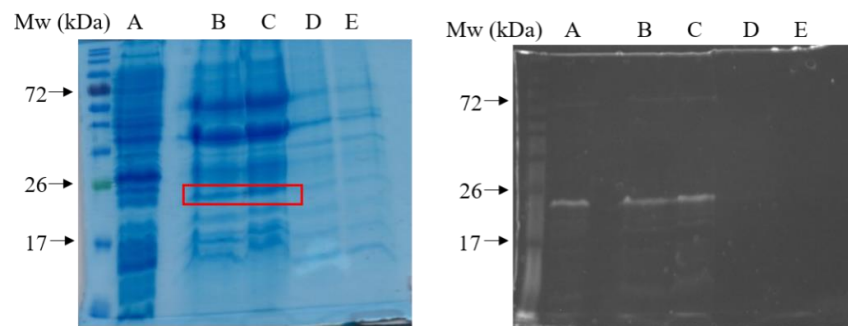


Figure 17. SDS-PAGE and zinc-blot of immunoprecipitation pretest *in vitro*. A: Supernatant of lysate (positive control); B: Pretreated *F.diplosiphon* antibody elution; C: Pretreated *P.marinus* antibody elution; D: Untreated *F.diplosiphon* antibody elution; E: Untreated *P.marinus* antibody elution

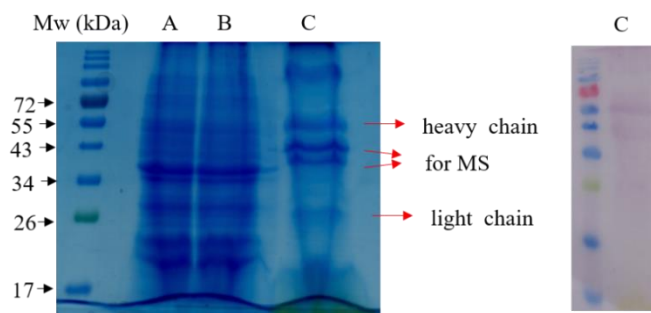


Figure 18. SDS-PAGE and β -PE blot of immunoprecipitation *in vivo*. A: Supernatant of lysate; B: Washing step collection; C: Elution fraction

After the preliminary test, the enrichment procedure was performed using the soluble fraction (supernatant of lysate) from chapter 3.1.3. Afterward, the eluted proteins were analyzed by SDS-PAGE and Western Blot (Fig. 18). However, no signal was observed around 21 kDa as expected,

but faint signals were recorded at 37 and 45 kDa in the western blot. The two signals were analyzed via MS, but unfortunately, no CpeB or CpeA were identified (data not shown).

3.2 Expression of the *P. marinus* SS120 PE cluster in a heterologous host using the TREX system

Since all *in vivo* approaches to enrich PE-III and identify the chromophorylation state failed, we went ahead to express the whole PE cluster in *E. coli*. The approach is based on the recently described TREX system (transfer and expression of biosynthetic pathways) by Drepper and coworkers (Loeschcke *et al.* (2013)). It comprises all functional elements necessary for the delivery and concerted bidirectional expression of biosynthetic gene clusters.

The TREX system comprises functional elements such as DNA transfer through conjugation, chromosomal integration via randomized transposition, and T7 RNA polymerase-dependent bidirectional gene expression, as illustrated in Figure 19. The system utilizes the 9.5 kb plasmid pIC20H-RL, which is a multi-copy *E. coli* vector derived from pUC19 and carries the TREX cassettes along with an Ap^R resistance gene. The TREX cassettes include resistance markers (Tc^R and Gm^R), an oriT for conjugational transfer, transposon Tn5 elements, and T7 promoters for bidirectional transcription of DNA fragments by T7 RNA polymerase. The TREX system is designed to facilitate comparative expression studies with biosynthetic gene clusters across a wide range of bacterial expression hosts, thus enabling the identification and characterization of valuable natural products.

The TREX system was evaluated by expressing the carotenoid biosynthesis gene cluster (*crt*) from *P. ananatis* in *P. putida*, *R. capsulatus*, and *E. coli* (Loeschcke *et al.* (2013)). The study addressed two main questions: (i) whether simultaneous bidirectional expression of a gene cluster using T7 RNA polymerase is feasible, and (ii) whether the system is applicable in a broad range of host bacteria. T7 RNAP was shown to be particularly useful for the expression of clustered genes as it ignores bacterial termination sites and therefore synthesizes long transcripts (Arvani *et al.* (2012)). Due to the inability to use the suicide plasmid in our lab, we refrained from conjugating and integrating the PE cluster into the *E. coli* chromosomal. Rather, we utilized the system solely as a general vector for transformation.

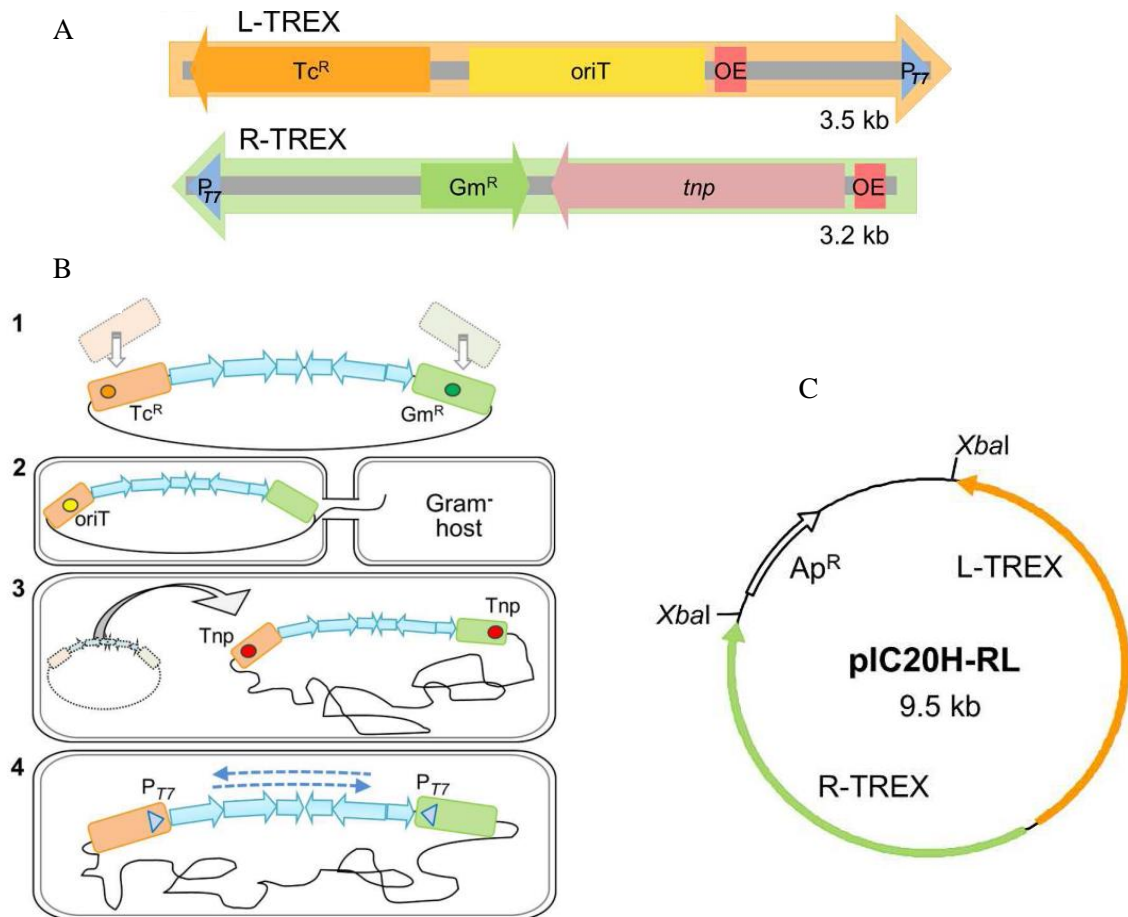


Figure 19. **A.** Structure and function of the pathway transfer and expression system TREX. The TREX system consists of two cassettes, the L-TREX (orange) and R-TREX (green) cassette, which comprise all elements for establishing a biosynthetic pathway in a heterologous bacterial host. Tc^R: tetracycline resistance gene (dark orange); oriT: origin of transfer (yellow); OE: outside end of transposon (red); P_{T7}: T7 bacteriophage promoter (blue); Gm^R: gentamicin resistance gene (dark green); tnp: transposase gene (light red). **B.** The expression procedure of all clustered genes. **C.** pIC20H-RL carrying the <L-TREX-R> module was constructed encompassing the L-TREX and R-TREX cassettes in an “inside-out” fashion with the T7 promoters pointing outward (indicated by arrow heads), flanked by XbaI restriction sites. Ap^R: ampicillin resistance gene. Figure adapted from Ref (Loeschcke *et al.* (2013))

To use this system for the expression of the PE cluster of *P. marinus* SS120 in *E. coli*, the gene cluster from *cpeB* at the 5'-end to *ppeC* at the 3'-end was amplified by PCR from genomic DNA. Using Gibson cloning, this ~ 6 kb fragment was cloned between the two TREX cassettes of the TREX system (Fig. 20). Two RBS were generated separately after T7 bacteriophage promoter (P_{T7}) because the pIC20H-RL vector did not contain the necessary expression elements, including RBS. The insertion of the fragment was verified via agarose gel electrophoresis using double digestion

(Fig. 21). For a functional PE cluster expression, the chromophore biosynthesis of PEB should also be involved in the system.

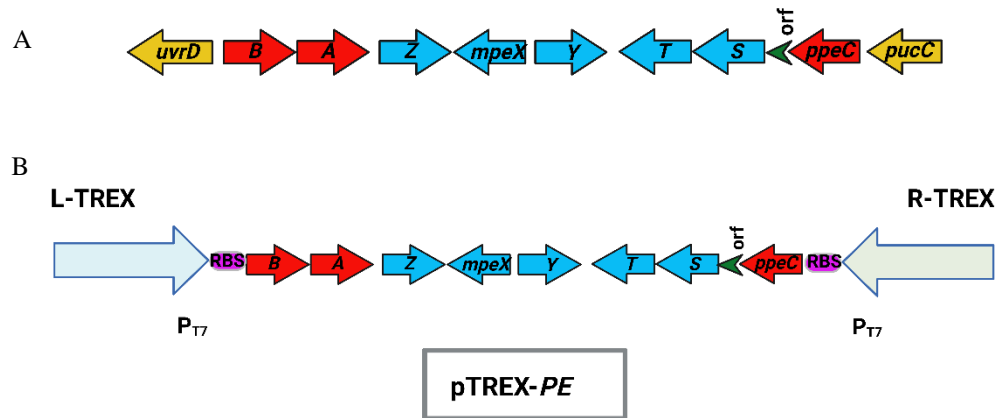


Figure 20. A. PE gene cluster in *P. marinus* SS120. B. Structure of the TREX labeled PE cluster. Red arrows correspond to genes encoding apo- or linker proteins (*cpeA*, *cpeB* and *ppeC*), blue arrows correspond to genes encoding putative PBP lyases (*cpeZ*, *mpeX*, *cpeY*, *cpeT* and *cpeS*). The green arrow depicts an open reading frame of an unknown function. Orange arrows mark the flanking genes *uvrD*, a DNA helicase and *pucC*, a bacteriochlorophyll synthase. Only the parts between the small red box from the PE cluster were integrated into the pIC20H-RL vector, including two RBS, and that the resulting plasmid was named pTREX-PE.

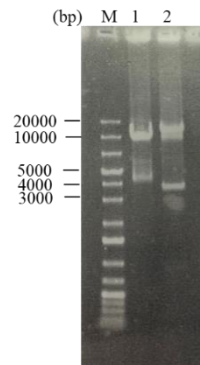


Figure 21. Agarose gel electrophoresis of pTREX-PE. Lane 1: *KpnI* digested pTREX-PE; Lane 2: *KpnI* and *MluI* double digested pTREX-PE. Fragment 1: 12002 bp; fragment 2: 3690 bp.

3.2.1 PE cluster transcription analysis in *E. coli*

An analysis of mRNA was conducted in *E. coli* cells to determine whether the T7 promoters of the pTREX-PE vector allowed for bidirectional transcription of cluster fragments. The RNA extraction protocol (described in chapter 2.3.3) was applied successfully for the isolation of RNA from *E. coli*

culture. Agarose gel electrophoresis of the isolated RNA demonstrated the presence of intact 23S, 16S and 5S rRNA molecules (Fig. 22A). RNA was of purity by PCR checking. Then, RNA was converted to cDNA using ProtoScript® II first strand cDNA synthesis (M-MuLV reverse transcriptase with reduced RNase H activity and increased thermostability). The calculated amount of cleaned-up cDNA mixture was estimated around 23.3 ng/μL. Serial dilutions of cDNA preparations were prepared (10^{-1} , 5×10^{-1} , 10^{-2}) and samples of each dilution were used as a template for PCR amplification. The PCR products were visible in all samples (Fig. 25B). It proved that genes inserted into the TREX system from *P. marinus* SS120 can be transcribed in *E. coli*.

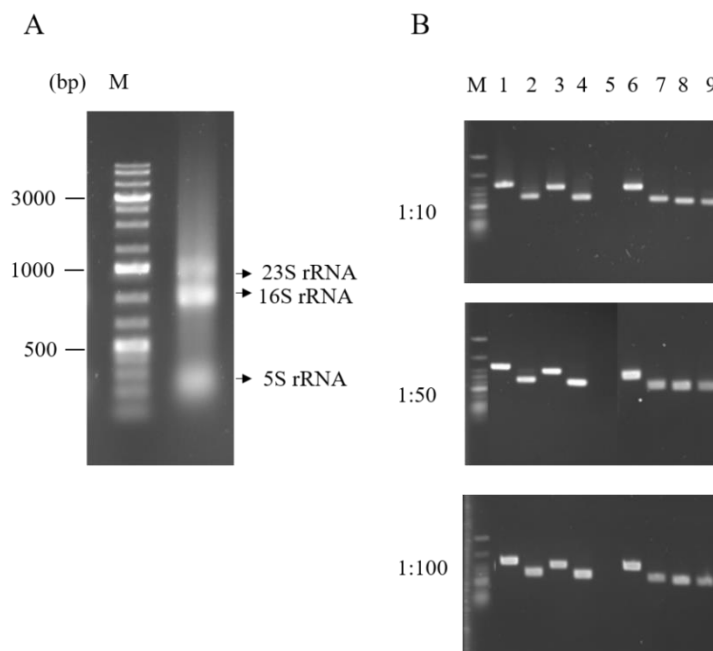


Figure 22. A. Agarose gel electrophoresis of 167 ng isolated RNA from *E. coli* pTREX-PE. B. Test PCR after cDNA synthesis of *E. coli* pTREX-PE. Lane 1-10: The synthesized cDNA was tested in PCR reactions with *rbla*, *rcpeB*, *rcpeA*, *rcpeZ*, *rcpeY*, *rppeC*, *rcpeS*, *rcpeT* and *rmpeX* primers. Afterward, agarose gel electrophoresis on 2 % agarose gel was performed. Amplified fragments using the following dilutions 1:10, 1:50, and 1:100 of 23 ng of cDNA as a template.

3.2.2 PE cluster translation analysis in *E. coli*

After confirming the transcription of the PE cluster from the pTREX-PE plasmid, the next step was to determine if the genes are also being translated in *E. coli*. Therefore, plasmid pTREX-PE, which comprises high-copy replication ori *pMB1*, was transformed both in *E. coli* BL21 (DE3) and PEB biosynthesis (PEB biosynthesis was encoded by the vector pTD*holpebS*) in *E. coli* BL21 (DE3). *E. coli* cells were incubated at 37 °C to allow for the selection of transposon mutants which showed

gentamicin resistance. PE genes expression was induced by adding 0.5 mM (final concentration) IPTG at an optical density of approximately 0.6 (OD_{600 nm}). As a negative control, a strain containing a plasmid with no fragment inserted was also cultured in the same conditions.

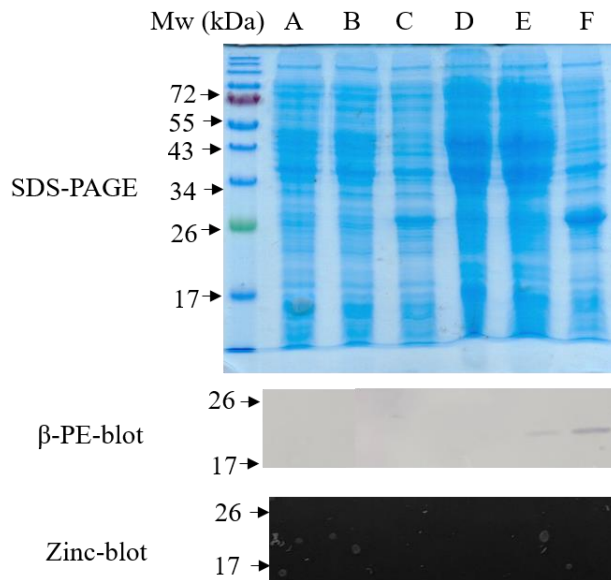


Figure 23. SDS-PAGE, β -PE-blot and zinc-blot of pTREX-PE test expression. Lane A-C: pIC20H-RL, pTREX-PE and pTREX-PE with pTDho1pebS before IPTG induction in *E. coli* BL21 DE3; Lane D-F: pIC20H-RL, pTREX-PE and pTREX-PE with pTDho1pebS after IPTG induction overnight.

Analysis of PE cluster translation was evaluated via SDS-PAGE, Western-blot. Samples were compared before and after induction. The SDS-PAGE did not show any specific bands, but the β -PE blot in lane E and F exhibited a clear signal at approximately 20 kDa, suggesting the production of CpeB (Fig. 23). Mass spectrum data further confirmed the translation of *cpeB*, but other essential PE assembly proteins, including CpeA, CpeZ, CpeY, MpeX, CpeT, CpeS, and PpeC, were not detected in the results. In the coexpression sample (pTREX-PE with pTDho1pebS), the signal was observed only in the western blot of β -PE and not in the zinc-blot. It was directly proven that PE-III could not be assembled by TREX system in the *E. coli*. Based on the findings, it can be concluded that even though only CpeB was identified, the genes responsible for PE assembly were transcribed. It is possible that the RBS of the PE cluster may not be recognizable by the *E. coli* system, resulting in the issue.

3.3 *cpeBA* expression in *Synechococcus* sp. PCC 7002

As the TREX system was not successful in producing PE-III in *E. coli*, a new approach was taken. As mentioned earlier, it is crucial to ensure that the ribosome recognizes the genes of the PE cluster correctly and initiates translation. The main challenge here is that the ribosome binding site (RBS) of *Prochlorococcus* is not easily identifiable by a suitable host. *Synechococcus* sp. PCC 7002 (*Syn.* 7002), a cyanobacterium related to *Prochlorococcus* species, is an ideal model for functional genomics and biotechnological applications through metabolic engineering. Additionally, *Synechococcus* sp. PCC 7002 does not possess any phycoerythrin. Therefore, it was selected as a host for *Prochlorococcus* gene expression to achieve PE cluster expression.

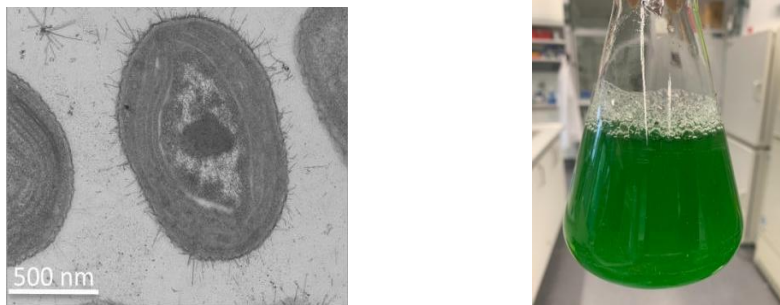


Figure 24. *Synechococcus* sp. PCC 7002 **A.** Transmission electron micrograph of *Synechococcus* sp. PCC 7002. Scale bar, 500 nm (Credit: original image by Prof. Donald Bryant's lab, Penn State University). **B.** *Synechococcus* sp. PCC 7002 in medium A⁺.

Synechococcus sp. PCC 7002 (*Agmenellum quadruplicatum* PR-6) is a unicellular, euryhaline cyanobacterium, which was isolated on Magueyes Island, Puerto Rico from “fish pens” in a mud sample (Fig. 24; Van Baalen (1962)). Under optimal conditions (38 °C, 1 % (v/v) CO₂ in air, at saturating irradiation of ~250 μmol photons m⁻² s⁻¹), it has a fast doubling time around 2.6 h with a reduced nitrogen source (Ludwig & Bryant (2012)). PBS of *Synechococcus* sp. PCC 7002 are assembled from rods containing two or three hexamers of phycocyanin (α-PC and β-PC) and a core containing three cylindrical subassemblies of allophycocyanin (Gómez-Lojero *et al.* (2003), Shen *et al.* (2008)). *Synechococcus* sp. PCC 7002 is an ideal host for functional genomics and biotechnological applications through metabolic engineering as it is naturally transformable with high recombination capacity (Stevens Jr & Porter (1980), Xu *et al.* (2011)). The genome has been completely sequenced, consisting of a 3 Mbp chromosome and six endogenous plasmids, denoted pAQ1 (4809 bp), pAQ3 (16,103 bp), pAQ4 (31,972 bp), pAQ5 (38,515 bp), pAQ6 (124,030 bp),

and pAQ7 (186,459 bp) (Roberts & Koths (1976)). The largest two plasmids (pAQ6 and pAQ7) always appear to have the same copy number as the chromosome. Methods of gene mutagenesis and overexpression have been established (Frigaard *et al.* (2004)). Although *Prochlorococcus* and *Synechococcus* differ in many ways, such as the photosynthetic apparatus, genome size and the ability to grow in oligotrophic waters (Rocap *et al.* (2003), Zhaxybayeva *et al.* (2009), Yu *et al.* (2012)), analysis of their 16S rDNA has shown a close phylogenetic relationship (Fig. 25). While whole-genome phylogenies clearly separate *Prochlorococcus* from *Synechococcus*, the phylogenies of many individual gene families cluster LL adapted *Prochlorococcus* more closely with *Synechococcus* than with HL adapted *Prochlorococcus*.

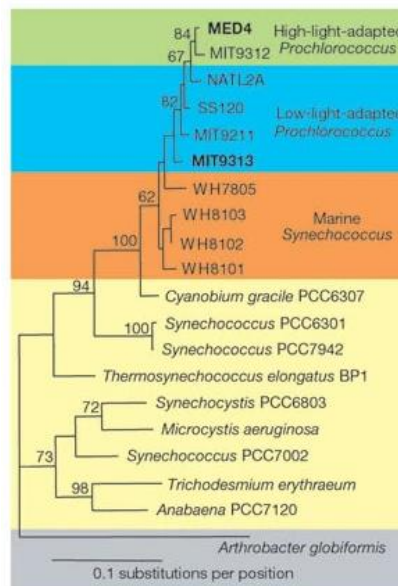


Figure 25. Relationships between *Prochlorococcus* and *Synechococcus* inferred using 16S rDNA (figure took from Rocap *et al.* (2003)).

There are several vectors constructed for gene expression in *Synechococcus* sp. PCC 7002, mostly derived from endogenous pAQ1. Plasmid pAQ1 is the smallest plasmid in *Synechococcus* sp. PCC 7002 and has the highest copy numbers (Akiyama *et al.* (1998)). It encodes three predicted genes and is absolutely indispensable for unknown reasons. An integrative expression vector usually consists of a gene expression cassette, selectable markers, two flanking DNA segments that facilitate recombination onto targeted neutral sites, and an *E. coli* replicon that allows plasmid duplication in *E. coli* (Fig. 26).

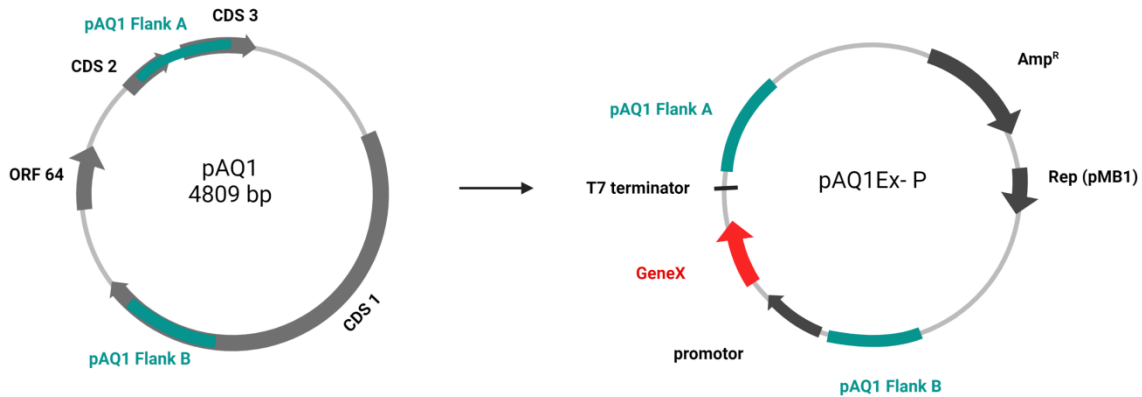


Figure 26. pAQ1 and a generic expression vector that can be used for the introduction of genes into *Synechococcus* sp. PCC 7002. (A) Endogenous, wild type plasmid pAQ1 from *Synechococcus* sp. PCC 7002. (B) A generic expression vector. Flank A and Flank B are regions of homology; Rep (pMB1) (origin of replication) are from pGEM-7zf; Amp^R (ampicillin resistance cassette).

Unlike other cyanobacteria models, only a few native promoters have been characterized in *Synechococcus* sp. PCC 7002 (Berla *et al.* (2013)). A lot of expression systems in *Synechococcus* sp. PCC 7002 are designed using heterologous constitutive promoters from *Escherichia coli*, P_{trc} , *Fremyella diplosiphon*, P_{cpeC} and *Synechocystis* sp. PCC 6803, P_{cpeB} and P_{psbA2} (Xu *et al.* (2011), Markley *et al.* (2015)). In addition, recently by overexpressing the riboflavin biosynthesis gene cluster from *Bacillus subtilis* in *Synechococcus* sp. PCC 7002, light-sensitive vitamin B2 could be successfully produced (Kachel & Mack (2020)).

3.3.1 Transformation of *Syn.* 7002 pAQ1::*GFP*

To have a positive control of this new system, linear fragments of DNA should be used to transform *Synechococcus* sp. PCC 7002. pAQ1::*GFP* plasmid was linearized by *AhdI* and immediately mixed with fresh liquid *Syn.* 7002 culture and incubated under saturating illumination overnight. After incubation, the mixture was transformed to a medium A⁺ agarose plate containing spectinomycin antibiotic. After having successfully isolated a single colony resistant to the antibiotic, detection of GFP expression in a fresh flask was performed. The GFP-overexpression accumulated a massive amount of GFP protein in the cells and a green color appeared masking the intrinsic red autofluorescence (Fig. 27).

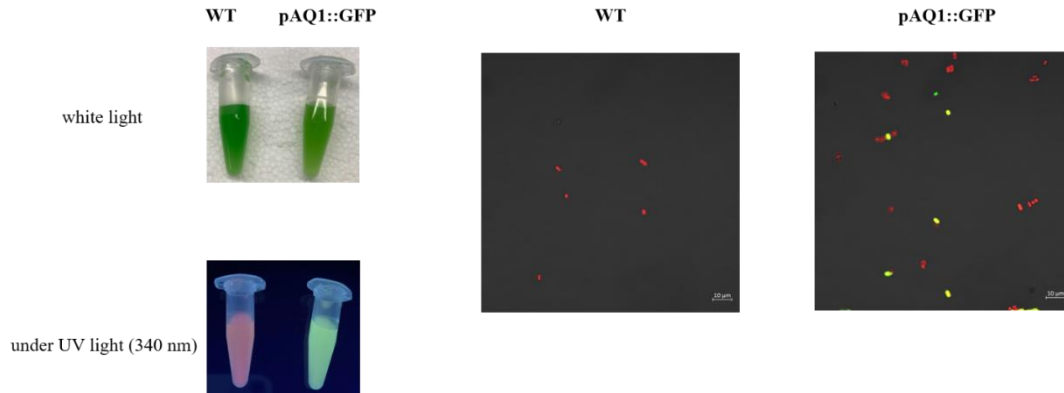


Figure 27. Comparison of *Syn. 7002* (WT) and *Syn. 7002* pAQ1::*GFP* cells under different light conditions and microscopy pictures. Under the white light, there is no visible difference, however, under the UV condition, the large amount of GFP protein hides the red fluorescence, showing green color. Images were acquired by fluorescence microscopy. The representative fluorescence images of WT (red colored) and over-expressed GFP (yellow colored) are shown in the right legend.

3.3.2 Construction of *Syn. 7002* pAQ1::*cpeBA*

To test, if the *Syn. 7002* could be an appropriated host for *Prochlorococcus* PE gene expression, two genes *cpeB* and *cpeA* were selected as a control. pAQ1-*cpeBA* plasmid was created following the AQUA cloning protocol (chapter 2.3.15). To facilitate later identification of the translation levels of the *cpeB* and *cpeA* genes, different tags were assigned to each gene at the cloning stage (Fig. 28).

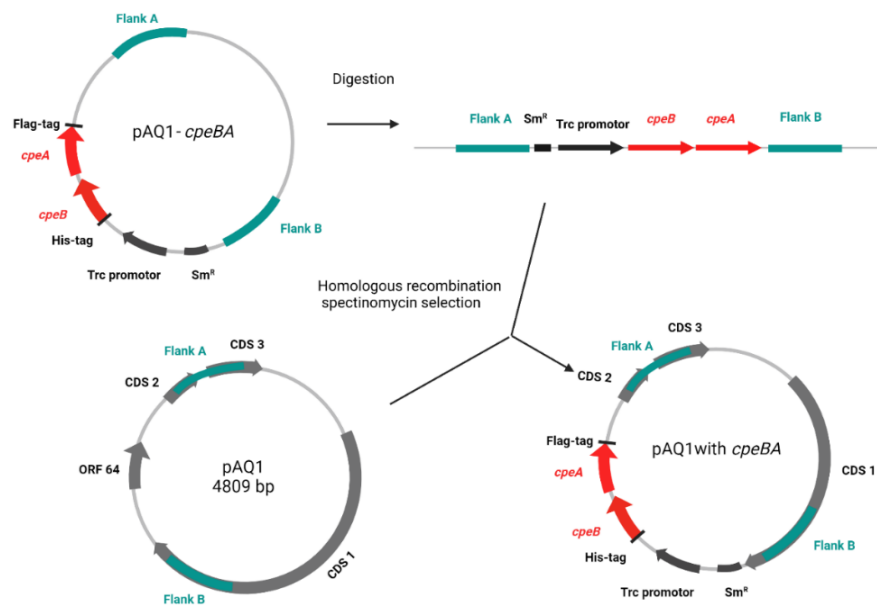


Figure 28. Construction of pAQ1::*cpeBA*. pAQ1-*cpeBA* assembly via AQUA cloning. pAQ1-*cpeBA* plasmid was linearized by AhdI (NEB) and immediately transformed into *Syn. 7002* and *Syn. 7002* tolerant strain. Using spectinomycin to do the selection. The *trc* promoter is constitutive, without *lacIq*.

Because medium A⁺ contains no organic carbon source, *Synechococcus* sp. PCC 7002 may exhibit slow growth when genes affecting the photosynthetic apparatus are expressed. Improved growth may be obtained by providing 10 mM glycerol, which allows mixotrophic (photoheterotrophic or heterotrophic) growth, as an additional carbon and energy source under such conditions. We prepared four different strains: *Syn.* 7002, *Syn.* 7002 “glycerol tolerant”, *Syn.* 7002 pAQ1::*cpeBA* and *Syn.* 7002 pAQ1::*cpeBA* “glycerol tolerant” and we grew them in medium A⁺ at 30 °C under the same saturating illumination (about 60 μE/m²s). Generally, tolerant cultures are growing almost twice as fast as non-tolerant (Fig. 29).

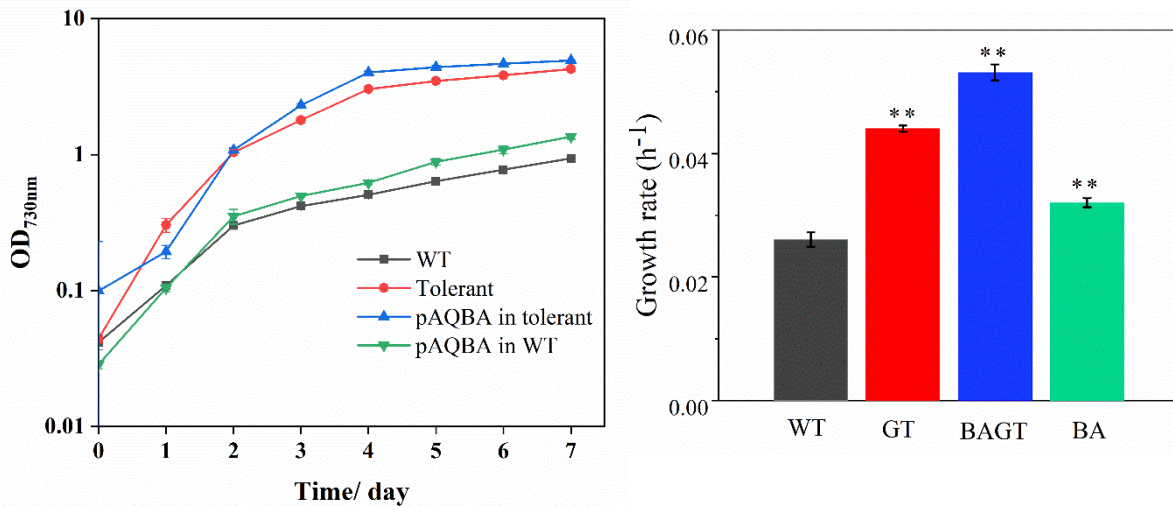


Figure 29. Growth curve of *Synechococcus* sp. PCC 7002. The shown graph displays three biological replicates, each consisting of three technical replicates. Error bars indicate the standard deviation. GT: Glycerol tolerant *Syn.* 7002; BAGT: *Syn.* 7002 pAQ1::*cpeBA* “glycerol tolerant”; BA: *Syn.* 7002 pAQ1::*cpeBA* (** P < 0.01, determined by Student’s T-test)

3.3.3 *cpeBA* transcription analysis in *Synechococcus* sp. PCC 7002

The RNA extraction protocol already described was applied successfully for the isolation of RNA from the *Syn.*7002 cultures. Residual DNA was removed using DNase I and an agarose gel electrophoresis of the isolated RNA showed the presence of intact 23S, 16S and 5S rRNA molecules (Fig. 30A). RNA purity was analyzed by PCR and then, the RNA was converted to cDNA (chapter 2.3.4). Calculated amount of cleaned-up cDNA mixture was estimated around 10.8 ng/μL. Serial dilutions of cDNA were prepared (1:5, 1:10, 1:20, 1:50) and samples of each dilution were used as a template for PCR amplification. The PCR products were visible in all samples (Fig.

30B). It proved that two genes *cpeB* and *cpeA* from *P. marinus* SS120 both can be transcribed in the *Synechococcus* sp. PCC 7002.

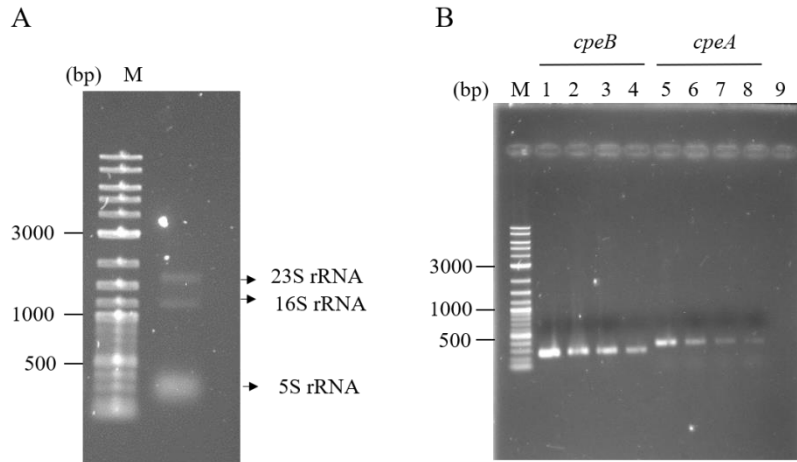


Figure 30. A. Agarose gel electrophoresis of 23 ng isolated RNA from *Syn. 7002* pAQ1::*cpeBA*; B. PCR after cDNA synthesis of *Syn. 7002* pAQ1::*cpeBA*; The synthesized cDNA was tested in PCR reactions with *rcpeB* and *rcpeA* primers. Afterwards agarose gel electrophoresis on 2 % agarose gel was performed. Lane 1-4: amplify *cpeB* fragment using 1:5, 1:10, 1:20, 1:50 dilution cDNA as template; Lane 5-9: amplify *cpeA* fragment using 1:5, 1:10, 1:20, 1:50 dilution cDNA as template; Lane 9: negative control, PCR with no template.

3.3.4 *cpeBA* translation analysis in *Synechococcus* sp. PCC 7002

After we confirmed that both *cpeB* and *cpeA* could be transcribed in *Syn.7002*, we checked whether each gene could be translated. Wild type and mutant strains of *Synechococcus* sp. PCC 7002 were standardly cultivated in Medium A⁺ at 30 °C under white light illumination on a shaker. Cells of 50 mL culture of *Syn. 7002* and *Syn. 7002* pAQ1::*cpeBA* were harvested when OD_{730 nm} reached 2.5 by centrifugation at 5000g, 4 °C, 5 min. Pelleted cells were resuspended in 10 mL lysis buffer (50 mM Na₂HPO₄, 300 mM NaCl, pH 7.5) and disrupted by sonication. Solubilized crude extracts of the wild type and the overexpressed *cpeBA* were prepared and analyzed via SDS-PAGE and western blot (Fig. 31).

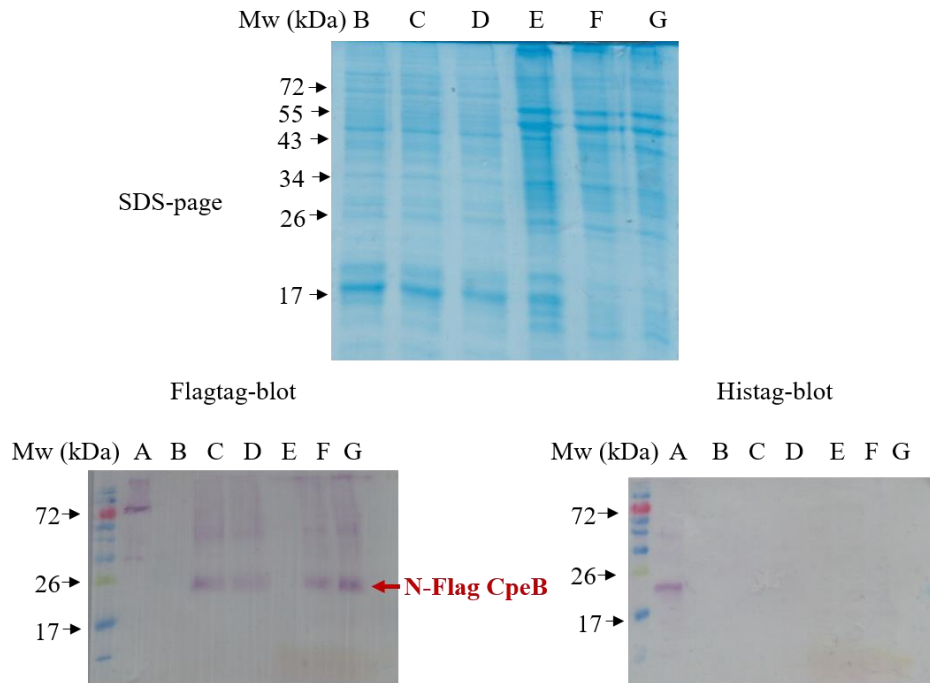


Figure 31. SDS-PAGE and Western blots of *Syn. 7002* (WT) and *Syn. 7002* pAQ1::*cpeBA* A: Positive control of Western-blot; B: Soluble fraction of *Syn. 7002* (WT); C: Soluble fraction of *Syn. 7002* pAQ1::*cpeBA* colonie1; D: Soluble fraction of *Syn. 7002* pAQ1::*cpeBA* colonie2; E: Insoluble fraction of *Syn. 7002* (WT); F: Insoluble fraction of *Syn. 7002* pAQ1::*cpeBA* colonie1; G: Insoluble fraction of *Syn. 7002* pAQ1::*cpeBA* colonie2; The calculated molecular weight of N-Flag CpeB is ~ 22.1 kDa. The calculated molecular weight of C-Histag CpeA is ~ 18.1 kDa.

Compared with the WT sample, there was an additional signal that appeared around 24 kDa in the flagtag western blot corresponding to the N-Flagtag CpeB (~ 22.1 kDa). However, when we analyzed the histag western blot, no signal corresponding to the Histag CpeA (~ 18.1 kDa) was detected (Fig. 31). To further detection of CpeA, we prepared 500 mL culture of *Syn. 7002* pAQ1::*cpeBA* for protein enrichment by affinity chromatography. Cells were disrupted by French Press and samples from each purification step were analyzed via SDS-PAGE and Western blot (Fig. 32). After affinity chromatography, the elution samples did not show a protein band corresponding to Histag CpeA. Concentrated elution fractions pool also did not show any purified protein or western blot signal. On the other hand, three bands appeared in the zinc-blot which corresponded to phycobiliprotein β -PC, α -PC and β -APC. Overall, although *cpeB* and *cpeA* two genes both could be transcribed in the host, only CpeB was translated. A possible reason for this observation could be the cyanobacterium host *Syn. 7002* can not identify the RBS of *Prochlorococcus*.

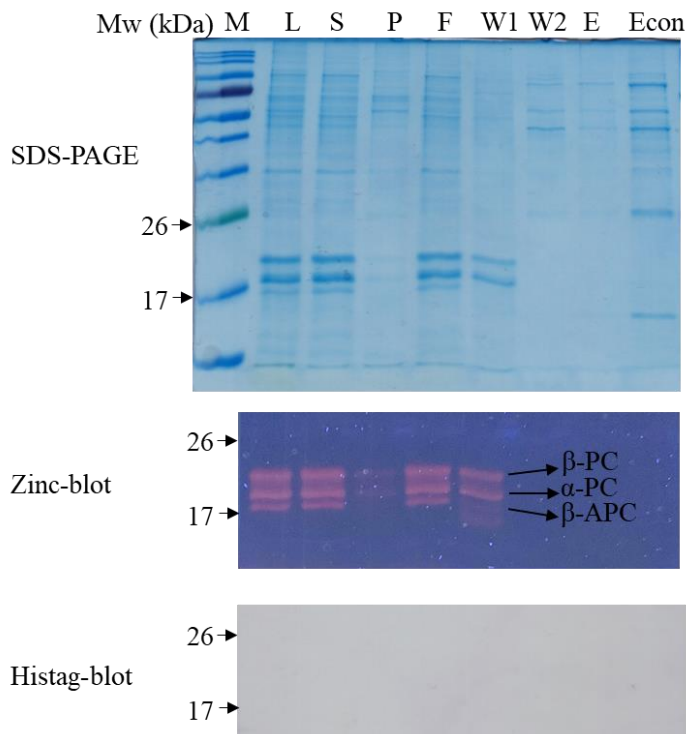


Figure 32. SDS-PAGE, zinc-blot and Western blot of the affinity chromatography purification samples of Histag CpeA. L: Lysate; S: Soluble fraction; P: Insoluble fraction; F: Flow-through fraction; W1: Washing fraction without imidazole; W2: Washing fraction with 10 mM imidazole; E: Elution fraction; Econ: Concentrated elution fraction. zinc-blot detected under 380nm.

3.3.5 Isolation of phycobiliprotein from *Synechococcus* sp. PCC 7002

Although we confirmed that CpeB can be overproduced in *Synechococcus* sp. PCC 7002, whether it can assemble into phycobilisomes still needs further studies. Amino acid sequence analysis of SS120 CpeB showed 59 % similarity with the PC β -subunit (CpcB) and 63 % identity with the APC β -subunit (ApcB) of *Synechococcus* sp. PCC 7002 (Fig. 33). In *Syn.* 7002, it has been proven that ApcB binds one PCB at Cys-81 and CpcB has two PCB attaching sites, Cys-82 and Cys-153 respectively (Shen *et al.* (2008)). While *P. marinus* CpeB also shows binding possibility at both residues.

CpcB	MFDIFTRVVSQADARGEFISSDKLEALKKVAEGTKRSDAVSRMTNNAASSIVTNAARQLF	60
CpeB	MLDAFSRAVVSADSKGATIGSAELSSLRKYVADANKRIDATLAIQTQNVSCIAADAISGMV	60
ApcB	MQDAITSVINSADVQGKYLDGSAMDKLGKAYFTTGALRVRAASTISANAAAIVKEAVAKSL	60
	* * :: .: .* * : * . . . : * : .: . * * . : : * . . * . : *	
CpcB	ADQPQLIAPGGNAYTNRRMAACL	120
CpeB	CENTGLTQPGGHCPTRRMAACL	120
ApcB	-LYSDVTRPGGNMYTTRRYAAC	119
	: * * * : * . * * * * : * * * : * * : * * * * * : * * * * * : *	
CpcB	GVPGASVAAGVRAMGKAAVAIVMDPA-----G---VTSGDC	170
CpeB	GVPLSNAIRAIEIMKIATVAIMTETNSGRKMFEGINSGSGAEC	180
ApcB	GVPVGSTVQAIQAMKEVTAGLVGADA-G-----	159
	* * * : * : * * * : * * * : * * * : *	
CpcB	VE	172
CpeB	LN	182
ApcB	LS	161
	:.:	

Figure 33. Sequence alignment of the amino acids of the β -subunits CpcB: *Synechococcus* sp. PCC 7002 PC; ApcB: *Synechococcus* sp. PCC 7002 APC; CpeB: *Prochlorococcus marinus* SS120 PE. Red box marked cystine residue attached to phycocyanobilin. Figure was prepared with Mega 11.

Once, the transformation of the *cpeBA* into *Synechococcus* sp. PCC 7002 has been successful it was investigated if the overexpressed protein CpeB from *Prochlorococcus* can be involved in PBS assembly in the host strain. After examination of the growth of this cyanobacterial strain (Fig. 29), isolation of PBSs of mid-exponential growing cultures was conducted. Separation of PBS was performed using a discontinuous sucrose gradient. The obtained colored layers were isolated and further analyzed using UV/Vis spectroscopy (Fig. 34). Absorbance peaks are characteristic for the different phycobiliproteins. Phycocyanin (PC) is blue and absorbs at $\lambda_{\max} = 610-620$ nm, whereas allophycocyanin (APC) is light blue and shows absorbance at $\lambda_{\max} = 650-655$ nm. The displayed colored fractions obtained is light blue. Peak 1 and peak 2 fractions both show an absorption maximum at ~ 630 nm thus probably representing the PC. The absorption spectrum of the Peak 3 fraction shows two maxima at ~ 626 nm and ~ 646 nm, which is probably a blended sample containing PC and APC. Prolonged centrifugation or an adapted sucrose gradient should be tested in order to achieve better separation and thus pure fractions.

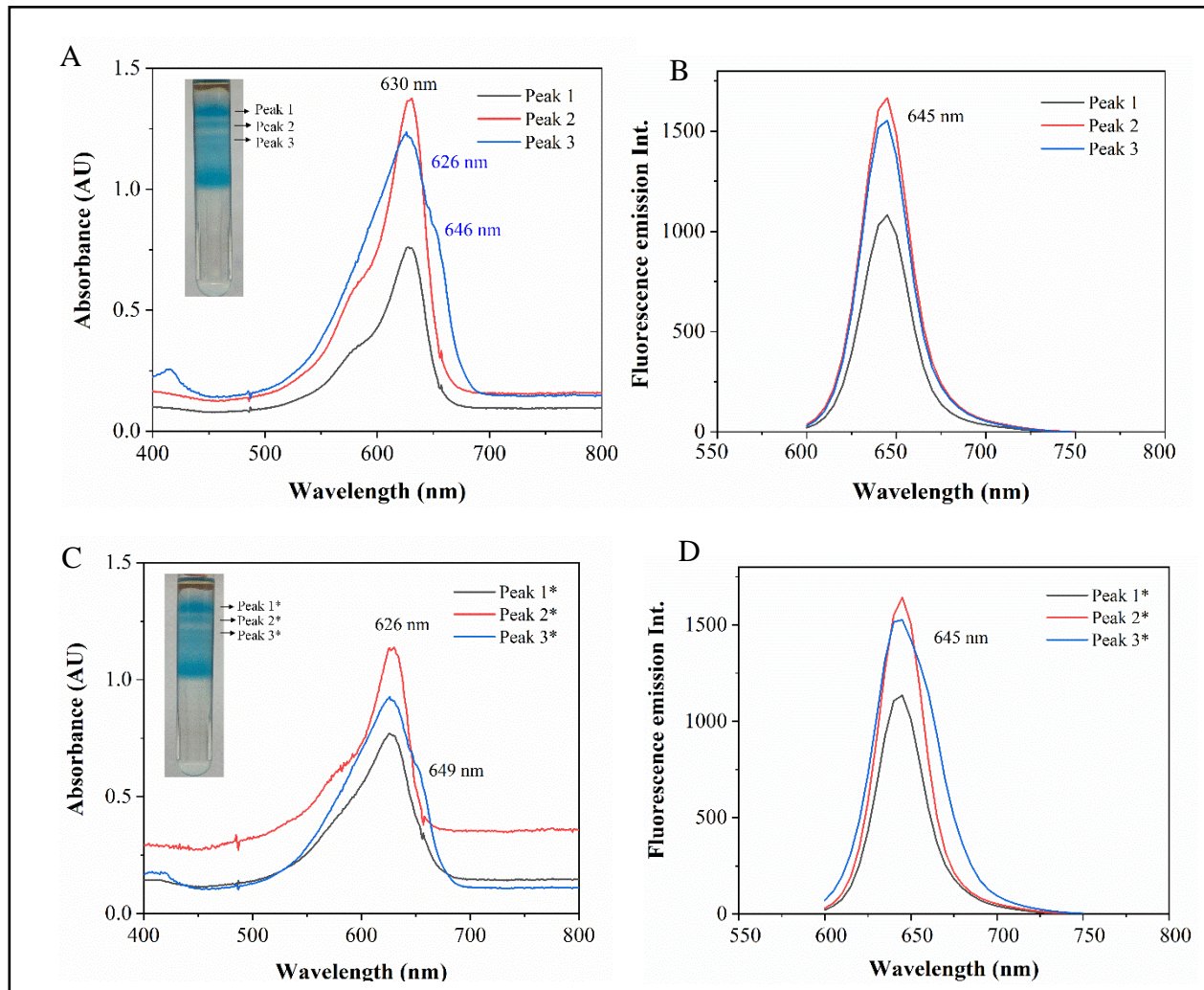


Figure 34. Separation of *Syn. 7002* (WT) and *Syn. 7002 pAQ1::cpeBA* cell lysate by discontinuous sucrose density gradient and UV/Vis analysis. UV/Vis, Fluorescence spectra of *Syn. 7002* (WT) of respective colored fractions harboring phycobiliproteins (A-B). UV/Vis, Fluorescence spectra of *Syn. 7002 pAQ1::cpeBA* of respective colored fractions harboring phycobiliproteins (C-D). Sucrose density gradient consisting of 0.5 M, 0.75 M, 1 M and 1.5 M sucrose dissolved in potassium-phosphate buffer 0.75 M (pH 7). Centrifugation was carried out at 18 °C for 15 h in an ultracentrifuge (L8-M ultracentrifuge, Beckman Coulter-swing-out rotor SW 40) at 120 000g.

The obtained fractions were applied to SDS-PAGE with heating the samples beforehand. The SDS-PAGE shows the proteins present in each fraction (Fig. 35). Signals in all fractions at ~ 18 kDa are visible in the zinc blot, which only detects covalently chromophorylated proteins, i.e. phycobiliproteins. The further signals on the SDS-PAGE represent, among others: linker proteins of the phycobilisome and other non-pigment harboring proteins that were isolated. Except for the phycobiliproteins, no other protein in the purified sample should be chromophorylated thus not be

detectable in the zinc blot. Signals on the flag tag blot only appeared in the *Syn. 7002* pAQ1::*cpeBA* lysate fractions which confirmed CpeB can integrate into the host phycobilisome. Most possibility is instead part of CpcB's function. In conclusion, it can be proven that expression of *P. marinus* SS120 leads to CpeB protein synthesis and likely assembly into the host PBS.

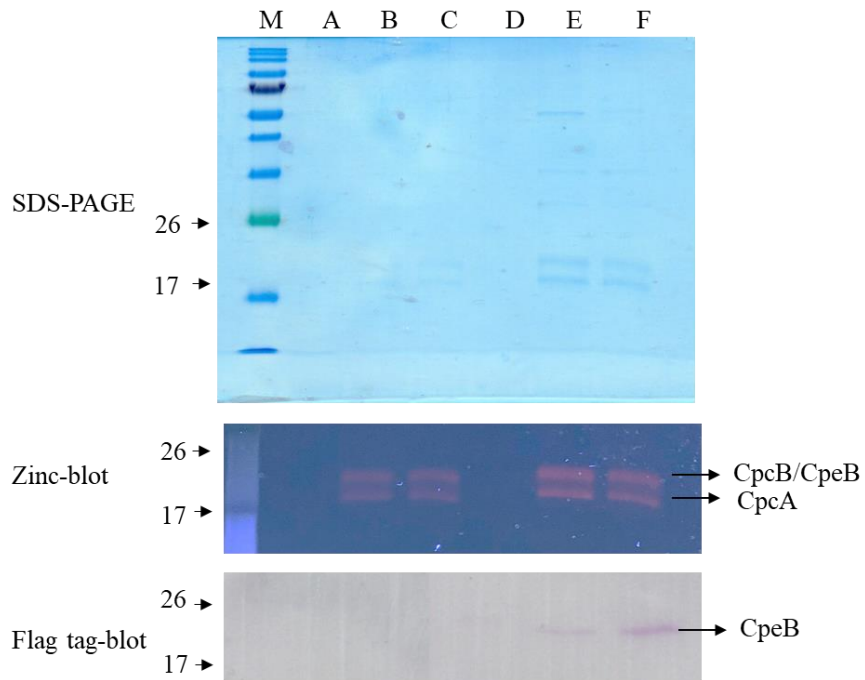


Figure 35. SDS-PAGE and zinc-blot of fractions obtained after ultracentrifugation of *Syn. 7002* (WT) and *Syn. 7002* pAQ1::*cpeBA* lysate. Lane A: Peak 1 of WT; Lane B: Peak 2 of WT; Lane C: Peak 3 of WT; Lane D: Peak 1* of *Syn. 7002* pAQ1::*cpeBA*; Lane E: Peak 2* of *Syn. 7002* pAQ1::*cpeBA*; Lane F: Peak 3* of *Syn. 7002* pAQ1::*cpeBA*. (CpcB is 18.3 kDa; CpcA is 17.6 kDa; ApcB is 17.2 kDa; N-Flag CpeB is ~ 22.1 kDa)

3.4 *In vivo* characterization of different lyases involved in the chromophorylation of PE-III

Another approach to investigate the chromophorylation of PE-III and to determine the PBP lyases required for chromophorylation was a heterologous *E. coli* expression using the pDuet™ vector system (Novagen-Merck). Compared to the TREX cluster system, it helps to dissect the function of the individual lyases. Genes were expressed using compatible vectors and different combinations of lyases were tested for their activity on the PE-III subunit (CpeB and CpeA). The created recombinant strains included an expression vector containing either *cpeB* or *cpeA*, along with a plasmid responsible of the phycobilin biosynthesis machinery (PEB, PCB and PUB) by using the genes *hoI*, *pebS*, *pcyA* and *PUBS*.

3.4.1 CpeS is a lyase specific for attachment of 3Z-PEB to Cys82 of CpeB

Chromophore binding is particularly pronounced with the S-type lyases (Zhao *et al.* (2006)). According to the X-ray crystal structure of the CpcS/CpcU family, lyases in this group possess a 10-stranded anti-parallel β -sheet with a beta-barrel fold with an α -helix (Kronfel *et al.* (2013)). The main feature of the S/U lyases is high binding site specificity, but a very low specificity for the chromophore and the receptor apoprotein. For example, CpcS from *Nostoc* sp. PCC 7120 rapidly forms an adduct with PCB and the latter can be transferred in a much slower reaction to cysteine 84 of the β -subunits of phycocyanin or phycoerythrocyanin (Zhao *et al.* (2006)).

The best results in heterologous expression of the genes encoding the PE components from *P. marinus* SS120 were obtained for CpeS. In *P. marinus* SS120, the 543-bp *cpeS* gene is located ~200 bp upstream from the *ppeC* operon. To gain insight into the potential role of CpeS (20.6 kDa) we analyzed its predicted amino acid sequence and we found 41-74 % sequence similarity to phycobiliprotein lyases. CpeS showed 50 % similarity to TeCpcS from *Thermosynechococcus elongatus* BP-1 and 67 % to MED4CpeS from *Prochlorococcus marinus* MED4 respectively (Fig. 36). When the *Prochlorococcus marinus* SS120 CpeS phycobiliprotein lyase was co-expressed in *E. coli* with the biosynthetic genes of PEB and the apoprotein CpeB, a strong pink staining of the cells was observed. Analysis of the purified HT-CpeB confirmed that CpeS from *P. marinus* SS120 is a specific lyase for attachment of 3Z-PEB to Cys82 of CpeB.

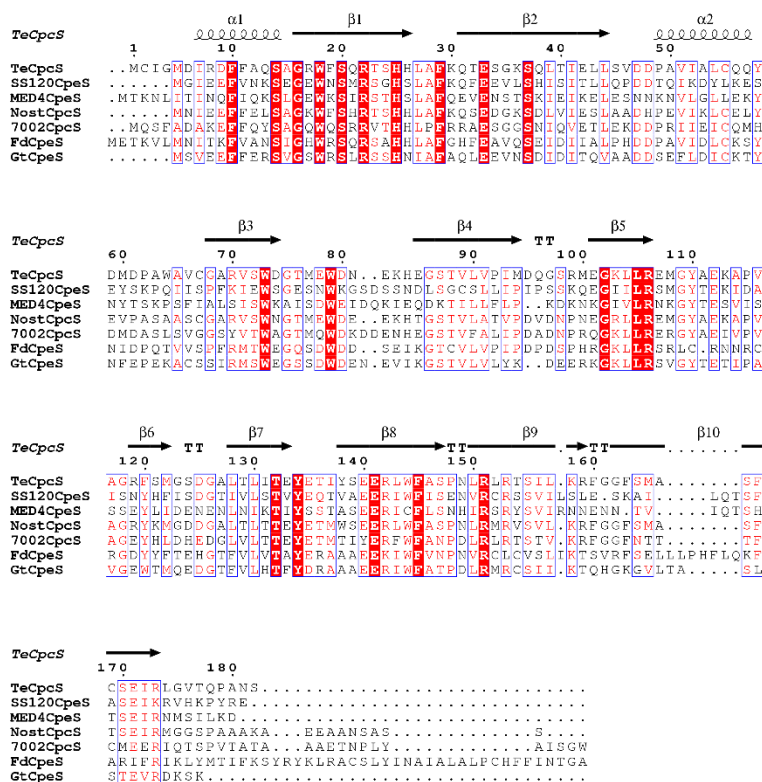


Figure 36. Multiple sequence alignment of representative S-type lyases. For each sequence, the name of the organism appears before the protein: *Thermosynechococcus elongatus* BP-1 (Te), *Nostoc* sp. PCC 7120 (Nost), *Synechococcus* sp. PCC 7002 (7002), *Fremyella diplosiphon* (Fd) and *Guillardia theta* (Gt). Identical and conservatively replaced residues in all sequences are shown in red and blue box, respectively. Secondary structural elements, observed in the crystal structure of TeCpcS, are shown above the alignment with α -helices and β -strands represented by rectangles and arrows, respectively.

3.4.1.1 Identification of the chromophore used by the CpeS lyase

To identify the PEB isomer of the CpeS: PEB complex, the purified complex was prepared with 0.1 % TFA solution. The phycobilin was further isolated through a Sep-Pak filter and a HPLC analysis was performed (Phenomenex - Luna 5 μ m C18 (2) 100 Å). By comparison with 3(*E*)- and 3(*Z*)-PEB standards, the chromophore bound to the CpeS was identified as 3(*Z*)-PEB. The small amounts of the 3(*E*)-PEB isomer in the sample are due to the processing procedure. The 3(*Z*)-PEB is extremely temperature-sensitive and changes to 3(*E*)-PEB when the temperature is increased.

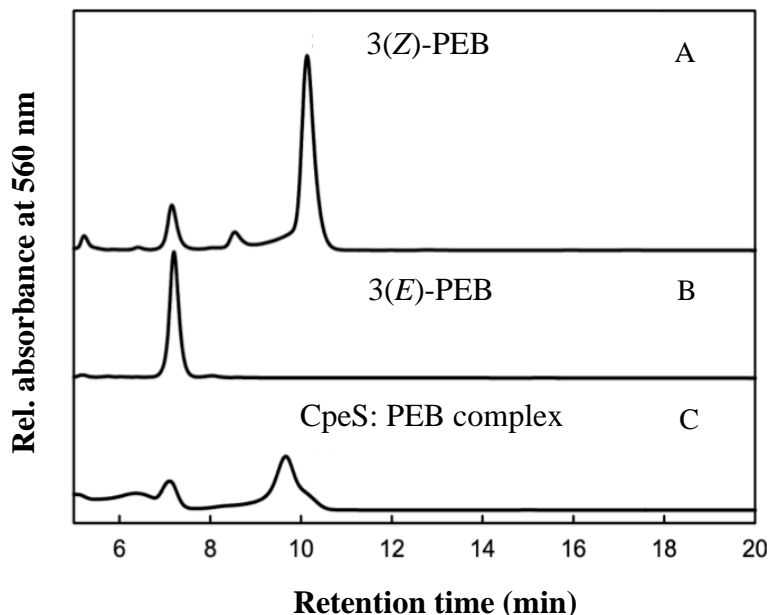


Figure 37. HPLC analysis of the PEB isomer from the CpeS: PEB complex. The isolated isomer was compared with phycobilin standards **A**) 3(Z)-PEB and **B**) 3(E)-PEB. **C**) The PEB from the CpeS: PEB complex could be identified as 3(Z)-PEB. The mobile phase consisted of 50 % (v/v) acetone and 50 % (v/v) 20 mM formic acid. Relative absorbance at 560 nm. (Figure adapted to Julia Schwach)

3.4.1.2 Size exclusion chromatography of HT-CpeB coproduced with CpeS

A heterologous *E. coli* expression system (pETDuet-1-*cpeB*; pCDFDuet-1-*cpeS*; pTD*holpebS* (no His)) was used to determine the function of CpeS. An analysis of HT-CpeB coproduced with CpeS lyase is given in Fig. 38, including SDS-PAGE and zinc-induced fluorescent assay. To test CpeB for covalent bound bilins the SDS-PAGE gel was subjected to zinc acetate. Samples coming from coexpression with the lyase gene *cpeS* exhibited fluorescence at 312 nm, indicating bound chromophore(s). After affinity chromatography, the elution fractions showed several bands on SDS-PAGE and only one signal on zinc-blot.

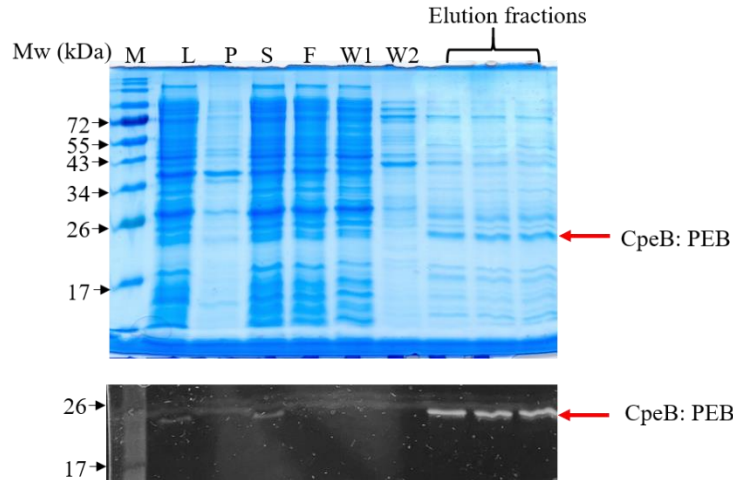


Figure 38. SDS-PAGE and zinc-blot of HT-CpeB purified by affinity chromatography. M: Protein marker (color prestained protein standard broad range (10-250 kDa); NEB); L: Lysate; P: Pellet; S: Supernatant; F: Flow-through; W1: Washing fraction without imidazole; W2: Washing fraction with 10 mM imidazole. The elution fractions of HT-CpeB (MW = 20.9 kDa).

For further purification and follow-up analysis of HT-CpeB, a SEC was performed. After affinity chromatography, the eluted CpeB was concentrated and was separated on the Superdex™ 75 10/300 GL column (GL Healthcare). The purified CpeB:PEB showed an elution volume of ~ 9.754 mL (Fig. 39 A). Based on the calibration curve (Fig. 39 C), this corresponds to a relative MW of ~ 47.1 kDa. The estimated molecular weight of the protein is ~ 20.9 kDa. Hence, the purified HT-CpeB is most likely present as a dimer and the minor peaks eluting at smaller volumes are most likely caused by impurities of the sample.

Another question that should be addressed was, whether it is possible to distinguish between a dimer and a trimer, if they have a similar shape and diameter. Therefore, the same protein sample was also separated on the Superdex™ 200 Increase 10/300 GL column (Fig. S1). According to the MW standards HT-CpeB eluted as a complex of ~ 45 kDa at 14.578 mL (Fig. 39C). which correlates with the calculated mass of a homodimer (41.8 kDa). The slight difference between the calculated and the determined MW is most likely related to the shape of the protein. Nevertheless, it can be concluded that HT-CpeB is present as a dimeric state after purification. The model is shown in Fig. 40.

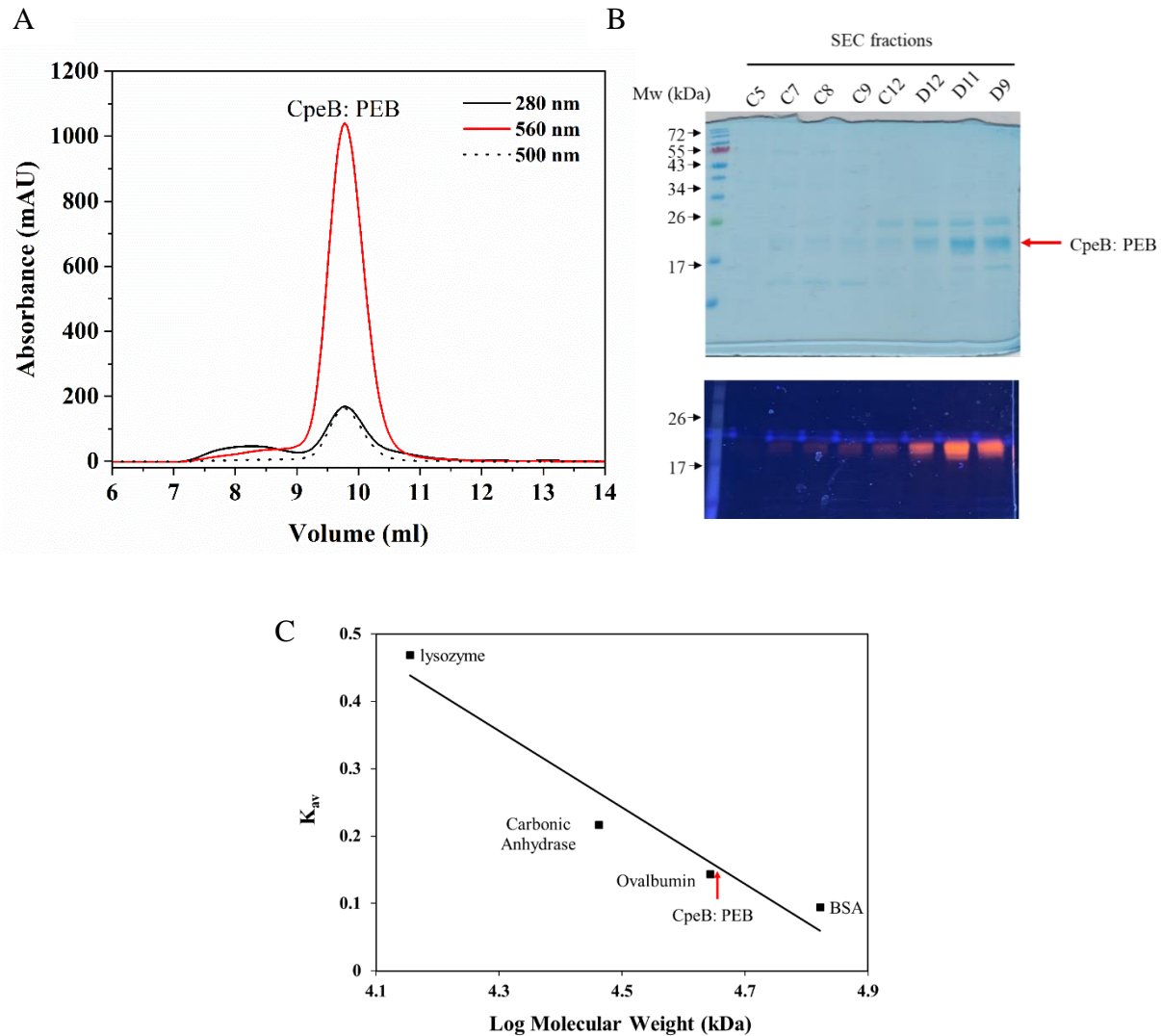


Figure 39. Size exclusion chromatography (SEC) of HT-CpeB coproduced with CpeS lyase from *E. coli*. **A.** The SEC elution profile of CpeB:PEB (CpeS) produced in *E. coli* BL21 (DE3). The protein was separated via a Superdex™ 75 10/300 GL column (GE Healthcare), sample volume 500 μ L, flow rate 0.1 mL/min with Na_2HPO_4 buffer and the absorbance was monitored at 280 nm, 500nm and 560 nm wavelengths. **B.** Elution fractions (C5-D9) were separated by SDS-PAGE and analyzed by Coomassie staining and zinc-induced fluorescence. **C.** The SEC standard curve in Na_2HPO_4 buffer and the calculated size of CpeB:PEB (CpeS) produced in *E. coli* BL21 (DE3). Molecular weight of standard proteins: Blue Dextran (2000 kDa), bovine serum albumin (66.4 kDa), Ovalbumin (44 kDa) and carbonic anhydrase (29 kDa), lysozyme (14.3 kDa). Void volume (V_0) correlates with V_e of Blue Dextran. The elution volume of standards with known molecular weight was used to determine the oligomerization state of CpeB

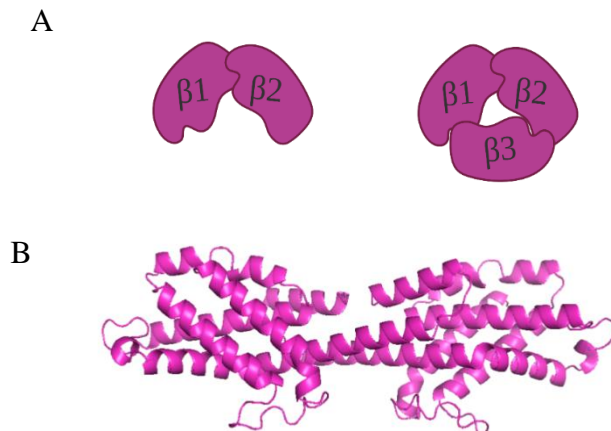


Figure 40. The model of CpeB oligomerization state from *E. coli*. **A.** Two hypothetical schematic oligomerization states are represented. The angle between two subunits had to be decreased to fit in a third unit. **B.** Modified dimer model by AlphaFold. The model even showed a maximum diameter of 96.8 Å with pLDDT 88, ptmscore 0.822. The model was predicted by AlphaFold and the maximum diameter was given by HullRad.

3.4.1.3 Characterization of HT-CpeB coproduced with CpeS

After SEC, purified HT-CpeB was analyzed by SDS-PAGE and Western blots (Fig. 41A). After separating the purified HT-CpeB on SDS-PAGE, the bilin content of each protein was examined by zinc-enhanced fluorescence staining of the SDS-polyacrylamide gel. During the SEC step, CpeB:PEB complex shows a single band. CpeB accumulated in soluble form in *E. coli* after PEB was covalently attached in the presence of CpeS. Fig. 41B shows the absorbance and fluorescence emission spectra of the resulting CpeB product after purification from cells producing CpeS. The CpeB:PEB produced in the presence of CpeS had an absorbance maximum at 555 nm and a fluorescence emission maximum at 567 nm. No significant ligation of PEB to CpeB occurred in the absence of CpeS (Table S1).

Purified HT-CpeB was digested with trypsin and resulting peptides were desalted via a C18 Sep-Pak column (Waters). Peptides were separated by HPLC on a Jupiter C4 (300 Å) column (Phenomenex). Isolated chromopeptides were dissolved in 50 % acetonitrile, 1 % TFA, and analyzed by HPLC and MS/MS. HPLC analysis gave the major peak for a chromopeptide with a retention time of ~ 8.8 min and a strong absorption at 556 nm (Fig. 42B, peak 1). Two minor peaks were detected for peptides eluting slightly earlier, with absorption at 542 nm and 548 nm separately (Fig. 42B, peaks 2 and 3). MS/MS were used to identify the peptides from the sample (Dr. Jonathan C. Trinidad, Director of Biological Mass Spectrometry, Department of Chemistry, Indiana University). Evidence was found for PEB attachment at Cys82 on two peptides((R)MAACLR(D)

and MAACLR) of CpeB. A review of the tandem mass spectra did not show an attachment to any other peptide. These results confirm that the CpeS bilin lyase specifically attaches PEB to Cys82 of CpeB.

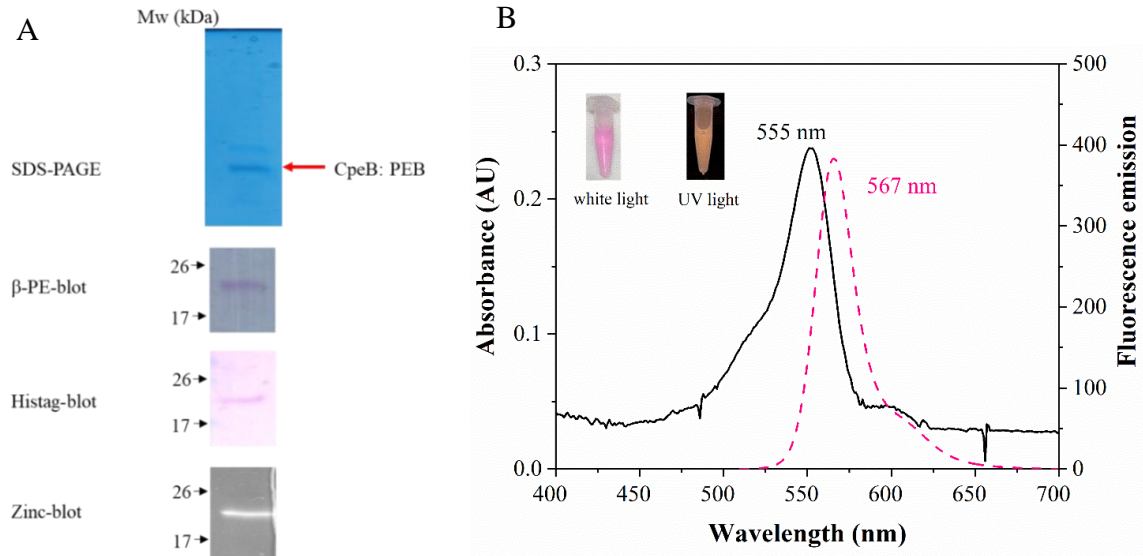


Figure 41. Analyses of purified HT-CpeB coproduced with CpeS lyase A. purified HT-CpeB was analyzed by SDS-PAGE, immunodetection with β -PE and Histag and zinc-induced fluorescence B. Absorbance (solid line) and fluorescence emission (dashed line, excitation set at 490 nm) spectra of purified HT-CpeB obtained from *E. coli*.

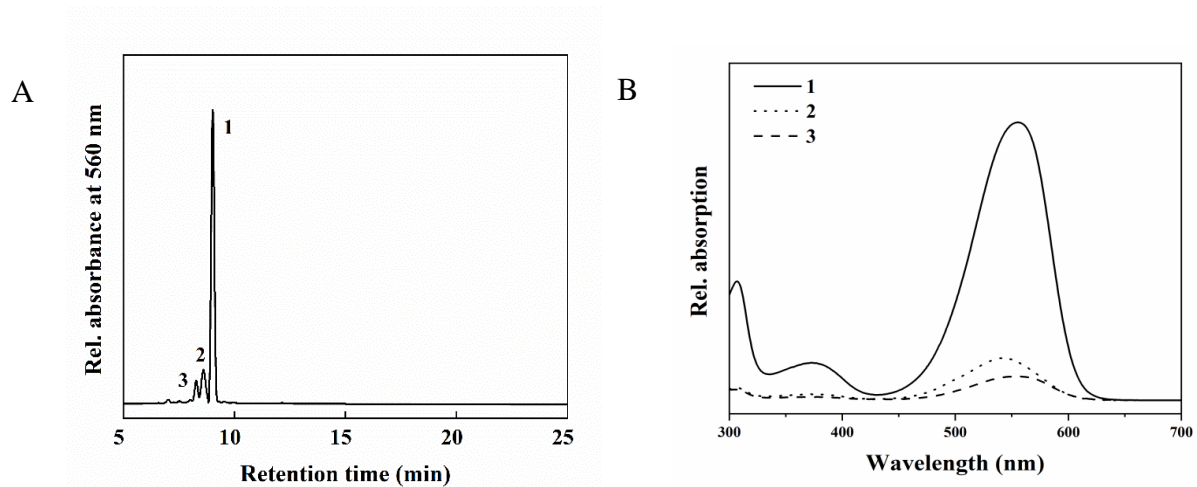


Figure 42. HPLC separation of tryptic bilin peptides of HT-CpeB coproduced with CpeS lyase A. HPLC elution profiles of tryptic bilin peptides of HT-CpeB. HT-CpeB was reconstituted with CpeB, CpeS and PEB as indicated HPLC elution spectrum. The elution profile shows the absorption at 560 nm. B. Three different bilin peptides (1, 2, 3) were obtained and their absorption spectra were in HPLC solvent.

3.4.2 Analysis of recombinant T-type lyases on HT-CpeB

CpcT-type lyases are similar in structure to CpcS/U-type lyases and consist of a calyx-shaped β -barrel fold (Zhou *et al.* (2014)). Until now, only two T-type lyase structures are reported (Zhou *et al.* (2014), Gasper *et al.* (2017)). Comparison with CpcT shows that P-HM1CpeT is smaller, which might be expected for a viral protein. P-HM1CpeT adopts a typical barrel-like fold with 10-strands. When aligned of T-type lyase sequences, several highly conserved amino acid residues are apparent (Fig. 43). Residues that may be important in bilin binding include Glu-54, Asp-165, Gln-55, and Asn-20 (using *Nostoc* sp. PCC 7120 CpcT numbering). There are two highly conserved cysteines (Cys-116 and Cys-137) and additional His-33 that could play roles in catalysis or in transient bilin binding (Zhao *et al.* (2005), Shen *et al.* (2006)).

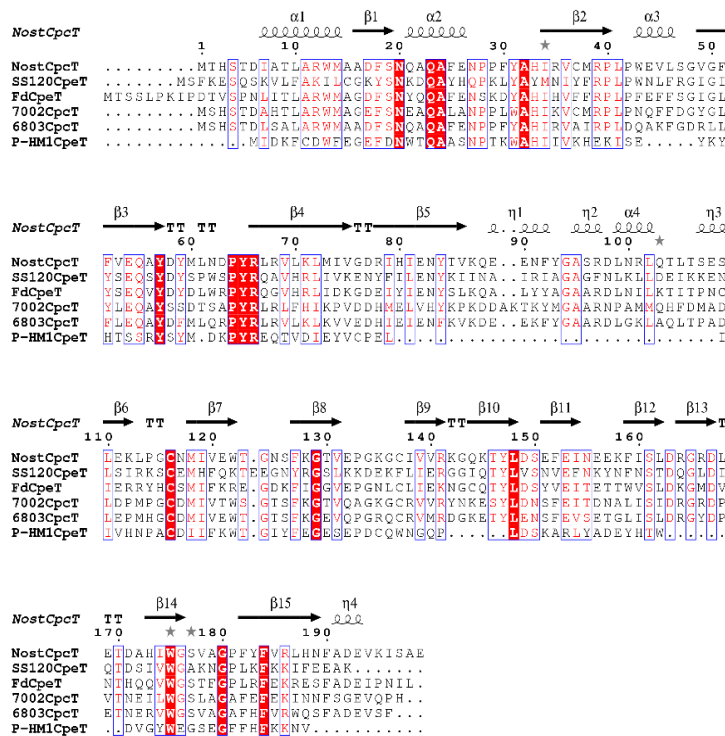


Figure 43. Multiple sequence alignment of representative T-type lyases. For each sequence, the name of the organism appears before the protein: *Nostoc* sp. PCC 7120 (Nost), *Synechococcus* sp. PCC 7002 (7002), *Fremyella diplosiphon* (Fd), *Synechocystis* sp. PCC 6803 (6803) and *Prochlorococcus phage P-HM1* (P-HM1). Identical and conservatively replaced residues in all sequences are shown in red and blue box, respectively. Secondary structural elements, observed in the crystal structure of NostCpcT, are shown above the alignment with α -helices and β -strands represented by rectangles and arrows, respectively.

3.4.2.1 T-type lyases binding PEB

In this part, it was demonstrated that lyases CpeT from *Prochlorococcus marinus* SS120 (SS120CpeT) and CpeT from *Prochlorococcus phage* P-HM1 (P-HM1CpeT) both can bind PEB. Lyase *SS120cpeT* was overexpressed in *E. coli* BL21(DE3) as a recombinant protein attached to the trigger factor chaperon (TF) and containing the His-Tag to produce TF-SS120CpeT: PEB. Cells were induced by addition of 0.4 mM IPTG at 30 °C for 2 h, followed by 15 °C overnight incubation. The result suggested that TF-SS120CpeT can bind PEB as it was detected by its fluorescence emission at 635 nm (Fig. 44).

In a similar manner, lyase *cpeT* from *Prochlorococcus phage* P-HM1 was overexpressed as a fusion protein containing an N-terminal StrepII-tag (StrepII-P-HM1CpeT) and produced in *E. coli* BL21 (DE3) in combination with the biosynthetic gene cluster of the phycobilin PEB. The resulting complex after the co-production was characterized by strong fluorescence and high stability. After affinity chromatography purification, the StrepII-P-HM1CpeT: PEB complex shows a strong fluorescence emission at 617 nm (Fig. 45). The PEB isomer of the complex was identified as the 3(Z)-isomer of PEB by HPLC (Gaspar *et al.* (2017)).

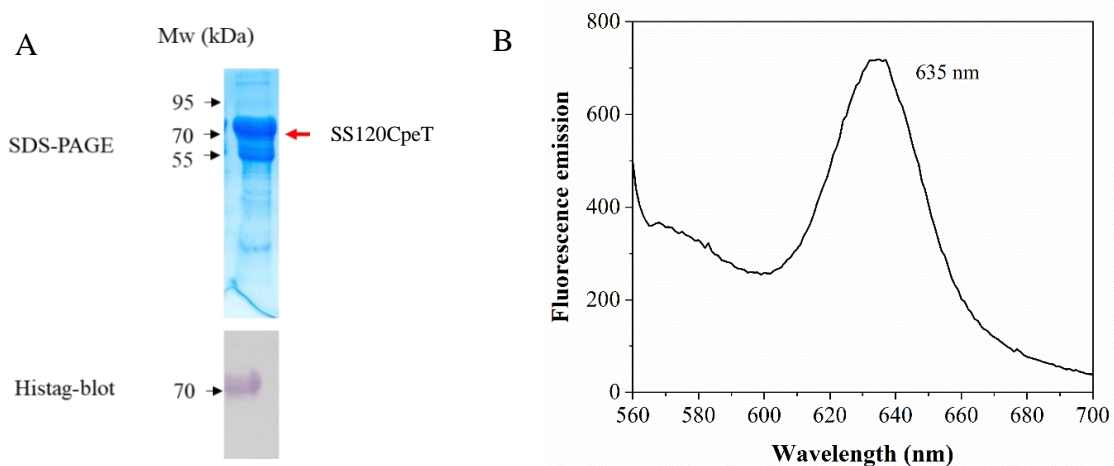


Figure 44. Analysis of the SS120CpeT: PEB complex. A. SDS-PAGE and Western blot analysis of purified SS120CpeT: PEB complex using affinity chromatography. TF-SS120CpeT protein (75 kDa). Western blot transfer and immunological detection via anti-Histag antibody. B. Fluorescence spectroscopy of the SS120CpeT: PEB complex. SS120CpeT: PEB complex shows a strong fluorescence emission at 635 nm after excitation with 540 nm.

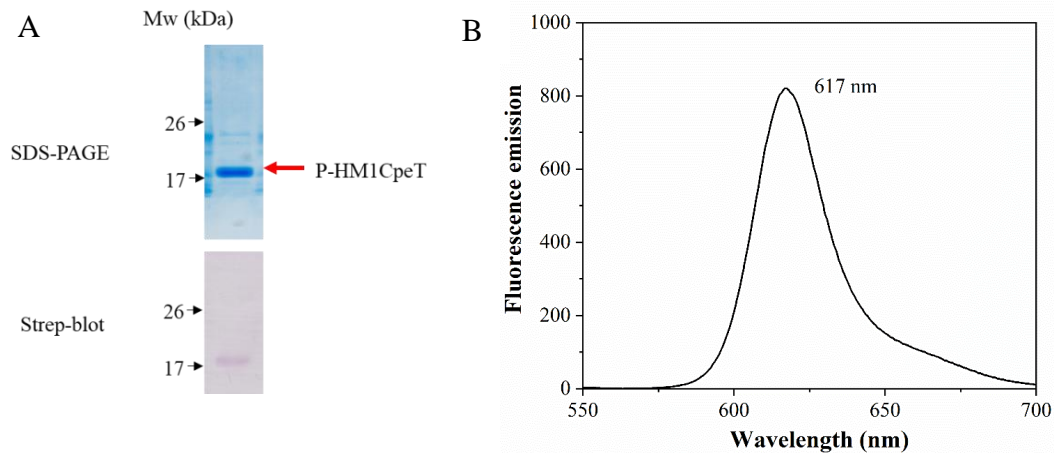


Figure 45. Analysis of the P-HM1CpeT: PEB complex. A. SDS-PAGE and Western blot analysis of purified P-HM1CpeT: PEB complex using affinity chromatography. StrepII-P-HM1CpeT protein (19 kDa). Western blot transfer and immunological detection via anti-StrepII-tag antibody. B. Fluorescence spectroscopy of the P-HM1CpeT: PEB complex. P-HM1CpeT: PEB complex shows a strong fluorescence emission at 617 nm after excitation with 540 nm.

3.4.2.2 HT-CpeB coproduced with SS120CpeT and P-HM1CpeT

The bilin lyase activity of SS120CpeT and P-HM1CpeT was studied using the Duet coexpression system in *E. coli*. Gene coexpression was done in a recombinant *E. coli* strain containing the R-phycoerythrin subunit beta gene *cpeB* and the PEB synthesis genes *pebS* and *hoI* that encoded a phycoerythrobilin synthase and heme oxygenase respectively. After expression, HT-CpeB was purified using TALON Metal affinity chromatography and analyzed by fluorescence emission spectroscopy and SDS-PAGE (Figure S2, S3). Purified HT-CpeB from these coexpression experiments did not show any fluorescence emission spectra. SDS-PAGE and zinc blot analysis of the sample revealed that there was no chromophorylation of CpeB.

Lyase CpeT from *Fremyella diplosiphon* was recently described to bind PEB to the β -subunit of PE at Cys165, but lyase CpeZ is required for the correct and efficient attachment of PEB (Nguyen *et al.* (2020)). According to that, we tried to coexpress *SS120cpeT* and *P-HM1cpeT* in combination with CpeZ from *Fremyella diplosiphon* and is equivalent in *Prochlorococcus marinus* SS120. In all of these experiments, no chromophorylation of CpeB was detected either with SS120CpeT or with P-HM1CpeT.

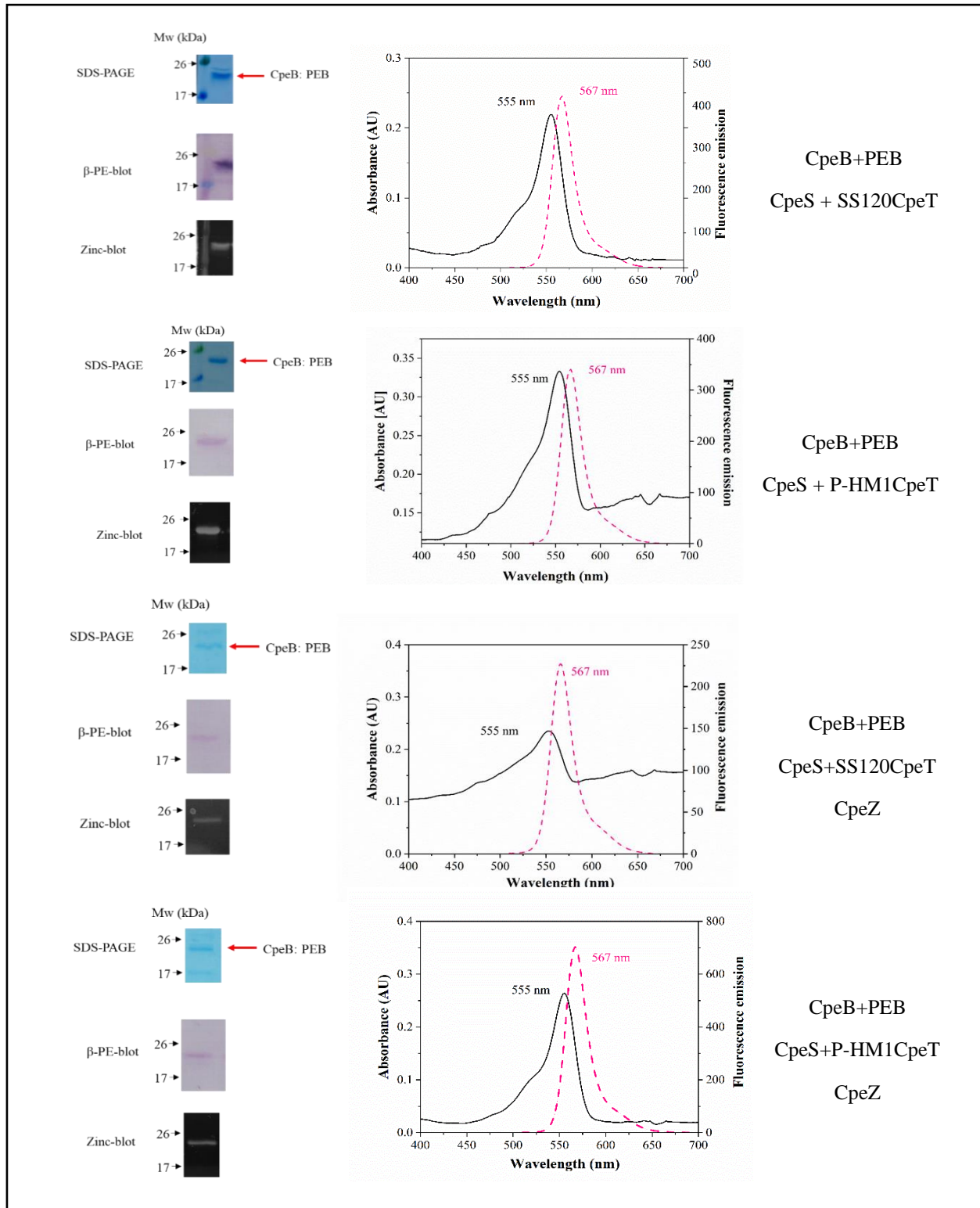


Figure 46. Analyses of purified HT-CpeB coproduced with T-type lyases. On the left, purified HT-CpeB was analyzed by SDS-PAGE, immunodetection with β -PE and zinc-induced fluorescence. On the right, absorbance (solid line) and fluorescence emission (red dashed line, excitation set at 490 nm) spectra of purified HT-CpeB obtained from *E. coli*. Protein combinations are indicated beside right of the graphs.

These results suggest that sequential addition of the chromophores to the R-phycoerythrin β -subunit could be essential. Therefore, T-type lyases *SS120cpeT* and *P-HM1cpeT* were independently coexpressed with lyase CpeS and CpeB. After affinity chromatography and SEC purified HT-CpeB, from *E coli* strains containing PEB genes *pebS* and *hol*, *cpeB*, *SS120cpeT* or *P-HM1cpeT*, and eventually *cpeZ*, was analyzed by SDS-PAGE. The fluorescence emission spectra of HT-CpeB show the same absorbance peak at 555 nm. After excitation at 490 nm fluorescence an emission peak at 567 nm was detected (Fig. 46). This fluorescence emission corresponds to PEB bound to the CpeB β subunit. Samples from these coexpression experiments were digested with trypsin and analyzed by HPLC but any new chromophore peptide, in comparison with the control experiment without T-type lyases, was detected (Fig. 47). It means that two T-type lyases both could not transfer chromophore PEB to CpeB in the pDuetTM coexpression system.

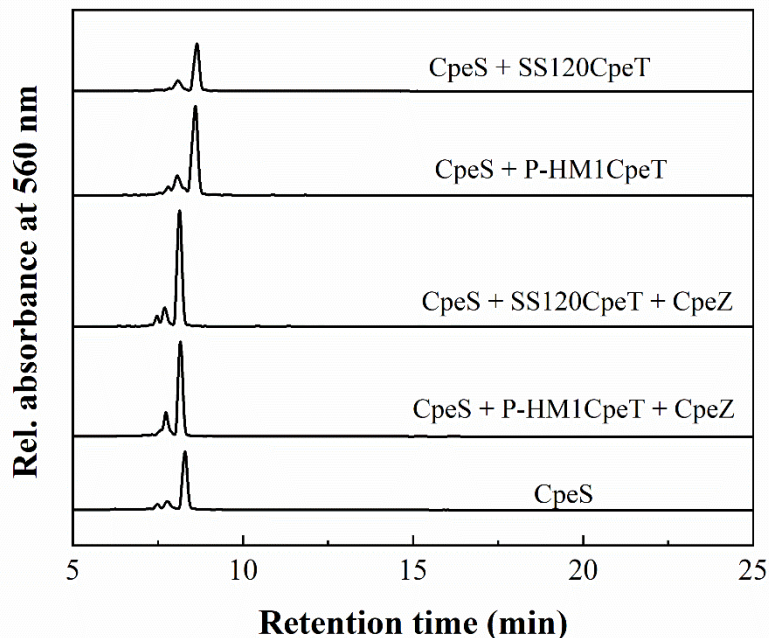


Figure 47. HPLC analyses of HT-CpeB peptides in different co-expression system. HT-CpeB was digested with trypsin after affinity chromatography purification and SEC (Superdex 75 Increase 10/300 GL). Peptides were monitored at a wavelength of 560 nm. Around 100-200 μ g of protein were loaded onto the HPLC column (Jupiter[®] 5 μ m C4 300 \AA , Phenomenex).

3.4.3 Analysis of recombinant E/F-type lyases on HT-CpeB and HT-CpeA

The E/F-type phycobiliprotein lyases represent the best-studied group of the phycobiliprotein lyases. According to bioinformatic predictions, members of this group typically have HEAT/PBS-HEAT-like repeats or at least Armadillo-type folds (Bretaudeau *et al.* (2012)). The putative MpeX, CpeY and CpeZ phycobiliprotein lyases from *Prochlorococcus marinus* SS120 can be assigned to the E/F-type phycobiliprotein lyases. Similar to the E/F type phycobiliprotein lyases, the *Prochlorococcus marinus* SS120 putative gene product Pro1634 contains two HEAT-repeat domains which have been attributed an important role in protein-protein interactions (Morimoto *et al.* (2003)). Furthermore, several phycobin lyase-isomerases were reported in this group ((Blot *et al.*, 2009, Mahmoud *et al.*, 2017)).

Phylogenetic analysis of the putative gene products CpeY and CpeZ assigned these proteins to a family of structurally related cyanobacterial proteins that includes CpcE/CpcF phycocyanin alpha-subunit lyase of *Synechococcus sp.* PCC 7002 and the PecE/PecF phycoerythrocyanin alpha-subunit lyase of *Nostoc sp.* PCC 7120 (Fig. 48). Two other phycobiliprotein lyases of the E/F group have been characterized from *Fremyella diplosiphon*: CpeY and CpeZ. CpeY transfers PEB to α -Cys82-PE, and the efficiency of the transfer is significantly enhanced by CpeZ. CpeZ alone is not able to transfer PEB to the PE subunit (Biswas *et al.* (2011)).

However, considering the phylogenetic analysis, MpeX seems to be closely related to the genes MpeU and MpeV, while the whole MpeU/V/X clade could have emerged from CpeF-like ancestors. MpeX could have a similar function as other members of the CpeF family. The putative lyase MpeX of *Prochlorococcus marinus* SS120 shares 33 % amino acid identity over the whole length with CpeF of freshwater cyanobacterium *F. diplosiphon*, 43 % with MpeU and 42 % with MpeV of *Synechococcus* RS9916. Interestingly, Pro1634 is sorted into a group termed IaiH (IscA-interacting Heat-repeats-containing protein), which is hardly characterized and until now there is no proof that these proteins are genuine phycobin lyases, although they are undeniably related to iron-sulfur cluster formation in cyanobacteria (Morimoto *et al.* (2003), Gao (2020)). Pro1634 shares 21 % and 23 % amino acid identity with CpeF and CpeZ of freshwater cyanobacterium *F. diplosiphon*, 21.67 % /22.47 % with CpcE/F from *Nostoc sp.* PCC712 and 19 % /20 % with PecE/F from *Mastigocladus laminosus* (Fig. 48).

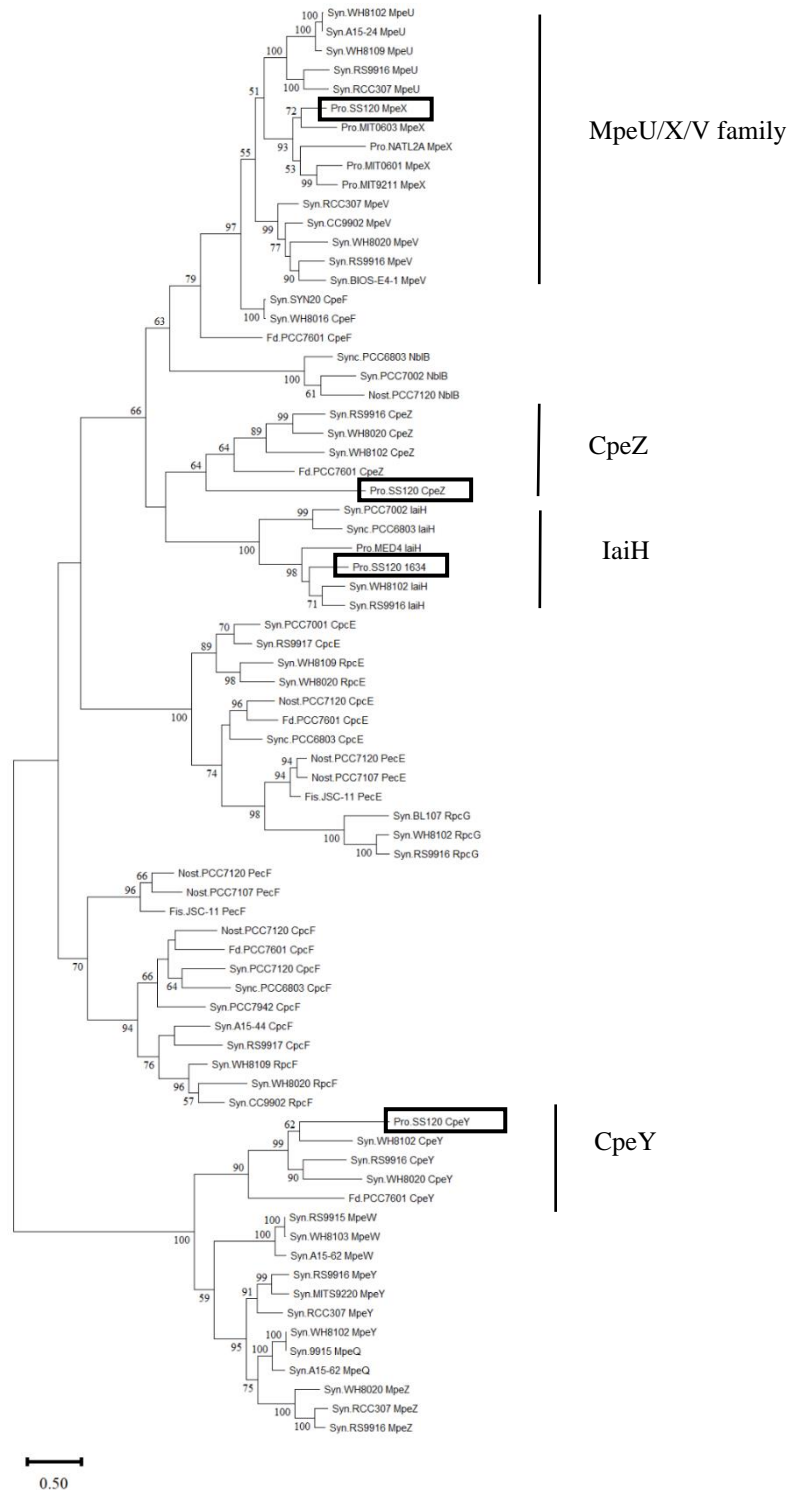


Figure 48 Maximum likelihood (ML) phylogenetic tree of a E/F-type lyases. Putative lyases MpeX, Pro1634, CpeY and CpeZ of *P. marinus* SS120 are highlighted with rectangles. Lyase family names are given on the right side. Sequence names include abbreviation of the genus, the strain name and the lyases name. Bootstrap values for ML are given at nodes of the tree. Only values higher than 50 % for ML bootstrap values are shown. Fis.: *Fischerella* Fd.: *Fremyella*; Nost.: *Nostoc*; Pro.: *Prochlorococcus*; Syn.: *Synechococcus*. Tree was created with MEGA11.

3.4.3.1 Characterization of HT-CpeA coproduced with CpeY and CpeZ

The PE-III α -subunit CpeA from *P. marinus* SS120 should carry one chromophore PUB at Cys 73. It is suggested that the CpeY and CpeZ from *F. diplosiphon* play a role in PE biosynthesis, possibly as a lyases in the attachment of PEB to the α -subunit (Kahn *et al.* (1997)). Moreover, heterologous expression of *cpeZ* in *Escherichia coli* increases the activity of the lyase CpeY, by a chaperone-type role, assisting the interactions between CpeA and the lyase CpeY. On the other hand, it has been published that the CpeY homolog lyase from *Synechococcus* sp. RS9916 is able to attach PEB to CpeA in a similar manner than CpeY from *F. diplosiphon* but without the requirement of the chaperone-like protein CpeZ (Biswas *et al.* (2011), Kronfel *et al.* (2019)). According to that, we did several co-expression experiments using the α -subunit *cpeA*, PEB genes *pebS* and *hol* in combination with *cpeY* and both *cpeZ* genes. HT-CpeA was later purified by affinity chromatography but did not show any signal in the zinc-blot (Fig. 49). CpeY alone, CpeZ alone or CpeY with CpeZ, showed no detectable bilin addition resembling CpeA with no addition of lyases.

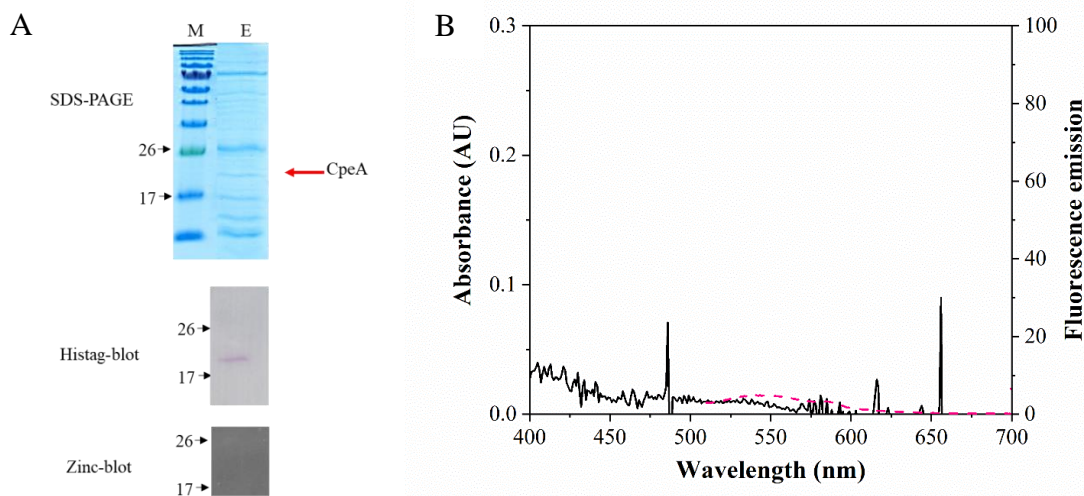


Figure 49. Analyses of purified HT-CpeA coproduced with CpeY and CpeZ lyases A. purified HT-CpeA was analyzed by SDS-PAGE, immunodetection with anti-Histag and zinc-induced fluorescence B. Absorbance (solid line) and fluorescence emission (dashed line, excitation set at 490 nm) spectra of purified HT-CpeA obtained from *E. coli*.

3.4.3.2 Characterization of HT-CpeB coproduced with MpeX and Pro1634

The independent co-expression in an *E. coli* recombinant strain containing the β -subunit *cpeB* and PEB genes *pebS* and *hol* of the genes *mpeX* and *pro1634* as well as the co-expression of both genes together, showed no detectable bilin addition to the CpeB. In the presence of lyase CpeS, at least one PEB was attached to CpeB as indicated by an absorbance peak at 555 nm and a strong fluorescence emission at 567 nm (Fig. 50). After SEC, purified HT-CpeB was analyzed by SDS-PAGE, Western and zinc (Fig. 51). Moreover, absorbance and fluorescence emission spectra of the resulting CpeB product after the purification was analyzed (Fig. 52). Neither an absorption peak at ~ 500 nm nor fluorescent emission was detected for potential PUB binding. Interestingly, HPLC analysis of the sample from the recombinant *E. coli* strain co-expressing the genes *cpeS*, *mpeX* and *pro1634*, exhibited a new peak at a retention time of 20.3 minutes (Fig. 52). The eluting peptide showed a slightly elevated absorption at 585-600 nm. To confirm possible doubly linked PEB/PUB at Cys50/61 these samples were concentrated and analyzed by mass spectroscopy. However, a bilin doubly bound to Cys50/61 was not detected in this peptide. Alternatively, if PEB/PUB at Cys50/61 in a small subset of proteins, it could have been overlooked by mass spectrometry. Large proteins with low levels of doubly-bound bilins and a high m/z value are typically challenging to detect (Kronfel *et al.* (2019)).

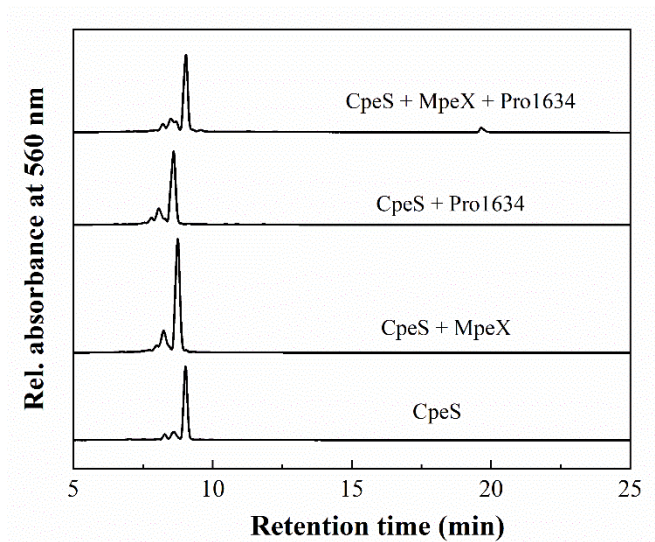


Figure 50. HPLC analysis of CpeB peptides from the recombinant strain of *E. coli* containing the β -subunit *cpeB* and PEB genes *pebS* and *hol* and different lyases. HT-CpeB was digested with trypsin after SEC purification (Superdex 75 Increase 10/300 GL). The compounds were monitored at a wavelength of 560 nm. Around 100-200 μ g of protein were loaded onto the column (Jupiter[®] 5 μ m C4 300 Å, Phenomenex).

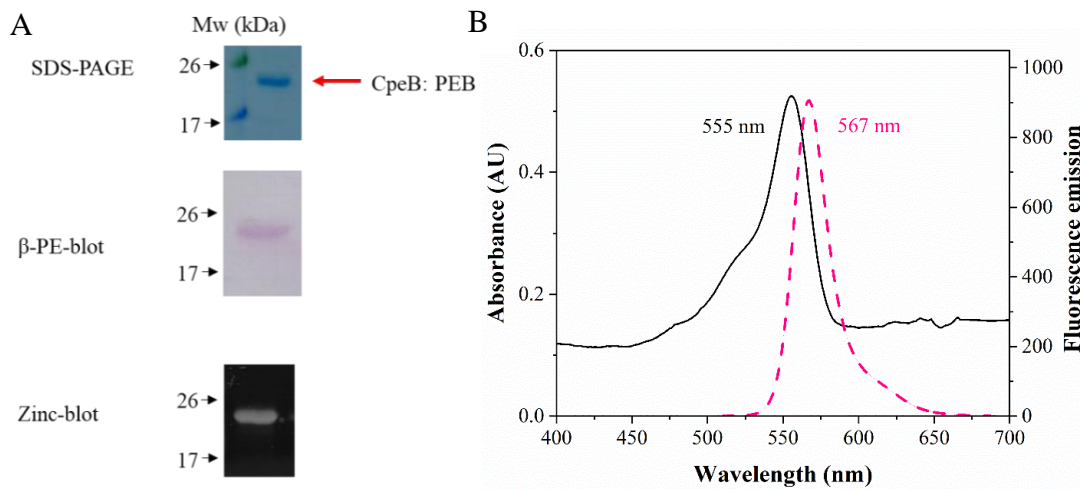


Figure 51. Analyses of purified HT-CpeB coproduced with CpeS, MpeX and Pro1634 lyases. A. Purified HT-CpeB analyzed by SDS-PAGE, immunodetection with β -PE and anti-Histag and zinc-induced fluorescence **B.** Absorbance (solid line) and fluorescence emission (red dashed line, excitation set at 490 nm) spectra of purified HT-CpeB.

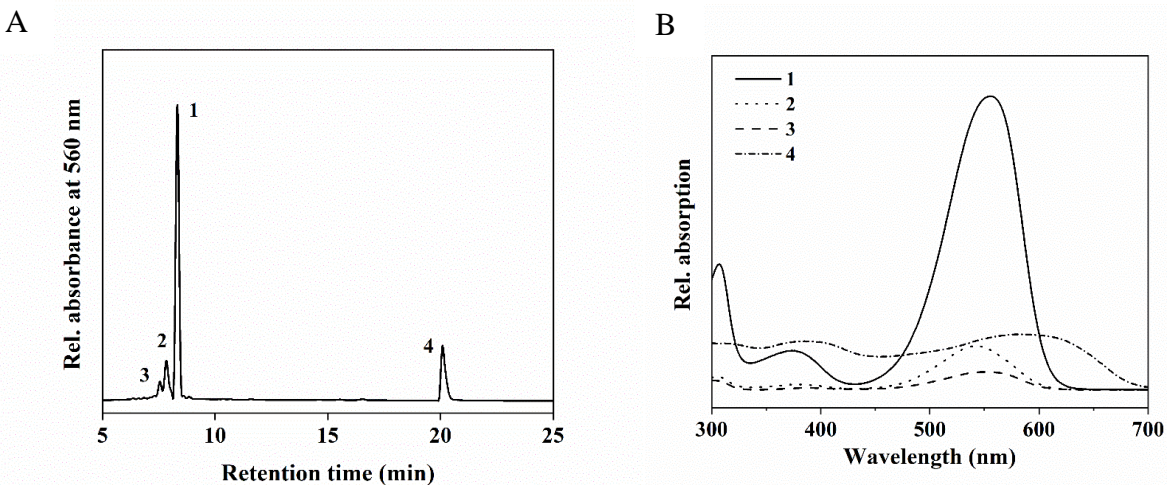


Figure 52. Analysis of CpeB from the recombinant strain of *E. coli* containing the β -subunit *cpeB* and PEB genes *pebS* and *ho1* and the genes *cpeS*, *mpeX* and *pro1634*. A. HPLC chromatogram of the trypsin digested peptides of CpeB. **B.** Four different bilin peptides (1, 2, 3 and 4) were obtained and their absorption spectra were detected in HPLC solvent.

4 Discussion

Prochlorococcus is a genus of small, unicellular, marine cyanobacteria that are considered to be the most abundant photosynthetic organisms on Earth (Partensky *et al.* (1999)). Unlike many other cyanobacteria, *Prochlorococcus* lacks phycobilisomes (PBS) but instead uses divinyl chlorophyll (DV-Chl) binding proteins, also known as prochlorophyte chlorophyll binding protein (Pcb) (Dufresne *et al.* (2003)). Additionally, LL-adapted *P. marinus* SS120 possesses PE-III, which is believed to have three phycourobilin (PUB) and one phycoerythrobilin (PEB) attached to it (Hess *et al.* (1999), Steglich *et al.* (2003)). Lyases play a significant role in the assembly of phycobiliproteins (PBP) by facilitating the covalent attachment of phycobilins to apoproteins. The main focus of the project should be on the function of putative lyase members and the assembly of PE-III from *P. marinus* SS120.

4.1 Assembly of phycobiliprotein

This work mainly focused on the putative lyases and their involvement in the PE-III chromophorylation. Zhao *et al.* developed the reconstitution system for a phycobiliprotein, holo-CpcB (Zhao *et al.* (2006)). In this thesis, a multi-plasmid expression system for the reconstitution of phycobiliproteins in *E. coli* was successfully established. After cloning the apo-phycobiliprotein, phycobilin biosynthesis and lyase genes of several cyanobacteria, various phycobiliproteins could be biosynthesized in the heterologous *E. coli* system using the dual pDuet™ plasmids containing their respective genes.

4.1.1 Codon usage

Synonymous codon substitution might keep silence in the amino acid sequence but can impact gene expression levels and protein folding. There may be translational differences due to differences in codon usage between *Prochlorococcus* and *E. coli*. Although the initiation step of mRNA translation is considered rate-limiting, codon usage is known to affect elongation rate and can be a limiting factor in product yield. Since translation kinetics would still differ from those in *Prochlorococcus* (Tagwerker *et al.* (2012)), just optimizing the genes of lyases for the expression in *E. coli* might not necessarily solve the problem. The Codon Adaptation Index (CAI) is a measure of the synonymous codon usage bias for sequence and quantifies codon usage similarities between a gene and a reference set (Puigbò *et al.* (2008)). The CAI of PE-III genes around 0.5-0.6 showed

so far lower than considered ideal. Codon usage tables showed a bias in codon usage between *Prochlorococcus* and *E. coli*. For example, *E. coli* uses the Arginine AGA codon and the Glutamin codon CAA twice as much compared to SS120 (Fig. S5). Non-adapted genes from *Prochlorococcus* overexpressed in *E. coli* were already shown to cause an increase in the amount of insoluble and misfolded proteins (Cortazzo *et al.* (2002)). *Synechococcus* and *Prochlorococcus* have made great contributions to earth's photosynthetic biomass. Surprisingly, although the two marine cyanobacteria are phylogenetically close, they are distinct dramatically in codon usage patterns (Fig. S6). Yu *et al* revealed in *Prochlorococcus*, the amino acids of valine and serine are preferred to be encoded by GUU and CCA. However, in *Synechococcus*, they are prone to use GUG and CCC (Yu *et al.* (2012)). We still need to mention that, in *Syn.* 7002 host, original *cpeB* from *P. marinus* SS120 could be successfully expressed (chapter 3.3).

4.1.2 Production condition

The co-expression system in *E. coli* was proven to be successful for the lyase CpeS. However, other lyases that are also suited for the system are still unknown. For CpeY, CpeZ, MpeX, Pro1634 and CpeT, although the formation of inclusion bodies made the purifications unfeasible, we were able to confirm their expression in *E. coli* by the immunological detection procedure Western blot (Weber (2019), Hackh (2022)). A recurring problem with the expression of cyanobacterial genes in *E. coli* is the occurrence of insoluble proteins. For example, *in vitro* experiments reported, only a small amount of apo-protein was soluble, but PEB ligation increased its solubility (Biswas *et al.* (2011)). Therefore, we infer that produced lyases were possibly wrongly folded and, consequently, inactive in *E. coli*. As of now, several improvements were found to decrease the extent of this issue. One is using a lower temperature to grow the main culture (Carrigee *et al.* (2021)). Another involves the use of an autoinducer medium or additional medium like LB-sorbitol (Tomazic *et al.* (2021), Carrigee *et al.* (2022)). Moreover, there is also the possibility that in the applied expression system we lost essential parts which are needed for PE-III assembly. Such as, the gene cluster contains a gene encoding a linker protein (*ppeC*), likely involved in anchoring the PE to the thylakoid membrane and an open reading frame (orf 62) of unknown function possibly encoding a micro protein (Staudt & Wenkel (2011)).

4.1.3 Regulation of gene expression

The genomes of *Prochlorococcus* are characterized by low levels of guanine and cytosine, a high concentration of compact intergenic regions, and a limited number of genes responsible for transcription, signal transduction, and gene expression regulation (Dufresne *et al.* (2003), Rocap *et al.* (2003)). Gene expression is regulated on multiple levels, and the stability of RNA is a key regulatory step for it. The relative amounts of RNAs reflect the balance between transcription and degradation. The estimated global average mRNA lifetime in *Prochlorococcus* is 2.5 minutes, with 80% of transcripts having a lifetime between 1.1 and 8 minutes (Steglich *et al.* (2010)). These numbers are consistent with the estimated lifetimes of transcripts in heterotrophic bacteria. So far, 24 antisense RNAs (asRNAs; 100-600 nucleotides in length) were reported for *Prochlorococcus* (Steglich *et al.* (2008)). The abundance of asRNAs in *Prochlorococcus* compared to protein regulators may account for the relatively brief length of the 5'UTRs, which play a crucial role in gene regulation by protein regulators (and trans-acting non-coding RNAs), but have a lesser impact on gene regulation mediated by asRNAs (Steglich *et al.* (2008)). These short asRNAs in *Prochlorococcus* allow for efficient pairing with mRNA and can serve as excellent substrates for ribonuclease III, which recognizes double-stranded RNA. Moreover, the partial overlap of mRNA-asRNA duplexes may produce additional entry sites in single-stranded regions, thereby facilitating the action of ribonuclease E, which is the primary ribonuclease in regulated mRNA degradation (Stazic *et al.* (2011)).

Ribosome binding sites (RBS) are well-characterized genetic tools used to control protein production in model organisms. Different RBS sequences will affect the expression level, as translational efficiency varies to more than 10^3 fold (Farasat *et al.* (2014)). The accessibility of this site and complementarity to the 16S rRNA in the ribosome is a major determinate of protein expression. Most cyanobacteria such as *Synechococcus* sp. PCC 7002, *Synechocystis* sp. PCC 6803 have the portion of the 16S rRNA that pairs with mRNA sequence of ACCTCCTTT which would suggest optimal pairing with mRNA with a central region of the RBS being AGGAGG (Gordon & Pflieger (2018)). However, in *Prochlorococcus*, it is difficult to observe common RBS. Until now, only one consensus RBS sequence "GGAGG", located 6-10 nucleotides upstream of the start codon, has been analyzed in *Prochlorococcus*. This sequence is relatively weak compared to some other bacterial RBS sequences, which may be reflective of the streamlined genome and efficient protein synthesis in *Prochlorococcus*. Although there is not much information about RBS of

Prochlorococcus, it can be stated that their RBS are unusual in contrast to other cyanobacteria. Potential RBS sequences present in the *Prochlorococcus* cluster could eventually not be recognized by the host *E. coli* or *Synechococcus*, preventing efficient expression. Furthermore, it is also likely that *Prochlorococcus* does not rely on RBS for translation initiation (Voigt *et al.* (2014)). While, translation initiation in *Synechococcus* may depend on either ribosomal protein S1 or the direct binding of a 70 S monosome to start sites of leaderless mRNA (Mutsuda & Sugiura (2006); Voigt *et al.* (2014); Read *et al.* (2017)).

4.2 Function of lyases

4.2.1 CpeS is a PEB-specific phycobiliprotein lyase

The S-type phycobiliprotein lyase CpeS from *P. marinus* SS120 was investigated in this study. S/U-type lyases are classified into five groups. Thus far, only members of groups CpcS-I, CpcS-III, and CpcU were characterized. These lyases attach PCB to β Cys84 of PC or PEC and to α Cys82 and β Cys82 of APC (Zhao *et al.* (2006), Biswas *et al.* (2010)). On the other hand, CpeS and CpeU, due to their encoding in gene clusters associated to PE maturation, were found to attach PEB to PE subunits, (Shen *et al.* (2008)). Through coexpression of CpeS with the PEB biosynthetic genes, a highly stable CpeS:PEB complex could be generated. The HPLC analysis conducted afterwards indicated that the attached chromophore is 3(Z)-PEB, consistent with the PEB extracted from the eukaryotic S-type lyase found in *Guillardia theta* (Tomazic *et al.* (2021)). It is worth noting that 3(Z)- and 3(E)- PEB differ in the A-ring, the presence of two possible stereoisomeric ethylidene groups at the C31 carbon atom. The attachment of phycobilins to phycobiliproteins can generate a new chiral center, and the 3(Z) vs 3(E) configuration of the chromophore can play an important role in this process (Gossauer & Weller (1978)). Different configurations can exist at different cysteine residues, potentially affecting the efficiency of energy transfer in photosynthesis. For example, the phycocyanin from *Synechococcus* sp. PCC 7002 has been shown to exhibit different chiral configurations at different cysteine residues. The chiral C3¹ carbons of the PCB chromophores attached at α Cys84 and β Cys82 are in the R configuration, while the C3¹ carbon of the PCB at β Cys153 is in the S configuration (Shen *et al.* (2006)). This highlights the importance of understanding the specific configurations of phycobilins in relation to their attachment to phycobiliproteins and their role in photosynthesis.

CpeS from *Prochlorococcus* MED4 was proved to be able to transfer a PEB chromophore to MED4CpeB (Wiethaus *et al.* (2010)). In contrast to the β -PE subunit from *P. marinus* SS120, the β -PE subunit from *P. marinus* MED4 carries only one potential chromophore binding site, the β -Cys82-PE. In fact, CpeS from *P. marinus* SS120 did not attach PCB to CpeB and PEB to CpeA in this *E. coli* system (data not shown). Moreover, CpeS from *F. diplosiphon* could ligate PEB to both Cys82 and Cys139 of CpeA but very inefficiently. CpeY and CpeZ are the principal bilin lyases responsible for attachment of PEB at Cys82 on CpeA (Biswas *et al.* (2011)). In addition, this CpeS efficiently attached PEB to Cys80 of CpeB. CpcS from *Nostoc* sp. PCC 7120 showed broad PBP substrate recognition and transferred PCB to Cys82 of CpcA (Zhao *et al.* (2007)). PecE and PecF, which belong to the CpcE/F family, could ligate photoactive PVB on PEC α -subunit (PecA) at Cys84 (Zhao *et al.* (2000)). Another CpcS family member, TeCpcS from *T. elongatus* BP-1 can ligate the cognate bilin, PCB, as well as two noncognate bilins PEB and P Φ B to Cys82 of different PBP substrates including CpcB and ApcA (Kronfel *et al.* (2013)). Starting from these considerations, a question arose: why are different lyases needed for attachment at Cys82 in α - or β -subunit? In cyanobacteria, the β -subunits of PC and PE tend to have a varied chromophore content. The E/F type lyases such as CpcE/CpcF were found to be specific for α -PC (Fairchild *et al.* (1992)). Furthermore, several EF types also require isomerizing activity, like PecE/PecF and RpcG (Zhao *et al.* (2000); Storf *et al.* (2001); Blot *et al.* (2009)). In addition, these chromophores are the ones that transfer energy to the terminal acceptor bilin present in Cys82 on β -subunits. This suggests that there is more flexibility of chromophore content here and that seems to be provided by the E/F type lyases, some of which evolved the isomerase activity. Overall, chromophorylation at the Cys82 equivalent position was obviously an important component in the solubility and accumulation of the folded proteins in *E. coli*. This observation suggests that chromophorylation at Cys82 might be an important first step in PBP biosynthesis in cyanobacteria as well.

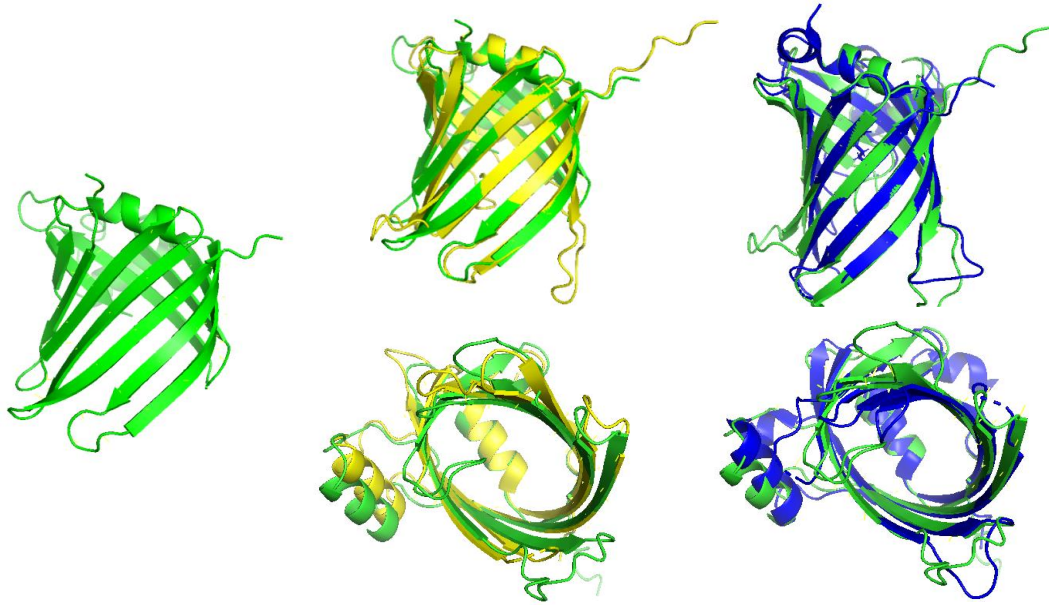


Figure 53. Structure alignment of CpeS to TeCpcS and GtCpeS. AlphaFold model of CpeS from *P. marinus* SS120 (green) and crystal structure of TeCpcS from *Thermosynechococcus elongatus* (yellow, PDB: 3BDR), GtCpeS from *Guillardia theta* (blue, PDB: 4TQ2). Structural alignment in top view. Lyases were superimposed in Pymol with a RMSD = 0.856 Å and 0.613 Å separately. AlphaFold scores: CpeS model with pLDDT = 91.09 and pTMScore = 0.8515.

TeCpcS is found as a homodimer in the crystal structure with the two α -helices, 10 β -strands, and the associated loops of each subunit. In the crystal structure, a phosphate ion forms a hydrogen-bond with the side chain of invariant Arg-151 located near the bottom of the funnel-like cavity. This interaction suggests that Arg-151 is possibly involved in substrate recognition. The D ring of the model substrate is buried at the bottom of the funnel, where its carbonyl group is hydrogen bound to the side chain of invariant Arg-151. When comparing the three barrel pockets of CpeS, GtCpeS and TeCpcS, the main difference is striking. Although the diameter at the bottom of the barrel is nearly identical on the basis of the main chain, the general barrel diameter of CpeS at the mouth is between GtCpeS and TeCpcS. The side chains of amino acid residues Arg-149, Glu-139, and Arg-151 are highly conserved among S-type lyases. The importance of Arg-149 or homologous amino acid residues for phycobilin binding has previously been confirmed for TeCpcS and GtCpeS. For Glu-139, the carboxylic function might be involved in positioning of the substrate by interaction with the tetrapyrrole nitrogens, as found for bilin-binding in FDBRs. In contrast, the more open binding pocket of TeCpcS would support the binding of a wider range of bilins.

4.2.2 T-type lyase

Is CpeT from *P. marinus* SS120 an active phycobiliprotein lyase? CpeT was heterologously overproduced with PEB biosynthesis in *E. coli*. It was demonstrated that SS120CpeT is indeed able to bind phycobilin. The complex of PEB and SS120CpeT showed an extremely strong fluorescence emission in the orange-red wavelength range (λ_{em} 635 nm) (Fig. 44). This attribute of a lyase:phycobilin complex has been described for other T-type phycobiliprotein lyases (CpcT) (Zhao *et al.* (2007)). Structural analysis of the CpcT:PCB complex revealed a rigidity in the PCB binding pocket. This leads to the tight embedding of PCBs in the binding pocket and results in the fluorescence of the complex (Zhou *et al.* (2014)). To investigate the ability of phycobilins transfer to apo-PBP, phycobilin transfer experiments were performed. The host β -PE subunit (CpeB from *P. marinus* SS120) was used as the apo-PBP. However, a direct PEB transfer could not be shown. So far, all described T-type lyases show specificity for β -Cys153. The sequence-dependent chromophorylation first postulated for *Nostoc* sp. PCC 7120 was later also proved in *F. diplosiphon* (Zhao *et al.* (2007), Kronfel *et al.* (2019)). Zhao *et al.* described that a correctly assembled PecB in *Nostoc* sp. PCC 7120 can only result from a sequential CpcT-catalyzed chromophorylation of Cys153 followed by Cys84 (Zhao *et al.* (2006)). In this study, we also described the coexpression tests with both S- and T-type lyases. However, analysis of the purified HT-CpeB by HPLC showed no chromophore peptide of PEB Cys-153.

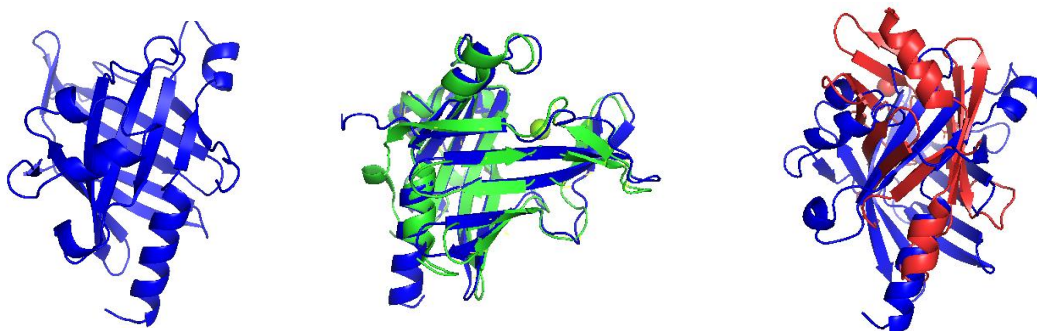


Figure 54. Structure alignment of CpeT to NostCpcT and PHM-1CpeT. AlphaFold model of CpeT from *P. marinus* SS120 (blue); crystal structure of NostCpcT from *Nostoc* sp. PCC 7120 (green, PDB: 4O4O) crystal structure of PHM-1CpeT from *Prochlorococcus* phage *P-HM1* (red, PDB: 5HI8). Lyases were superimposed in Pymol with a RMSD = 1.185 Å and RMSD = 13.105 Å respectively. AlphaFold scores: CpeT model with pLDDT = 93.87 and pTMscore = 0.8908.

CpcT from *Nostoc* sp. PCC 7120 was crystallized as a dimer and is able to bind PCB within the 10-stranded antiparallel β -barrel. It belongs to the fatty acid binding protein subfamily of the

calycin superfamily (Zhou *et al.* (2014)), a large protein family with a "barrel" like folding. They consist of antiparallel β -strands, which are often terminated by α -helices. Representatives of this group have been identified both within eukaryotes and prokaryotes (Chiu *et al.* (2010)) and are often involved in transport processes (Flower *et al.* (1993), Skerra (2008)). In addition, they are thought to function as a matrix for ligands. The AlphaFold model of CpeT from *P. marinus* SS120 reveals a similar β -barrel type structure. An amino acid sequence comparison shows that three T-type phycobiliprotein lyases CpeT from *P. marinus* SS120, CpcT from *Nostoc* sp. PCC 7120 and CpeT from the P-HM1 cyanophage have great similarities. To make the structural differences clear, the structures were superimposed. The structural comparison shows a basic similarity between both structures. However, there is a clear difference in the absence of some α -helices and a large number of loops in the P-HM1CpeT structure (Fig. 54).

4.2.3 E/F type lyase

In silico the structural analysis of CpeY, CpeZ, MpeX and Pro1634 support their belonging to the E/F group, which carries HEAT-like repeats and representative ARM-type folds (Fig. 43). Although the function of these four potential lyases could not be clarified in the coexpression system, valuable points are suggesting a function as PBP lyases. The general HEAT motifs occur by two anti-parallel helices connected by a short linker loop. Several repeat motifs build an α -solenoid protein shape, with the A-helix located at the outer, convex surface and the B-helix in the inner, concave area (Monecke *et al.* (2014), Zhao *et al.* (2017)). The typical ARM repeat consists of three helices (H1, H2, and H3). H2 and H3 helices build two layers in an antiparallel fashion and are roughly vertical to the shorter H1 helix, with a sharp bend between H1 and H2 (Andrade *et al.* (2001)). Being 439 amino acids long, CpeY is largest among the E/F family. However, there are examples of larger lyases that have been demonstrated to be involved in chromophore ligation and isomerization. One example is RpcG which is a fusion protein and this could explain the larger size and the capability to perform both ligation and isomerization (Blot *et al.* (2009)). CpeY from *F. diplosiphon* is a lyase involved in the attachment of PEB at Cys-82 of α -PE and it works along the chaperone-like protein CpeZ. As for MpeX, it mostly has a similar function to MpeUV or the CpeF family. The MpeV family also includes MpeU, which is a lyase isomerase that covalently attaches a doubly linked PUB to Cys50/61 on the β -subunit (Carrigee *et al.* (2021)). MpeU is found in all *Synechococcus* strains exhibiting a high PUB:PEB ratio (Mahmoud *et al.* (2017)). CpeF also

ligates doubly linked PEB at Cys50/61 on β -subunit but is not provided with an isomeric function (Kronfel *et al.* (2019)). Kumarapperuma *et al* proposed the lyase-isomerase is actually MpeQ, that is supposedly isomerizing PEB to PUB and binding it to Cys83 (Kumarapperuma *et al.* (2022)). In comparison to the amino acids sequence of MpeQ, MpeX has a valine at position 283, which, considering the crystal structure, is located in the active site and it is therefore crucial for isomerase activity. This consideration may explain the high PUB content of PE-III.

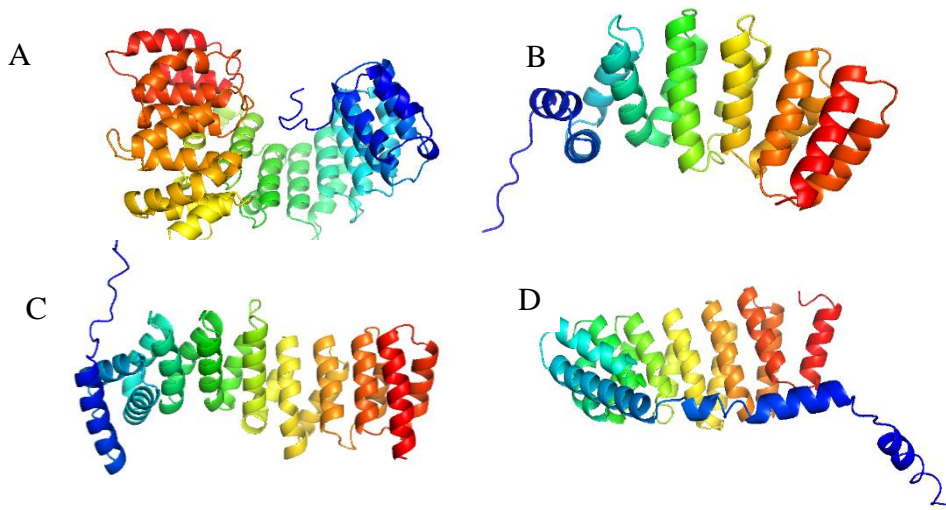


Figure 55 Structural model of E/F type lyases from *P. marinus* SS120. Structures resemble AlphaFold predictions of E/F putative lyases. A-D show the phycobilin lyase structure CpeY, CpeZ, MpeX and Pro1634 separately. MpeX might be involved in the isomerization of PEB to PUB and the attachment at β -Cys50/61, maybe assisted by Pro1634. CpeT could chromophorylate on the β -Cys163 with PEB or PUB. CpeY might attach PEB or PUB at on the α -Cys73, assisted by CpeZ. AlphaFold scores: CpeY model with pLDDT = 92.70 and pTMscore = 0.8919; CpeZ model with pLDDT = 93.87 and pTMscore = 0.8794; MpeX model with pLDD T= 92.84 and pTMscore = 0.8663; Pro1634 model with pLDDT = 90.48 and pTMscore = 0.7773

In addition to the entire lyases function group, there are phylogenetically related protein members. The typical example is the NblB family which is thought to play a role in the degradation of phycobilisomes during either sulfur or nitrogen limitation (Dolganov & Grossman (1999)). Similar to the other members of the E/F-type group, Pro1634 is characterized by HEAT-repeat domains. Phylogenetic analysis identified Pro1634 within IaiH type protein family (Fig. 48). Members of this group are known for their stabilizing effect on iron-sulfur [2Fe-2S] cluster-bearing proteins. *Synechocystis* PCC 6803 contains almost all candidates of the well-described iron-sulfur cluster system elements from *E. coli*. Only IscA2 forms a stable protein complex with the HEAT-repeat-containing protein IaiH, which functions to stabilize the [2Fe-2S] cluster bound to IscA2.

Furthermore, *P. marinus* SS120 Pro0137 shows the same three conserved cysteine residues and is closet to IscA2 (Hackh (2022)). In the HL MED4 strain a possible homolog of Pro1634 was found but, so far, it showed no lyase activity. Overall, based on the mentioned similarities, it is possible that Pro1634 has a similar function to IaiH.

4.3 Phycoerythrin structure

4.3.1 Chromophorylation PE-III from *P. marinus* SS120

Based on the results obtained in this work, extensive bioinformatic analyses and literature research, models for the assembly of the PE subunits from *P. marinus* SS120 were developed. *P. marinus* SS120 has a complete PE consisting of an α - and β - subunit. These carry conserved Cys residues that provide potential chromophore binding sites. While the α -subunit (CpeA) carries only one chromophore at the Cys73 position, the β -subunit (CpeB) is characterized by four potential binding sites (Cys50, Cys61, Cys82, Cys163) (Fig. 9A). The chromophore is bound twice via the A and D rings of the four-pyrrole ring system. The proposed chromophorylation of PE-III from *P. marinus* SS120 consists of PUB and PEB at a 3:1 ratio (Steglich *et al.* (2003)). So far, the PUB biosynthesis in *Prochlorococcus* has not been described but it is believed to be obtained by isomerization of PEB. On the other hand, it could also theoretically come from other phycobilins like PCB. This may be the reason why in *Prochlorococcus* genome there are genes involved in PCB biosynthesis. In *Synechocystis* sp. WH8501, which also obtains high PUB content, there are several PUB bound to α -Cys83, α -Cys140, β -Cys50/61 and β -Cys159, and PEB at β -Cys82 (Ong & Glazer (1991)). There is no ambiguity in the assignment of β -Cys82 (PEB) as the conserved terminal energy acceptor in phycoerythrin. CpeS was proven to link PEB to Cys82 of β -subunit, which would leave the remaining four cysteines to be attached to PUB. CpeY and CpeZ are known to promote PEB attachment on the α -subunit, which is contradictory with possible PUB chromophorylation. However, another possibility is that CpeY has also the isomerization function, similarly to what happens in *Synechococcus* sp. RS9916 where MpeZ was characterized as a Cys83 α -PE-II PEB lyase isomerase (Shukla *et al.* 2012). As for the β -subunit, one PUB could bind to Cys50/61 and the other to Cys163. MpeX might be involved in the isomerization of PEB to PUB and the attachment at β -Cys50/61, maybe assisted by Pro1634. Until now, T type lyase have not shown any isomerase function at β -Cys163 but they are not ruled out to facilitate isomerization and binding of PUB.

4.3.2 Predicted model of phycoerythrin from *Prochlorococcus*

Prochlorococcus is the only known prokaryote containing phycoerythrin in the presence of DV-Chls *a* and *b* as the major pigments (Hess *et al.* (1996)). LL adapted SS120 has a much higher DV-Chl *b* content than HL adapted strains, such as *P. marinus* MED4 (Moore *et al.* (1998)). As for the PE cluster, even though most of the genes were deleted in MED4, several genes (CpeS, CpeB) remained. Since MED4 only possesses a β -subunit but not a α -subunit, it is plausible that CpeB of SS120 could adopt the same structure. *In vitro*, the oligomerization of CpeB of *P. marinus* MED4 was determined as dimeric state. CpeB eluted mainly as complex of ~ 45 kDa on Superdex 75, correlating well with the calculated mass of a CpeB homodimer (Wiethaus *et al.* (2010)). In our study, SEC also revealed that purified HT-CpeB from *P. marinus* SS120, coproduced with CpeS and PEB biosynthesis proteins, elutes mainly as a dimer (chapter 3.4). Moreover, a dimer formation as the starting point for PBP assembly is an often-described model (Adir (2005)). Bilin attachment onto phycobiliprotein subunits is necessary for the assembly of ($\alpha\beta$) monomers. The spontaneous and highly stable formation of a ($\alpha\beta$) monomer is followed by the assembly into a ($\alpha\beta$)₃ trimer. Both subunits are significantly homologous on both sequence and structural levels, leading to a very even and highly symmetric structure (Adir *et al.* (2006)). A structural alignment of α - and β -subunit of *Prochlorococcus* to crystal structures of several PEs demonstrates the similarities between both subunits and supports the idea that two β -subunits could assemble as well to form a homodimer (Fig. 56).

Two phycoerythrin models of *Prochlorococcus* obtained by AlphaFold were described (Fig. 57-59). In *P. marinus* SS120 stereo view of $\alpha\beta$ monomer, both the polypeptides (α -subunit of 155 amino acids and β -subunit of 182 amino acids) possess a similar overall fold (globin family), and their folds are identical to that of other known cyanobacterium phycoerythrin structure. The $\alpha 1$, $\alpha 2$ and $\alpha 4$ helices of the two subunits are involved in extensive interaction and stabilize a $\alpha\beta$ heterodimer. The α -subunits contain 7 α helices ($\alpha 1$ - $\alpha 7$). The equivalent residues of β -subunits also adopt helical conformation with insertion residues (146-152), additionally adopting helical turn conformation. The chromophore PUB163 of the β -subunit is located near the central hexamer cavity (Fig. 57). Three $\alpha\beta$ monomers are arranged about a threefold axis and form a trimer ($\alpha\beta$)₃. The trimer model was described in Fig. 58. Although the model missed all potential chromophores, it still showed the typical phycoerythrin trimer skeleton configuration. For HL MED4 strain, there is only one shorter polypeptide (β -subunit of 175 amino acids). In contrast to the β -subunit of

SS120, it consists of 9 helices which are the N-terminal two spirals merging. Because of the longer helix, it would be more difficult to assemble $\beta\beta$ monomer. Using AlphaFold to model $(\beta\beta)_3$, the basic configuration is distorted. Each $\beta\beta$ looks like a separate individual, lacking interlocking effects. Although the structural prediction of phycoerythrin of *P. marinus* MED4 provides some interesting hypotheses, it lacks sufficient evidence to support it and therefore needs further investigation.

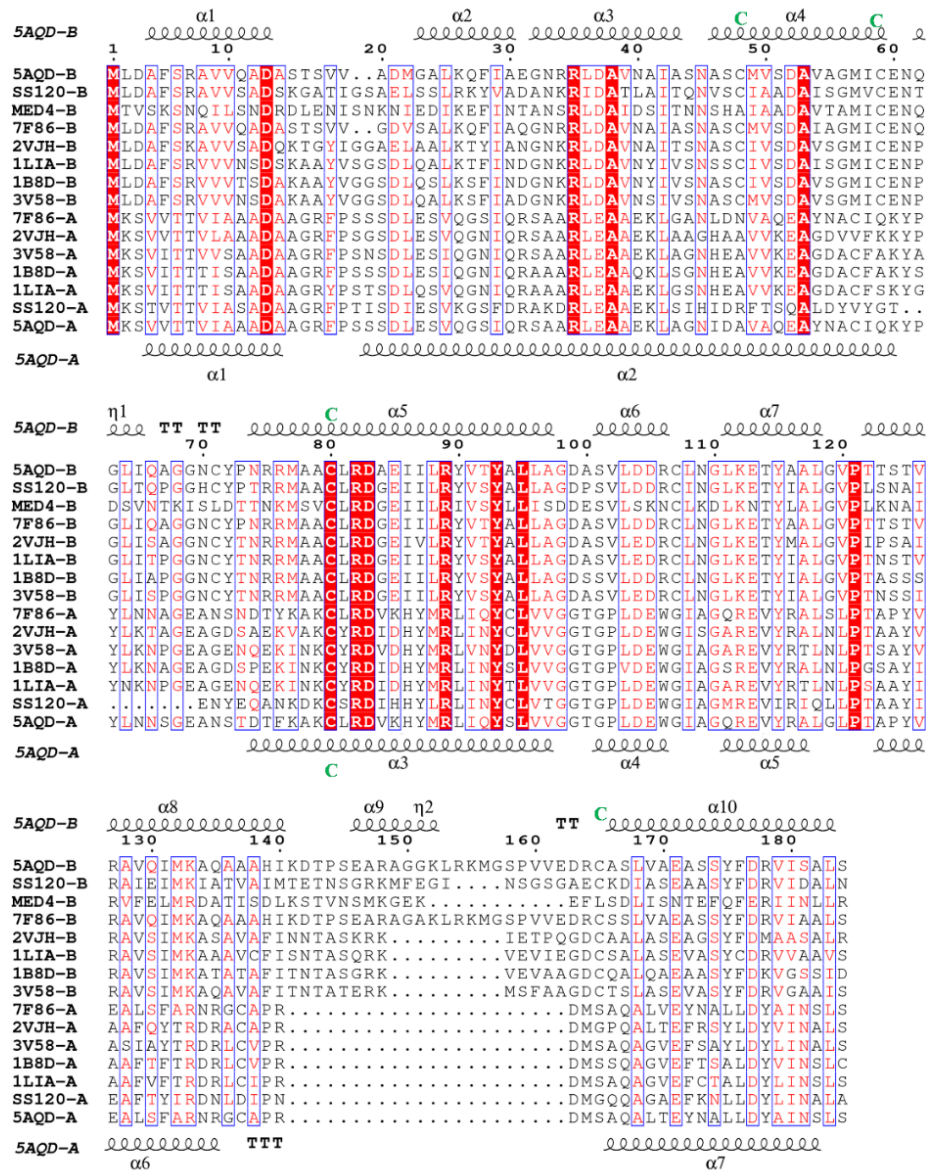


Figure. 56 Structure-based multiple sequence alignment. Atomic coordinates of α - and β -subunits from known crystal structures of cyanobacterial and red algal origin were superposed by Clustal W (5AQD, *Phormidium* sp. A09DM; 7F86, *Halomicronema* sp. R31DM; 1B8D, *G. monilis*; 3V58, *P. cruentum*; 2VJH, *G. violaceus*; 1L1A, *P. urceolata*; SS120, *P. marinus* SS120; MED4, *P. marinus* MED4). DSSP-assigned secondary structure (Kabsch & Sander (1983)) for the *Phormidium* protein is shown for β -subunit (top row) and for α -subunit (bottom row). Invariant residues are shaded red. Cysteine residues covalently linked to PEB or PUB chromophores are marked with letter C (green). Amino acids that might play a role in stability by hydrogen bonds were identified with Pymol. SS120- α -73-PEB: Asp76(D), Arg75(R), Lys72(K). SS120- β -82-PEB: Arg77(R), Arg78(R), Arg84(R), Asp85(D). SS120- β -50/61-(PUB): Asp54(D), Arg129(R), Asn146(N), Ser147(S) Gly184(G). SS120- β -163-(PEB): Asn35(N), Asp39(D), Ser159(S), Glu162(E), Lys28(K) on α -subunit Figure was prepared with ESPrpt 3.0 (Robert & Gouet (2014)).

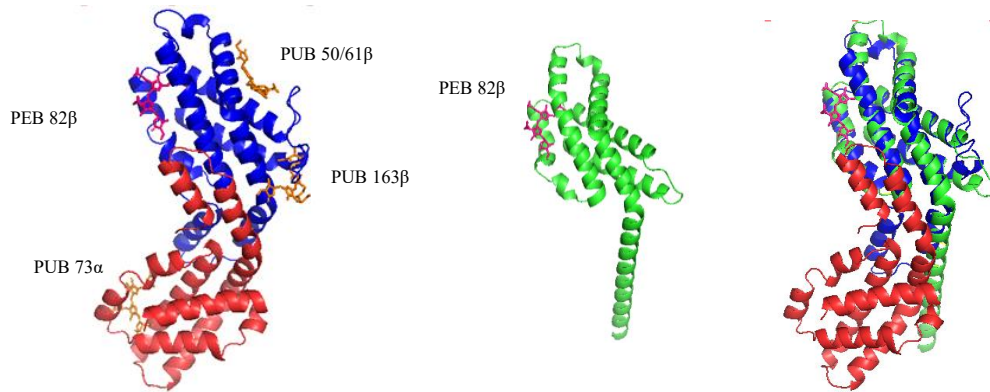


Figure 57. Stereo view of ribbon model of an $\alpha\beta$ monomer. AlphaFold predictions of *P. marinus* SS120 CpeB and CpeA were aligned with β -subunit of *P. marinus* MED4. The α - and β -subunits from SS120 strain are shown in red and blue colours, respectively. The β -subunit from MED4 is shown in green colour. PUB and PEB chromophores marked in pink and orange colours, respectively. Chromophores were not stereochemical adjusted to the structure, only proposed to attach conserved cysteines. *P. marinus* SS120 model with pLDDT = 91.40 and pTMscore = 0.8764. *P. marinus* MED4 model with pLDDT = 90.21 and pTMscore = 0.8516.

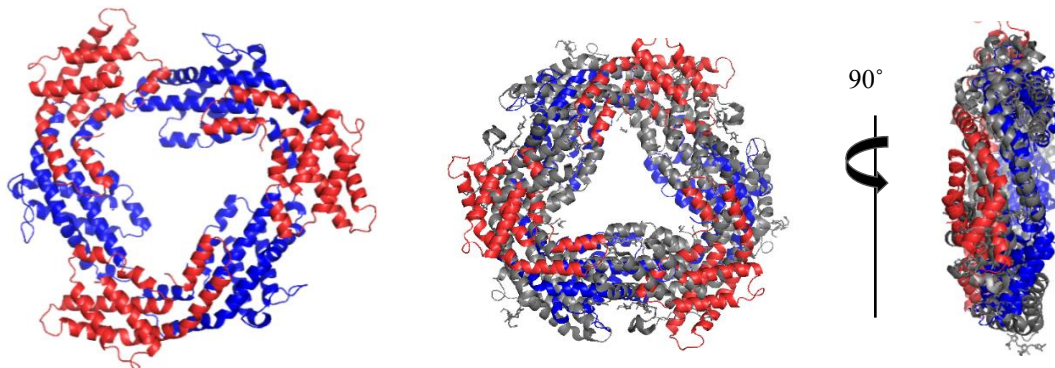


Figure 58. Stereo view of the model of PE-III of *P. marinus* SS120 trimer without chromophores. The trimer is constituted by three stable monomers (red: CpeA; blue: CpeB). Crystal structure analysis of C-phycocyanin from cyanobacterium *Phormidium* sp. A09DM (grey, PDB: 5AQD) were superimposed in Pymol with a RMSD = 43.123 Å. AlphaFold scores: PE-III of *P. marinus* SS120 with pLDDT = 90.4, pTMscore = 0.797

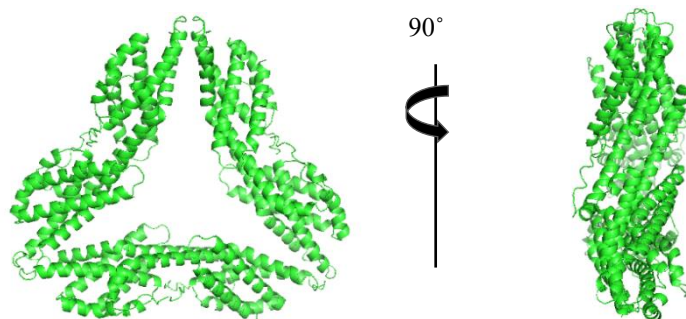


Figure 59. Stereo view of the model of phycoerythrin of *P. marinus* MED4 trimer without chromophore. AlphaFold scores: phycoerythrin of *P. marinus* MED4 with pLDDT = 64.7, pTMscore = 0.318 The structure has been rotated by 90°, revealing the monomer interface between the two subunits

5 Summary

Phycobilisomes (PBS) are the major light-harvesting complexes for the majority of cyanobacteria and allow these organisms to absorb in the so-called green gap. They consist of smaller units called phycobiliproteins (PBPs), which are composed of an α - and a β -subunit with covalently bound linear tetrapyrroles (phycobilins). The latter are attached to the apo-PBPs by phycobiliprotein lyases. Interestingly, cyanobacteria of the genus *Prochlorococcus* lack complete PBS and instead use prochlorophyte chlorophyll-binding proteins (Pcbs), which effectively utilize the energy of the blue light region. The low-light-adapted (LL) strain *Prochlorococcus marinus* SS120 has a single PBP, phycoerythrin-III (PE-III). It has been postulated that PE-III is chromophorylated with the phycobilins phycourobilin (PUB) and phycoerythrobilin (PEB) in a 3:1 ratio. Thereby, the function of PE-III remains unclear so far, so that light-gathering function and also photoreceptor function are discussed.

The main goal of this work was to characterize the assembly of PE-III and thus the function of the six putative phycobiliprotein lyases of *P. marinus* SS120. Previous work found that the individual lyases could not be produced in soluble form, so we switched to a dual pDuet™ plasmid system in *E. coli*, which was successfully established. Investigation of the binding of PEB to Apo-PE revealed that the CpeS lyase specifically chromophorylated Cys82 with 3Z-PEB. Unfortunately, additional chromophorylation could not be observed using the pDuet system. Therefore, in a second part of the work, the entire PE gene cluster from *P. marinus* SS120 was to be introduced into *E. coli* and expressed. Although the gene cluster was successfully transcribed within *E. coli*, no translation was observed, possibly due to incompatible translation initiation between *Prochlorococcus* and *E. coli*. The introduction of a mini PE cluster (CpeAB) into the cyanobacterium *Synechococcus* sp. PCC 7002 was also successfully performed, in which case production of CpeB but not CpeA from *Prochlorococcus* was detected. Recombinant CpeB was also detected together with intrinsic PBP in *Synechococcus* sp. 7002, indicating structural similarity and incorporation into PBS in *Synechococcus* sp. 7002. Overall, the obtained results suggest that a cyanobacterial host is a good option for the studies on the assembly of PE-III from *P. marinus* and, based on this, future work could aim at generating an artificial operon using synthetic biology to achieve efficient translation of all genes.

6 Zusammenfassung

Phycobilisomen sind die wichtigsten Lichtsammelkomplexe für den überwiegenden Teil der Cyanobakterien und ermöglichen es diesen Organismen in der sogenannten Grünücke zu absorbieren. Sie bestehen aus kleineren Einheiten, den sogenannten Phycobiliproteinen (PBP), die sich aus einer α - und einer β -Untereinheit mit kovalent gebundenen linearen Tetrapyrrolen (Phycobilinen) zusammensetzen. Letztere werden mit Hilfe von Phycobiliprotein-Lyase an die apo-PBPs gebunden. Interessanterweise fehlen Cyanobakterien der Gattung *Prochlorococcus* die kompletten Phycobilisomen und sie verwenden stattdessen Prochlorophyten-Chlorophyll-bindende Proteine (Pcbs), die die Energie des blauen Lichtbereichs effektiv nutzen. Der an schwaches Licht angepasste (LL) Stamm *Prochlorococcus marinus* SS120 besitzt ein einziges PBP, Phycoerythrin-III (PE-III). Es wurde postuliert, dass PE-III mit den Phycobilinen Phycocourobilin (PUB) und Phycoerythrobilin (PEB) in einem Verhältnis von 3:1 chromophoryliert ist. Dabei bleibt die Funktion von PE-III bislang ungeklärt, so dass Lichtsammelfunktion und auch Photorezeptor-Funktion diskutiert werden.

Das Hauptziel dieser Arbeit war es, die Assemblierung des PE-III und damit die Funktion der sechs mutmaßlichen Phycobiliprotein-Lyase von *P. marinus* SS120 zu charakterisieren. Frühere Arbeiten ergaben, dass die einzelnen Lyase nicht in löslicher Form hergestellt werden konnten, daher wurde hier auf ein duales pDuetTM-Plasmidsystem in *E. coli* umgestellt, welches erfolgreich etabliert wurde. Die Untersuchung der Bindung von PEB an Apo-PE ergab, dass die CpeS Lyase Cys82 spezifisch mit 3Z-PEB chromophoryliert. Zusätzliche Chromophorylierungen konnten mit Hilfe des pDuet Systems leider nicht beobachtet werden. Daher sollte in einem zweiten Teil der Arbeit das gesamte PE-Gencluster aus *P. marinus* SS120 in *E. coli* eingebracht und exprimiert werden. Obwohl das Gencluster erfolgreich in *E. coli* transkribiert wurde, konnte keine Translation nachgewiesen werden, was möglicherweise auf nicht kompatible Translationsinitiation zwischen *Prochlorococcus* und *E. coli* zurückzuführen ist. Auch das Einbringen eines mini PE-clusters (CpeAB) in das Cyanobakterium *Synechococcus* sp. PCC 7002 konnte erfolgreich durchgeführt werden, wobei hier die Produktion von CpeB, aber nicht CpeA aus *Prochlorococcus* nachgewiesen werden konnte. Rekombinantes CpeB konnte zudem zusammen mit den intrinsischen PBP in *Synechococcus* sp. 7002 nachgewiesen werden, was auf eine strukturelle Ähnlichkeit und den Einbau in die Phycobilisomen in *Synechococcus* sp. 7002 hinweist. Insgesamt legen die erzielten

Ergebnisse nahe, dass ein cyanobakterieller Wirt eine gute Option für die Studien zur Assemblierung von PE-III aus *P. marinus* darstellt und man darauf aufbauend mit Hilfe der synthetischen Biologie ein künstliches Operon erzeugen könnte, um eine effiziente Translation aller Gene zu erzielen.

References

- Acuña AM, Lemaire C, van Grondelle R, Robert B & van Stokkum IH** (2018) Energy transfer and trapping in *Synechococcus* WH 7803. *Photosynthesis Research* **135**: 115-124.
- Adir N** (2005) Elucidation of the molecular structures of components of the phycobilisome: reconstructing a giant. *Photosynthesis Research* **85**: 15-32.
- Adir N, Bar-Zvi S & Harris D** (2020) The amazing phycobilisome. *Biochimica et Biophysica Acta (BBA)-Bioenergetics* **1861**: 148047.
- Adir N, Dines M, Klartag M, McGregor A & Melamed-Frank M** (2006) Assembly and disassembly of phycobilisomes. *Complex Intracellular Structures in Prokaryotes* 47-77.
- Akiyama H, Kanai S, Hirano M & Miyasaka H** (1998) Nucleotide sequence of plasmid pAQ1 of marine cyanobacterium *Synechococcus* sp. PCC7002. *DNA Research* **5**: 127-129.
- Andrade MA, Petosa C, O'Donoghue SI, Müller CW & Bork P** (2001) Comparison of ARM and HEAT protein repeats. *Journal of Molecular Biology* **309**: 1-18.
- Arteni AA, Ajlani G & Boekema EJ** (2009) Structural organisation of phycobilisomes from *Synechocystis* sp. strain PCC6803 and their interaction with the membrane. *Biochimica et Biophysica Acta (BBA)-Bioenergetics* **1787**: 272-279.
- Arvani S, Markert A, Loeschcke A, Jaeger K-E & Drepper T** (2012) A T7 RNA polymerase-based toolkit for the concerted expression of clustered genes. *Journal of Biotechnology* **159**: 162-171.
- Averina S, Velichko N, Pinevich A, Senatskaya E & Pinevich A** (2019) Non-a chlorophylls in cyanobacteria. *Photosynthetica* **57**: 1109-1118.
- Awramik SM** (1992) The oldest records of photosynthesis. *Photosynthesis Research* **33**: 75-89.
- Bar-Eyal L, Shperberg-Avni A, Paltiel Y, Keren N, Adir N, Croce R, van Grondelle R, van Amerongen H & van Stokkum I** (2018) Light harvesting in cyanobacteria: the phycobilisomes. *Light harvesting in photosynthesis*, pp. 77-93. CRC Press.
- Berla BM, Saha R, Immethun CM, Maranas CD, Moon TS & Pakrasi HB** (2013) Synthetic biology of cyanobacteria: unique challenges and opportunities. *Frontiers in Microbiology* **4**: 246.

Beyer HM, Gonschorek P, Samodelov SL, Meier M, Weber W & Zurbriggen MD (2015) AQUA cloning: a versatile and simple enzyme-free cloning approach. *PLoS one* **10**: e0137652.

Bibby T, Nield J, Partensky F & Barber J (2001) Antenna ring around photosystem I. *Nature* **413**: 590-590.

Bibby T, Mary I, Nield J, Partensky F & Barber J (2003) Low-light-adapted *Prochlorococcus* species possess specific antennae for each photosystem. *Nature* **424**: 1051-1054.

Bibby TS, Nield J & Barber J (2001) Iron deficiency induces the formation of an antenna ring around trimeric photosystem I in cyanobacteria. *Nature* **412**: 743-745.

Bibby TS, Nield J, Chen M, Larkum AW & Barber J (2003) Structure of a photosystem II supercomplex isolated from *Prochloron didemni* retaining its chlorophyll a/b light-harvesting system. *Proceedings of the National Academy of Sciences* **100**: 9050-9054.

Biller SJ, Berube PM, Lindell D & Chisholm SW (2015) *Prochlorococcus*: the structure and function of collective diversity. *Nature Reviews Microbiology* **13**: 13-27.

Biswas A, Boutaghou MN, Alvey RM, Kronfel CM, Cole RB, Bryant DA & Schlachter WM (2011) Characterization of the activities of the CpeY, CpeZ, and CpeS bilin lyases in phycoerythrin biosynthesis in *Fremyella diplosiphon* strain UTEX 481. *Journal of Biological Chemistry* **286**: 35509-35521.

Biswas A, Vasquez YM, Dragomani TM, Kronfel ML, Williams SR, Alvey RM, Bryant DA & Schlachter WM (2010) Biosynthesis of cyanobacterial phycobiliproteins in *Escherichia coli*: chromophorylation efficiency and specificity of all bilin lyases from *Synechococcus* sp. strain PCC 7002. *Applied and Environmental Microbiology* **76**: 2729-2739.

Blank C & Sanchez-Baracaldo P (2010) Timing of morphological and ecological innovations in the cyanobacteria—a key to understanding the rise in atmospheric oxygen. *Geobiology* **8**: 1-23.

Blank CE (2004) Evolutionary timing of the origins of mesophilic sulphate reduction and oxygenic photosynthesis: a phylogenomic dating approach. *Geobiology* **2**: 1-20.

Blankenship RE (2015) Structural and functional dynamics of photosynthetic antenna complexes. *Proceedings of the National Academy of Sciences* **112**: 13751-13752.

Blot N, Wu X-J, Thomas J-C, Zhang J, Garczarek L, Böhm S, Tu J-M, Zhou M, Plöschner M & Eichacker L (2009) Phycourobilin in trichromatic phycocyanin from oceanic cyanobacteria is
CX

formed post-translationally by a phycoerythrobilin lyase-isomerase. *Journal of Biological Chemistry* **284**: 9290-9298.

Bretaudeau A, Coste F, Humily F, Garczarek L, Le Corguille G, Six C, Ratin M, Collin O, Schluchter WM & Partensky F (2012) CyanoLyase: a database of phycobilin lyase sequences, motifs and functions. *Nucleic Acids Research* **41**: D396-D401.

Bryant DA (2003) The beauty in small things revealed. *Proceedings of the National Academy of Sciences* **100**: 9647-9649.

Bumba L, Prasil O & Vacha F (2005) Antenna ring around trimeric photosystem I in chlorophyll b containing cyanobacterium *Prochlorothrix hollandica*. *Biochimica et Biophysica Acta (BBA)-Bioenergetics* **1708**: 1-5.

Carrigee LA, Frick JP, Karty JA, Garczarek L, Partensky F & Schluchter WM (2021) MpeV is a lyase isomerase that ligates a doubly linked phycourobilin on the β -subunit of phycoerythrin I and II in marine *Synechococcus*. *Journal of Biological Chemistry* **296**.

Carrigee LA, Frick JP, Liu X, Karty JA, Trinidad JC, Tom IP, Yang X, Dufour L, Partensky F & Schluchter WM (2022) The phycoerythrobilin isomerization activity of MpeV in *Synechococcus* sp. WH8020 is prevented by the presence of a histidine at position 141 within its phycoerythrin-I β -subunit substrate. *Frontiers in Microbiology* **13**: 1011189.

Chen M, Bibby TS, Nield J, Larkum A & Barber J (2005) Iron deficiency induces a chlorophyll d-binding Pcb antenna system around Photosystem I in *Acaryochloris marina*. *Biochimica et Biophysica Acta (BBA)-Bioenergetics* **1708**: 367-374.

Chen Y-R, Su Y-s & Tu S-L (2012) Distinct phytochrome actions in nonvascular plants revealed by targeted inactivation of phytybilin biosynthesis. *Proceedings of the National Academy of Sciences* **109**: 8310-8315.

Chisholm SW (2017) *Prochlorococcus*. *Current Biology* **27**: R447-R448.

Chisholm SW, Frankel SL, Goericke R, Olson RJ, Palenik B, Waterbury JB, West-Johnsrud L & Zettler ER (1992) *Prochlorococcus marinus* nov. gen. nov. sp.: an oxyphototrophic marine prokaryote containing divinyl chlorophyll a and b. *Archives of Microbiology* **157**: 297-300.

Chiu H-J, Bakolitsa C, Skerra A, Lomize A, Carlton D, Miller MD, Krishna SS, Abdubek P, Astakhova T & Axelrod HL (2010) Structure of the first representative of Pfam family PF09410

(DUF2006) reveals a structural signature of the calycin superfamily that suggests a role in lipid metabolism. *Acta Crystallographica Section F: Structural Biology and Crystallization Communications* **66**: 1153-1159.

Coleman ML & Chisholm SW (2007) Code and context: *Prochlorococcus* as a model for cross-scale biology. *Trends in Microbiology* **15**: 398-407.

Cortazzo P, Cerveňansky C, Marín M, Reiss C, Ehrlich R & Deana A (2002) Silent mutations affect in vivo protein folding in *Escherichia coli*. *Biochemical and Biophysical Research Communications* **293**: 537-541.

Dammeyer T & Frankenberg-Dinkel N (2006) Insights into phycoerythrobilin biosynthesis point toward metabolic channeling. *Journal of Biological Chemistry* **281**: 27081-27089.

Dammeyer T, Bagby SC, Sullivan MB, Chisholm SW & Frankenberg-Dinkel N (2008) Efficient phage-mediated pigment biosynthesis in oceanic cyanobacteria. *Current Biology* **18**: 442-448.

Dolganov N & Grossman AR (1999) A polypeptide with similarity to phycocyanin α -subunit phycocyanobilin lyase involved in degradation of phycobilisomes. *Journal of Bacteriology* **181**: 610-617.

Dufresne A, Salanoubat M, Partensky F, Artiguenave F, Axmann IM, Barbe V, Duprat S, Galperin MY, Koonin EV & Le Gall F (2003) Genome sequence of the cyanobacterium *Prochlorococcus marinus* SS120, a nearly minimal oxyphototrophic genome. *Proceedings of the National Academy of Sciences* **100**: 10020-10025.

Durchan M, Herbstová M, Fuciman M, Gardian Z, Vácha Fe & Polívka Ts (2010) Carotenoids in Energy Transfer and Quenching Processes in Pcb and Pcb- PS I Complexes from *Prochlorothrix hollandica*. *The Journal of Physical Chemistry B* **114**: 9275-9282.

Erdoğan A, Demirel Z, Eroğlu AE & Dalay MC (2016) Carotenoid profile in *Prochlorococcus* sp. and enrichment of lutein using different nitrogen sources. *Journal of Applied Phycology* **28**: 3251-3257.

Everroad C, Six C, Partensky F, Thomas J-C, Holtzendorff J & Wood AM (2006) Biochemical bases of type IV chromatic adaptation in marine *Synechococcus* spp. *Journal of Bacteriology* **188**: 3345-3356.

-
- Fairchild CD, Zhao J, Zhou J, Colson SE, Bryant DA & Glazer AN** (1992) Phycocyanin alpha-subunit phycocyanobilin lyase. *Proceedings of the National Academy of Sciences* **89**: 7017-7021.
- Farasat I, Kushwaha M, Collens J, Easterbrook M, Guido M & Salis HM** (2014) Efficient search, mapping, and optimization of multi-protein genetic systems in diverse bacteria. *Molecular Systems Biology* **10**: 731.
- Flombaum P, Gallegos JL, Gordillo RA, Rincón J, Zabala LL, Jiao N, Karl DM, Li WK, Lomas MW & Veneziano D** (2013) Present and future global distributions of the marine Cyanobacteria *Prochlorococcus* and *Synechococcus*. *Proceedings of the National Academy of Sciences* **110**: 9824-9829.
- Flower DR, North AC & Attwood TK** (1993) Structure and sequence relationships in the lipocalins and related proteins. *Protein Science* **2**: 753-761.
- Frankenberg N, Mukougawa K, Kohchi T & Lagarias JC** (2001) Functional genomic analysis of the HY2 family of ferredoxin-dependent bilin reductases from oxygenic photosynthetic organisms. *The Plant Cell* **13**: 965-978.
- Frigaard N-U, Sakuragi Y & Bryant DA** (2004) Gene inactivation in the cyanobacterium *Synechococcus* sp. PCC 7002 and the green sulfur bacterium *Chlorobium tepidum* using in vitro-made DNA constructs and natural transformation. *Photosynthesis Research Protocols*, pp. 325-340. Springer.
- Gao F** (2020) Iron–sulfur cluster biogenesis and iron homeostasis in cyanobacteria. *Frontiers in Microbiology* **11**: 165.
- Garczarek L, Hess WR, Holtzendorff J, van der Staay GW & Partensky F** (2000) Multiplication of antenna genes as a major adaptation to low light in a marine prokaryote. *Proceedings of the National Academy of Sciences* **97**: 4098-4101.
- Garczarek L, van der Staay GW, Hess WR, Le Gall F & Partensky F** (2001) Expression and phylogeny of the multiple antenna genes of the low-light-adapted strain *Prochlorococcus marinus* SS120 (Oxyphotobacteria). *Plant Molecular Biology* **46**: 683-693.
- Garczarek L, Dufresne A, Rousvoal S, West NJ, Mazard S, Marie D, Claustre H, Raimbault P, Post AF & Scanlan DJ** (2007) High vertical and low horizontal diversity of *Prochlorococcus* ecotypes in the Mediterranean Sea in summer. *FEMS Microbiology Ecology* **60**: 189-206.

Gasper R, Schwach J, Hartmann J, Holtkamp A, Wiethaus J, Riedel N, Hofmann E & Frankenberg-Dinkel N (2017) Distinct features of cyanophage-encoded T-type phycobiliprotein lyase Φ CpeT: The role of auxiliary metabolic genes. *Journal of Biological Chemistry* **292**: 3089-3098.

Gill SC & Von Hippel PH (1989) Calculation of protein extinction coefficients from amino acid sequence data. *Analytical Biochemistry* **182**: 319-326.

Glazer AN (1989) Light guides: directional energy transfer in a photosynthetic antenna. *Journal of Biological Chemistry* **264**: 1-4.

Gómez-Lojero C, Pérez-Gómez B, Shen G, Schluchter WM & Bryant DA (2003) Interaction of ferredoxin: NADP⁺ oxidoreductase with phycobilisomes and phycobilisome substructures of the cyanobacterium *Synechococcus* sp. strain PCC 7002. *Biochemistry* **42**: 13800-13811.

Gordon GC & Pflieger BF (2018) Regulatory tools for controlling gene expression in cyanobacteria. *Synthetic Biology of Cyanobacteria* 281-315.

Gossauer A & Weller J (1978) Synthesis of bile pigments. 9. Chemical total synthesis of (+)-(2R, 16R)- and (+)-(2S, 16R)-phycoerythrobilin dimethyl ester. *Journal of the American Chemical Society* **100**: 5928-5933.

Grébert T, Garczarek L, Daubin V, Humily F, Marie D, Ratin M, Devailly A, Farrant GK, Mary I & Mella-Flores D (2022) Diversity and evolution of pigment types in marine *Synechococcus* cyanobacteria. *Genome Biology and Evolution* **14**: evac035.

Grébert To (2017) Pigment diversity in marine *Synechococcus* sp.: molecular basis, evolution and ecological role. Thesis, Université Pierre et Marie Curie-Paris VI.

Grossman AR, Schaefer MR, Chiang GG & Collier J (1993) The phycobilisome, a light-harvesting complex responsive to environmental conditions. *Microbiological Reviews* **57**: 725-749.

Hackh J. (2022) Characterization of phycobiliprotein lyase Mpex and Pro1634 from *Prochlorococcus marinus* SS120. Masterarbeit.

Hamada F, Murakami A & Akimoto S (2017) Adaptation of divinyl chlorophyll a/b-containing cyanobacterium to different light conditions: three strains of *Prochlorococcus marinus*. *The Journal of Physical Chemistry B* **121**: 9081-9090.

Hess WR, Steglich C, Lichtlé C & Partensky F (1999) Phycoerythrins of the oxyphotobacterium *Prochlorococcus marinus* are associated to the thylakoid membrane and are encoded by a single large gene cluster. *Plant Molecular Biology* **40**: 507-521.

Hess WR, Partensky F, Van der Staay G, Garcia-Fernandez JM, Börner T & Vaultot D (1996) Coexistence of phycoerythrin and a chlorophyll *a/b* antenna in a marine prokaryote. *Proceedings of the National Academy of Sciences* **93**: 11126-11130.

Hess WR, Rocap G, Ting CS, Larimer F, Stilwagen S, Lamerdin J & Chisholm SW (2001) The photosynthetic apparatus of *Prochlorococcus*: insights through comparative genomics. *Photosynthesis Research* **70**: 53-71.

Humily F, Partensky F, Six C, Farrant GK, Ratin M, Marie D & Garczarek L (2013) A gene island with two possible configurations is involved in chromatic acclimation in marine *Synechococcus*. *PloS one* **8**: e84459.

Johnson PW & Sieburth JM (1979) Chroococcoid cyanobacteria in the sea: a ubiquitous and diverse phototrophic biomass 1. *Limnology and Oceanography* **24**: 928-935.

Johnson ZI, Zinser ER, Coe A, McNulty NP, Woodward EMS & Chisholm SW (2006) Niche partitioning among *Prochlorococcus* ecotypes along ocean-scale environmental gradients. *Science* **311**: 1737-1740.

Jumper J, Evans R, Pritzel A, Green T, Figurnov M, Ronneberger O, Tunyasuvunakool K, Bates R, Židek A & Potapenko A (2021) Highly accurate protein structure prediction with AlphaFold. *Nature* **596**: 583-589.

Kabsch W & Sander C (1983) Dictionary of protein secondary structure: pattern recognition of hydrogen-bonded and geometrical features. *Biopolymers: Original Research on Biomolecules* **22**: 2577-2637.

Kachel B & Mack M (2020) Engineering of *Synechococcus* sp. strain PCC 7002 for the photoautotrophic production of light-sensitive riboflavin (vitamin B2). *Metabolic Engineering* **62**: 275-286.

Kahn K, Mazel D, Houmard J, Tandeau de Marsac N & Schaefer MR (1997) A role for CpeYZ in cyanobacterial phycoerythrin biosynthesis. *Journal of Bacteriology* **179**: 998-1006.

Kolodny Y, Avrahami Y, Zer H, Frada MJ, Paltiel Y & Keren N (2022) Phycobilisome light-harvesting efficiency in natural populations of the marine cyanobacteria *Synechococcus* increases with depth. *Communications Biology* **5**: 1-7.

Komatsu H, Wada K, Kanjoh T, Miyashita H, Sato M, Kawachi M & Kobayashi M (2016) Unique chlorophylls in picoplankton *Prochlorococcus* sp. “Physicochemical properties of divinyl chlorophylls, and the discovery of monovinyl chlorophyll b as well as divinyl chlorophyll b in the species *Prochlorococcus* NIES-2086”. *Photosynthesis Research* **130**: 445-467.

Koontz L (2014) TCA precipitation. *Methods in enzymology*, Vol. 541 pp. 3-10. Elsevier.

Kronfel CM, Biswas A, Frick JP, Gutu A, Blensdorf T, Karty JA, Kehoe DM & Schluchter WM (2019) The roles of the chaperone-like protein CpeZ and the phycoerythrobilin lyase CpeY in phycoerythrin biogenesis. *Biochimica et Biophysica Acta (BBA)-Bioenergetics* **1860**: 549-561.

Kronfel CM, Kuzin AP, Forouhar F, Biswas A, Su M, Lew S, Seetharaman J, Xiao R, Everett JK & Ma L-C (2013) Structural and biochemical characterization of the bilin lyase CpcS from *Thermosynechococcus elongatus*. *Biochemistry* **52**: 8663-8676.

Kronfel CM, Hernandez CV, Frick JP, Hernandez LS, Gutu A, Karty JA, Boutaghou MN, Kehoe DM, Cole RB & Schluchter WM (2019) CpeF is the bilin lyase that ligates the doubly linked phycoerythrobilin on β -phycoerythrin in the cyanobacterium *Fremyella diplosiphon*. *Journal of Biological Chemistry* **294**: 3987-3999.

Kumarapperuma I, Joseph KL, Wang C, Biju LM, Tom IP, Weaver KD, Grébert T, Partensky F, Schluchter WM & Yang X (2022) Crystal structure and molecular mechanism of an E/F type bilin lyase-isomerase. *Structure* **30**: 564-574. e563.

Kuzin A, Su M, Seetharaman J, Forouhar F, Wang D, Janjua H, Cunningham K, Ma L, Xiao R & Liu J (2007) Crystal structure of fatty acid-binding protein-like Ycf58 from *Thermosynechococcus elongatus* target Ter13pdb ID: 3BDR. *Target Ter13* **200710**.

Ledermann B, Aras M & Frankenberg-Dinkel N (2017) Biosynthesis of cyanobacterial light-harvesting pigments and their assembly into phycobiliproteins. *Modern Topics in the Phototrophic Prokaryotes*, pp. 305-340. Springer.

Leonhardt K & Straus NA (1994) Photosystem II genes *isiA*, *psbDI* and *psbC* in *Anabaena* sp. PCC 7120: cloning, sequencing and the transcriptional regulation in iron-stressed and iron-repleted cells. *Plant Molecular Biology* **24**: 63-73.

Liu H, Zhang H, Niedzwiedzki DM, Prado M, He G, Gross ML & Blankenship RE (2013) Phycobilisomes supply excitations to both photosystems in a megacomplex in cyanobacteria. *Science* **342**: 1104-1107.

Liu L-N, Chen X-L, Zhang Y-Z & Zhou B-C (2005) Characterization, structure and function of linker polypeptides in phycobilisomes of cyanobacteria and red algae: an overview. *Biochimica et Biophysica Acta (BBA)-Bioenergetics* **1708**: 133-142.

Loeschcke A, Markert A, Wilhelm S, Wirtz A, Rosenau F, Jaeger K-E & Drepper T (2013) TREX: a universal tool for the transfer and expression of biosynthetic pathways in bacteria. *ACS Synthetic Biology* **2**: 22-33.

Lokstein H, Steglich C & Hess WR (1999) Light-harvesting antenna function of phycoerythrin in *Prochlorococcus marinus*. *Biochimica et Biophysica Acta (BBA)-Bioenergetics* **1410**: 97-98.

Ludwig M & Bryant DA (2012) *Synechococcus* sp. strain PCC 7002 transcriptome: acclimation to temperature, salinity, oxidative stress, and mixotrophic growth conditions. *Frontiers in Microbiology* **3**: 354.

MacGregor-Chatwin C, Jackson P, Sener M, Chidgey J, Hitchcock A, Qian P, Mayneord G, Johnson M, Luthey-Schulten Z & Dickman M (2019) Membrane organization of photosystem I complexes in the most abundant phototroph on Earth. *Nature Plants* **5**: 879-889.

Mahmoud RM, Sanfilippo JE, Nguyen AA, Strnat JA, Partensky F, Garczarek L, Abo El Kassem N, Kehoe DM & Schluchter WM (2017) Adaptation to blue light in marine *Synechococcus* requires MpeU, an enzyme with similarity to phycoerythrobilin lyase isomerases. *Frontiers in Microbiology* **8**: 243.

Markley AL, Begemann MB, Clarke RE, Gordon GC & Pflieger BF (2015) Synthetic biology toolbox for controlling gene expression in the cyanobacterium *Synechococcus* sp. strain PCC 7002. *ACS Synthetic Biology* **4**: 595-603.

Mauzerall D & Greenbaum NL (1989) The absolute size of a photosynthetic unit. *Biochimica et Biophysica Acta (BBA)-Bioenergetics* **974**: 119-140.

Mirdita M, Schütze K, Moriwaki Y, Heo L, Ovchinnikov S & Steinegger M (2022) ColabFold: making protein folding accessible to all. *Nature Methods* 1-4.

Monecke T, Dickmanns A & Ficner R (2014) Allosteric control of the exportin CRM 1 unraveled by crystal structure analysis. *The FEBS Journal* **281**: 4179-4194.

Moore J (1964) Gel permeation chromatography. I. A new method for molecular weight distribution of high polymers. *Journal of Polymer Science Part A: General Papers* **2**: 835-843.

Moore LR, Goericke R & Chisholm SW (1995) Comparative physiology of *Synechococcus* and *Prochlorococcus*: influence of light and temperature on growth, pigments, fluorescence and absorptive properties. *Marine Ecology Progress Series* 259-275.

Moore LR, Rocap G & Chisholm SW (1998) Physiology and molecular phylogeny of coexisting *Prochlorococcus* ecotypes. *Nature* **393**: 464-467.

Morel A, Ahn Y-H, Partensky F, Vaultot D & Claustre H (1993) *Prochlorococcus* and *Synechococcus*: a comparative study of their optical properties in relation to their size and pigmentation. *Journal of Marine Research* **51**: 617-649.

Morimoto K, Sato S, Tabata S & Nakai M (2003) A HEAT-repeats containing protein, IaiH, stabilizes the iron-sulfur cluster bound to the cyanobacterial IscA homologue, IscA2. *Journal of Biochemistry* **134**: 211-217.

Muramatsu M & Hihara Y (2012) Acclimation to high-light conditions in cyanobacteria: from gene expression to physiological responses. *Journal of Plant Research* **125**: 11-39.

Mutsuda M & Sugiura M (2006) Translation initiation of cyanobacterial rbcS mRNAs requires the 38-kDa ribosomal protein S1 but not the Shine-Dalgarno sequence: development of a cyanobacterial in vitro translation system. *Journal of Biological Chemistry* **281**: 38314-38321.

Neuwald AF & Hirano T (2000) HEAT repeats associated with condensins, cohesins, and other complexes involved in chromosome-related functions. *Genome Research* **10**: 1445-1452.

Nguyen AA, Joseph KL, Bussell AN, Pokhrel S, Karty JA, Kronfel CM, Kehoe DM & Schluchter WM (2020) CpeT is the phycoerythrobilin lyase for Cys-165 on β -phycoerythrin from *Fremyella diplosiphon* and the chaperone-like protein CpeZ greatly improves its activity. *Biochimica et Biophysica Acta (BBA)-Bioenergetics* **1861**: 148284.

-
- Ong L & Glazer A** (1991) Phycoerythrins of marine unicellular cyanobacteria. I. Bilin types and locations and energy transfer pathways in *Synechococcus* spp. phycoerythrins. *Journal of Biological Chemistry* **266**: 9515-9527.
- Partensky F, Blanchot J & Vaultot D** (1999) Differential distribution and ecology of *Prochlorococcus* and *Synechococcus* in oceanic waters: a review. *Bulletin-Institut Oceanographique Monaco-Numero Special-* 457-476.
- Paul S, Dutta A, Bag SK, Das S & Dutta C** (2010) Distinct, ecotype-specific genome and proteome signatures in the marine cyanobacteria *Prochlorococcus*. *BMC genomics* **11**: 1-15.
- Perry M, Talbot M & Alberte R** (1981) Photoadaptation in marine phytoplankton: response of the photosynthetic unit. *Marine Biology* **62**: 91-101.
- Pittera J** (2015) Adaptation des cyanobactéries marines du genre *Synechococcus* au gradient latitudinal de température. Thesis, Université Pierre et Marie Curie-Paris VI.
- Puigbò P, Bravo IG & Garcia-Vallve S** (2008) CAIcal: a combined set of tools to assess codon usage adaptation. *Biology Direct* **3**: 1-8.
- Read RW, Berube PM, Biller SJ, Neveux I, Cubillos-Ruiz A, Chisholm SW & Grzymalski JJ** (2017) Nitrogen cost minimization is promoted by structural changes in the transcriptome of N-deprived *Prochlorococcus* cells. *The ISME Journal* **11**: 2267-2278.
- Rippka R, Deruelles J, Waterbury JB, Herdman M & Stanier RY** (1979) Generic assignments, strain histories and properties of pure cultures of cyanobacteria. *Microbiology* **111**: 1-61.
- Roache-Johnson KH** (2013) Characterization of Phycoerythrin Physiology in Low-Light Adapted *Prochlorococcus* Ecotypes.
- Robert X & Gouet P** (2014) Deciphering key features in protein structures with the new ENDscript server. *Nucleic Acids Research* **42**: W320-W324.
- Roberts TM & Kothe KE** (1976) The blue-green alga *Agmenellum quadruplicatum* contains covalently closed DNA circles. *Cell* **9**: 551-557.
- Rocap G, Distel DL, Waterbury JB & Chisholm SW** (2002) Resolution of *Prochlorococcus* and *Synechococcus* ecotypes by using 16S-23S ribosomal DNA internal transcribed spacer sequences. *Applied and Environmental Microbiology* **68**: 1180-1191.

Rocap G, Larimer FW, Lamerdin J, Malfatti S, Chain P, Ahlgren NA, Arellano A, Coleman M, Hauser L & Hess WR (2003) Genome divergence in two *Prochlorococcus* ecotypes reflects oceanic niche differentiation. *Nature* **424**: 1042-1047.

Roche JL, Van der Staay G, Partensky F, Ducret A, Aebersold R, Li R, Golden S, Hiller R, Wrench P & Larkum A (1996) Independent evolution of the prochlorophyte and green plant chlorophyll a/b light-harvesting proteins. *Proceedings of the National Academy of Sciences* **93**: 15244-15248.

Saer RG & Blankenship RE (2017) Light harvesting in phototrophic bacteria: structure and function. *Biochemical Journal* **474**: 2107-2131.

Sagan L (1967) On the origin of mitosing cells. *Journal of Theoretical Biology* **14**: 225-IN226.

Sanfilippo JE, Garczarek L, Partensky F & Kehoe DM (2019) Chromatic acclimation in cyanobacteria: a diverse and widespread process for optimizing photosynthesis. *Annual Review of Microbiology* **73**.

Sato S & Tanaka A (2006) Identification of chlorophyllide a oxygenase in the *Prochlorococcus* genome by a comparative genomic approach. *Plant and Cell Physiology* **47**: 1622-1629.

Scheer H & Zhao KH (2008) Biliprotein maturation: the chromophore attachment. *Molecular Microbiology* **68**: 263-276.

Schluchter WM, Shen G, Alvey RM, Biswas A, Saunée NA, Williams SR, Mille CA & Bryant DA (2010) Phycobiliprotein biosynthesis in cyanobacteria: structure and function of enzymes involved in post-translational modification. *Recent Advances in Phototrophic Prokaryotes*, pp. 211-228. Springer.

Shen G, Schluchter WM & Bryant DA (2008) Biogenesis of phycobiliproteins: I. cpcS-I and cpcU mutants of the cyanobacterium *Synechococcus* sp. PCC 7002 define a heterodimeric phycocyanobilin lyase specific for β -phycocyanin and allophycocyanin subunits. *Journal of Biological Chemistry* **283**: 7503-7512.

Shen G, Saunee NA, Williams SR, Gallo EF, Schluchter WM & Bryant DA (2006) Identification and characterization of a new class of bilin lyase: the cpcT gene encodes a bilin lyase responsible for attachment of phycocyanobilin to Cys-153 on the β -subunit of phycocyanin in *Synechococcus* sp. PCC 7002. *Journal of Biological Chemistry* **281**: 17768-17778.

Sidler WA (1994) Phycobilisome and phycobiliprotein structures. *The Molecular Biology of Cyanobacteria*, pp. 139-216. Springer.

Singh R, Parihar P, Singh M, Bajguz A, Kumar J, Singh S, Singh VP & Prasad SM (2017) Uncovering potential applications of cyanobacteria and algal metabolites in biology, agriculture and medicine: current status and future prospects. *Frontiers in Microbiology* **8**: 515.

Six C, Thomas J-C, Garczarek L, Ostrowski M, Dufresne A, Blot N, Scanlan DJ & Partensky F (2007) Diversity and evolution of phycobilisomes in marine *Synechococcus* spp.: a comparative genomics study. *Genome Biology* **8**: 1-22.

Skerra A (2008) Alternative binding proteins: anticalins—harnessing the structural plasticity of the lipocalin ligand pocket to engineer novel binding activities. *The FEBS Journal* **275**: 2677-2683.

Stal LJ (2022) A Sea of Microbes: What's So Special about Marine Microbiology. *The Marine Microbiome*, pp. 1-44. Springer.

Staudt AC & Wenkel S (2011) Regulation of protein function by 'microProteins'. *EMBO Reports* **12**: 35-42.

Stazic D, Lindell D & Steglich C (2011) Antisense RNA protects mRNA from RNase E degradation by RNA–RNA duplex formation during phage infection. *Nucleic Acids Research* **39**: 4890-4899.

Steglich C, Frankenberg-Dinkel N, Penno S & Hess WR (2005) A green light-absorbing phycoerythrin is present in the high-light-adapted marine cyanobacterium *Prochlorococcus* sp. MED4. *Environmental Microbiology* **7**: 1611-1618.

Steglich C, Mullineaux CW, Teuchner K, Hess WR & Lokstein H (2003) Photophysical properties of *Prochlorococcus marinus* SS120 divinyl chlorophylls and phycoerythrin *in vitro* and *in vivo*. *FEBS Letters* **553**: 79-84.

Steglich C, Futschik ME, Lindell D, Voss B, Chisholm SW & Hess WR (2008) The challenge of regulation in a minimal photoautotroph: non-coding RNAs in *Prochlorococcus*. *PLoS Genetics* **4**: e1000173.

Steglich C, Lindell D, Futschik M, Rector T, Steen R & Chisholm SW (2010) Short RNA half-lives in the slow-growing marine cyanobacterium *Prochlorococcus*. *Genome Biology* **11**: 1-14.

Stevens Jr SE & Porter RD (1980) Transformation in *Agmenellum quadruplicatum*. *Proceedings of the National Academy of Sciences* **77**: 6052-6056.

Stickforth P, Steiger S, Hess WR & Sandmann G (2003) A novel type of lycopene ϵ -cyclase in the marine cyanobacterium *Prochlorococcus marinus* MED4. *Archives of Microbiology* **179**: 409-415.

Storf M, Parbel A, Meyer M, Strohmann B, Scheer H, Deng M-G, Zheng M, Zhou M & Zhao K-H (2001) Chromophore attachment to biliproteins: Specificity of PecE/PecF, a lyase-isomerase for the photoactive 31-Cys- α 84-phycoviolobilin chromophore of phycoerythrocyanin. *Biochemistry* **40**: 12444-12456.

Tagwerker C, Dupont CL, Karas BJ, Ma L, Chuang R-Y, Benders GA, Ramon A, Novotny M, Montague MG & Venepally P (2012) Sequence analysis of a complete 1.66 Mb *Prochlorococcus marinus* MED4 genome cloned in yeast. *Nucleic Acids Research* **40**: 10375-10383.

Takaichi S & Mochimaru M (2007) Carotenoids and carotenogenesis in cyanobacteria: unique ketocarotenoids and carotenoid glycosides. *Cellular and Molecular Life Sciences* **64**: 2607-2619.

Ting CS, Rocap G, King J & Chisholm SW (2002) Cyanobacterial photosynthesis in the oceans: the origins and significance of divergent light-harvesting strategies. *Trends in Microbiology* **10**: 134-142.

Tomazic N, Overkamp KE, Wegner H, Gu B, Mahler F, Aras M, Keller S, Pierik AJ, Hofmann E & Frankenberg-Dinkel N (2021) Exchange of a single amino acid residue in the cryptophyte phycobiliprotein lyase GtCPES expands its substrate specificity. *Biochimica et Biophysica Acta (BBA)-Bioenergetics* **1862**: 148493.

Ulloa O, Henríquez-Castillo C, Ramírez-Flandes S, Plominsky AM, Murillo AA, Morgan-Lang C, Hallam SJ & Stepanauskas R (2021) The cyanobacterium *Prochlorococcus* has divergent light-harvesting antennae and may have evolved in a low-oxygen ocean. *Proceedings of the National Academy of Sciences* **118**: e2025638118.

Van Baalen C (1962) Studies on marine blue-green algae.

Voigt K, Sharma CM, Mitschke J, Joke Lambrecht S, Voß B, Hess WR & Steglich C (2014) Comparative transcriptomics of two environmentally relevant cyanobacteria reveals unexpected transcriptome diversity. *The ISME Journal* **8**: 2056-2068.

Watanabe M & Ikeuchi M (2013) Phycobilisome: architecture of a light-harvesting supercomplex. *Photosynthesis Research* **116**: 265-276.

Weber Y. (2019) Analysis of different PBP T-type lyases from *P. marinus* SS 120 and the cyanophage P-HM1. Bachelorarbeit.

Whitaker JR & Granum PE (1980) An absolute method for protein determination based on difference in absorbance at 235 and 280 nm. *Analytical Biochemistry* **109**: 156-159.

Whitton BA & Potts M (2012) Introduction to the cyanobacteria. *Ecology of Cyanobacteria II*, pp. 1-13. Springer.

Wiethaus J, Busch AW, Dammeyer T & Frankenberg-Dinkel N (2010) Phycobiliproteins in *Prochlorococcus marinus*: biosynthesis of pigments and their assembly into proteins. *Eur J Cell Biol* **89**: 1005-1010.

Wiethaus J, Busch AW, Kock K, Leichert LI, Herrmann C & Frankenberg-Dinkel N (2010) CpeS is a lyase specific for attachment of 3Z-PEB to Cys82 of β -phycoerythrin from *Prochlorococcus marinus* MED4. *Journal of Biological Chemistry* **285**: 37561-37569.

Wikner J & Hagström Å (1988) Evidence for a tightly coupled nanoplanktonic predator-prey link regulating the bacterivores in the marine environment. *Marine Ecology Progress Series Oldendorf* **50**: 137-145.

Wyman M, Gregory R & Carr N (1985) Novel role for phycoerythrin in a marine cyanobacterium, *Synechococcus* strain DC2. *Science* **230**: 818-820.

Xu Y, Alvey RM, Byrne PO, Graham JE, Shen G & Bryant DA (2011) Expression of genes in cyanobacteria: adaptation of endogenous plasmids as platforms for high-level gene expression in *Synechococcus* sp. PCC 7002. *Photosynthesis Research Protocols*, pp. 273-293. Springer.

Yu T, Li J, Yang Y, Qi L, Chen B, Zhao F, Bao Q & Wu J (2012) Codon usage patterns and adaptive evolution of marine unicellular cyanobacteria *Synechococcus* and *Prochlorococcus*. *Molecular Phylogenetics and Evolution* **62**: 206-213.

Zhang J, Ma J, Liu D, Qin S, Sun S, Zhao J & Sui S-F (2017) Structure of phycobilisome from the red alga *Griffithsia pacifica*. *Nature* **551**: 57-63.

Zhao C, Höppner A, Xu Q-Z, Gärtner W, Scheer H, Zhou M & Zhao K-H (2017) Structures and enzymatic mechanisms of phycobiliprotein lyases CpcE/F and PecE/F. *Proceedings of the National Academy of Sciences* **114**: 13170-13175.

Zhao K-H, Su P, Böhm S, Song B, Zhou M, Bubenzer C & Scheer H (2005) Reconstitution of phycobilisome core–membrane linker, LCM, by autocatalytic chromophore binding to ApcE. *Biochimica et Biophysica Acta (BBA)-Bioenergetics* **1706**: 81-87.

Zhao K-H, Su P, Li J, Tu J-M, Zhou M, Bubenzer C & Scheer H (2006) Chromophore attachment to phycobiliprotein β -subunits: Phycocyanobilin: cysteine- β 84 phycobiliprotein lyase activity of CpeS-like protein from *Anabaena* Sp. PCC7120. *Journal of Biological Chemistry* **281**: 8573-8581.

Zhao K-H, Deng M-G, Zheng M, Zhou M, Parbel A, Storf M, Meyer M, Strohmann B & Scheer H (2000) Novel activity of a phycobiliprotein lyase: both the attachment of phycocyanobilin and the isomerization to phycoviolobin are catalyzed by the proteins PecE and PecF encoded by the phycoerythrocyanin operon. *FEBS Letters* **469**: 9-13.

Zhao K-H, Zhang J, Tu J-M, Böhm S, Plöscher M, Eichacker L, Bubenzer C, Scheer H, Wang X & Zhou M (2007) Lyase activities of CpcS- and CpcT-like proteins from *Nostoc* PCC7120 and sequential reconstitution of binding sites of phycoerythrocyanin and phycocyanin β -subunits. *Journal of Biological Chemistry* **282**: 34093-34103.

Zhaxybayeva O, Doolittle WF, Papke RT & Gogarten JP (2009) Intertwined evolutionary histories of marine *Synechococcus* and *Prochlorococcus marinus*. *Genome Biology and Evolution* **1**: 325-339.

Zhou J, Gasparich GE, Stirewalt VL, de Lorimier R & Bryant DA (1992) The cpcE and cpcF genes of *Synechococcus* sp. PCC 7002. Construction and phenotypic characterization of interposon mutants. *Journal of Biological Chemistry* **267**: 16138-16145.

Zhou W, Ding W-L, Zeng X-L, Dong L-L, Zhao B, Zhou M, Scheer H, Zhao K-H & Yang X (2014) Structure and Mechanism of the Phycobiliprotein Lyase CpcT*. *Journal of Biological Chemistry* **289**: 26677-26689.

Appendix

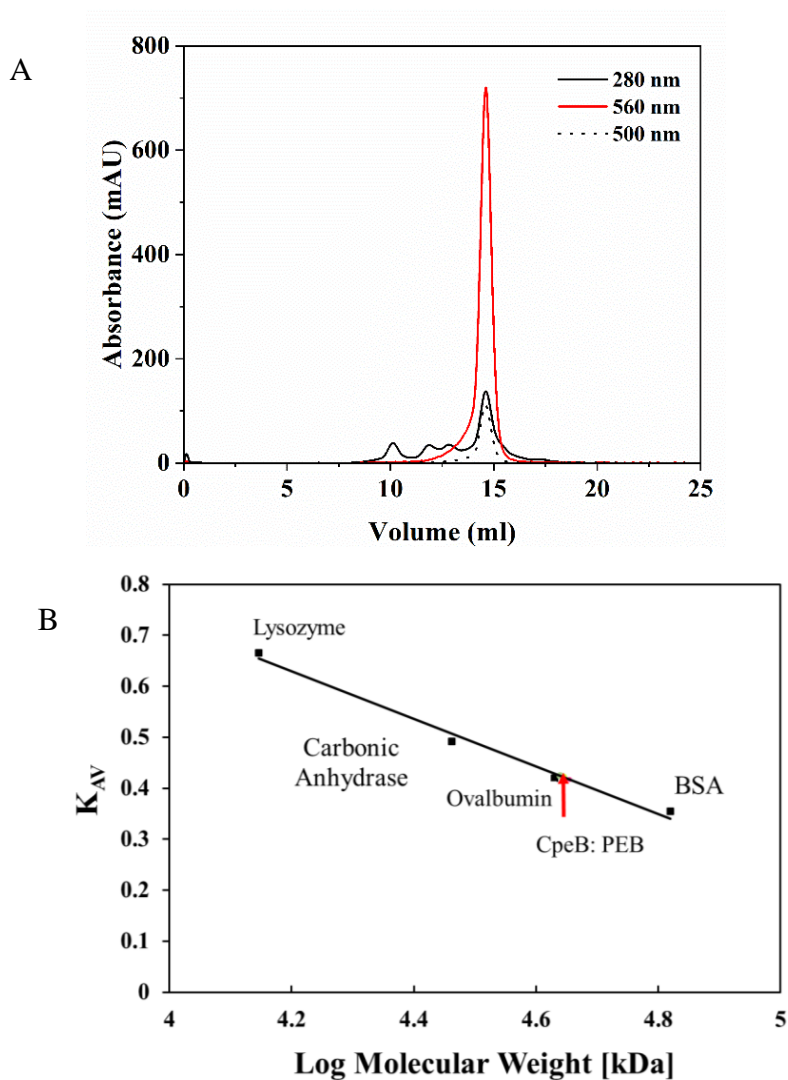


Figure S1. Size exclusion chromatography (SEC) analysis of HT-CpeB. **A.** The SEC elution profile of CpeB: PEB produced in *E. coli* BL21 (DE3) containing the *cpeS* and PEB biosynthetic genes *pebS* and *hol A*. CpeB was separated using a Superdex™ 200 10/300 GL column (GE Healthcare), sample volume 500 μ L, flow rate 0.1 mL/min, Na_2HPO_4 as eluent and the absorbance was monitored at 280 nm, 500 nm and 560 nm wavelengths. **B.** The SEC standard curve in Na_2HPO_4 with the calculated sizes of CpeB: PEB. Molecular weight of standards: Blue Dextran (2000 kDa), bovine serum albumin (66.4 kDa), Ovalbumin (44 kDa) and carbonic anhydrase (29 kDa), lysozyme (14.3 kDa).

Lyase	Phycobilin biosynthesized	Apo-protein	A _{max} / Em _{max}
	PEB	CpeB	No
CpeS	PEB	CpeB	555 nm/ 567 nm
	PCB	CpeB	No
	PEB	CpeA	No
SS120CpeT	PEB	CpeB	No
P-HM1CpeT	PEB	CpeB	No
MpeX	PEB	CpeB	No
	PUB	CpeB	No
Pro1634	PEB	CpeB	No
CpeY	PEB	CpeA	No
	PCB	CpeA	No
CpeZ	PEB	CpeA	No
	PCB	CpeA	No

Table S1. Overview of single lyase involved in Duet system. Different lyases from *P. marinus* SS120 and Cyanophage P-HM1 (designation P-HM1). The maximum absorption and fluorescence emission were detected after affinity chromatography.

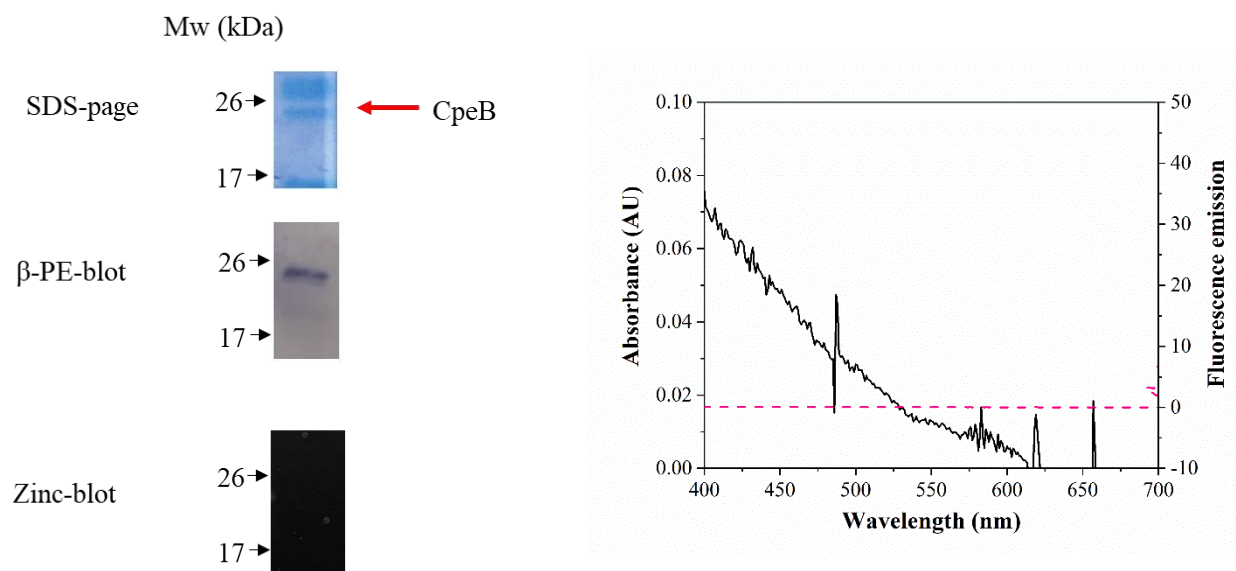


Figure S2. Analyses of purified HT-CpeB coproduced with SS120CpeT lyase A. Purified HT-CpeB was analyzed by SDS-PAGE, immunodetection with β -PE and zinc-induced fluorescence **B**. Absorbance (solid line) and fluorescence emission (red dashed line, excitation set at 490 nm) spectra of purified HT-CpeB obtained from *E. coli*.

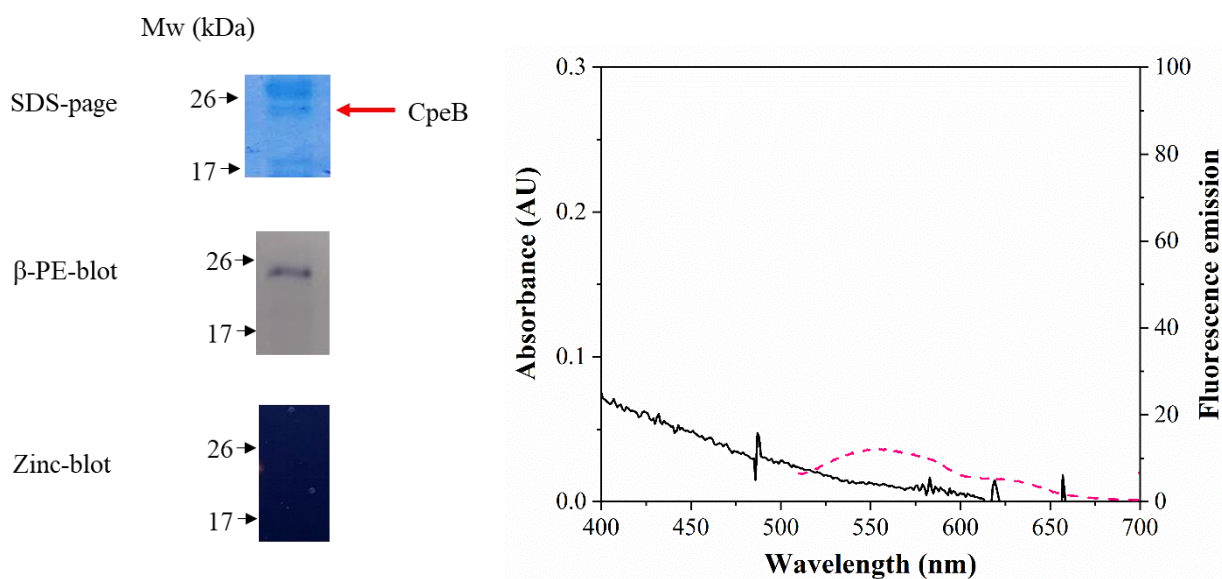


Figure S3. Analyses of purified HT-CpeB coproduced with P-HM1CpeT lyase A. Purified HT-CpeB was analyzed by SDS-PAGE, immunodetection with β -PE and zinc-induced fluorescence **B**. Absorbance (solid line) and fluorescence emission (red-dashed line, excitation set at 490 nm) spectra of purified HT-CpeB obtained from *E. coli*.

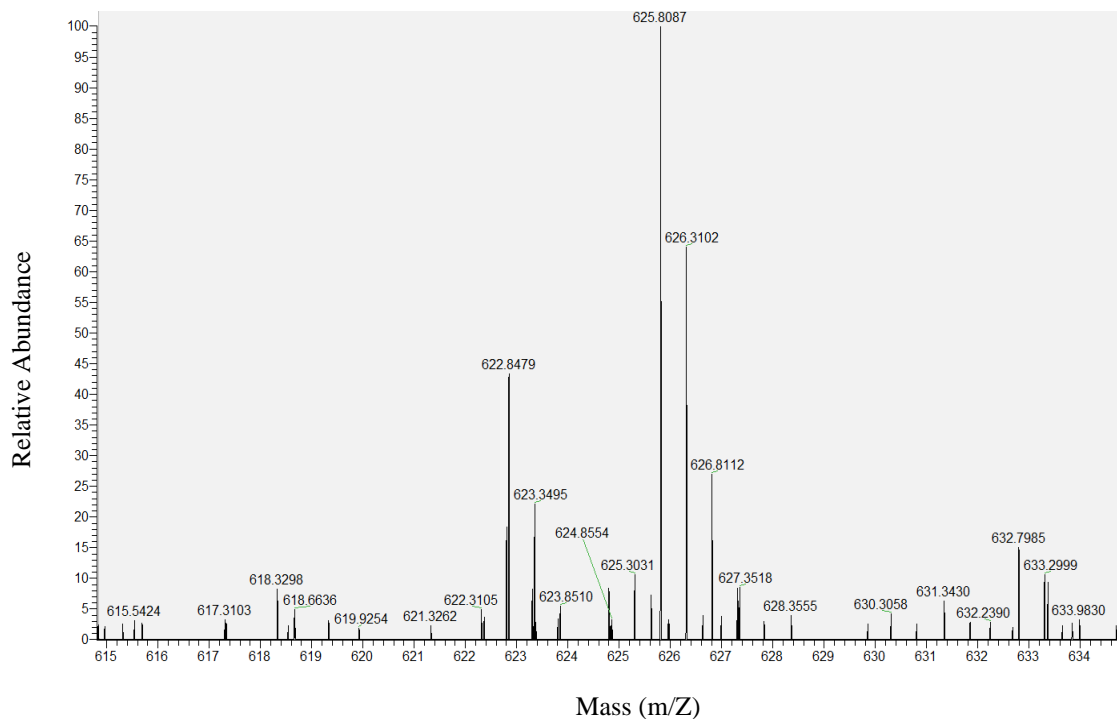
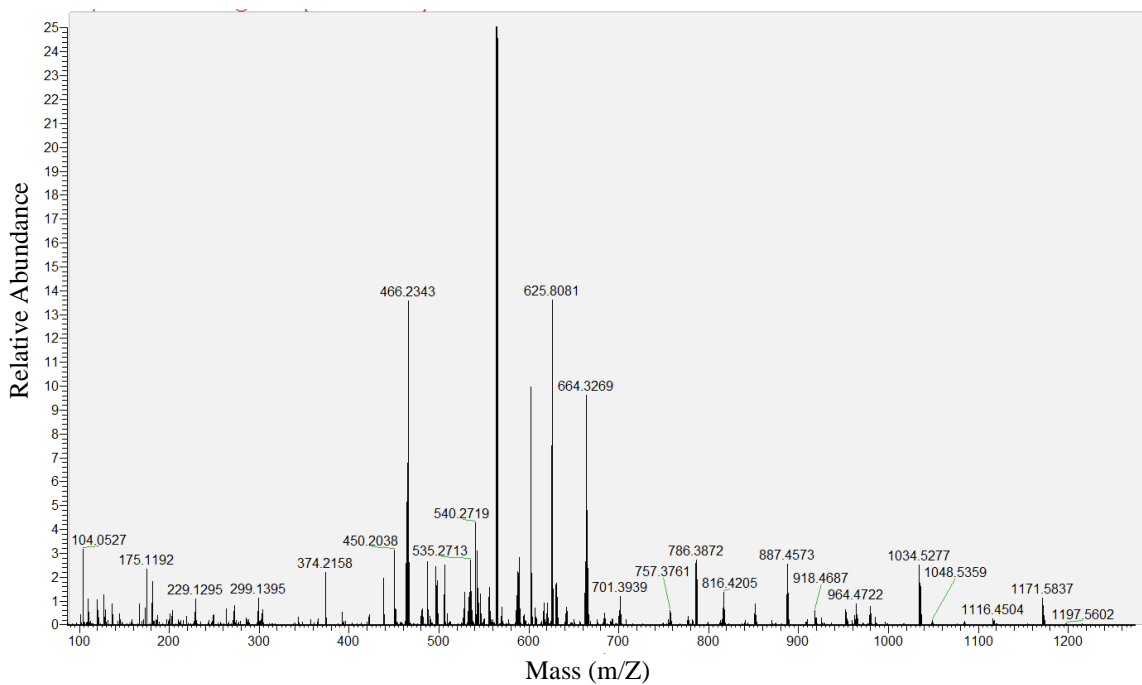


Figure S4. Mass spectrometric analysis of tryptic peptides of Holo-CpeB produced with CpeS lyase. A peptide fragment with a covalently bound PEB chromophore from trypsin digestion of the Holo-CpeB produced in the presence of CpeS. The peak at m/z 625.8 was attributed to a peptide containing a cysteine at position 82. The sequence of the peptide is (R)MAACLR (D).

Lyase 1	Lyase 2	Phycobilin biosynthesized	Apo-protein	A _{max} /Em _{max}
CpeS	SS120CpeT	PEB	CpeB	555 nm/ 567 nm
	PHM1CpeT	PEB	CpeB	555 nm/ 567 nm
	MpeX	PEB	CpeB	555 nm/ 567 nm
	Pro1634	PEB	CpeB	555 nm/ 567 nm
SS120CpeZ	CpeY	PEB	CpeA	No
		PCB	CpeA	No
		PUB	CpeA	No
MpeX	Pro1634	PEB	CpeB	No

Table S2. Overview of two lyases involved in Duet system. Different lyases from *P. marinus* SS120 and Cyanophage P-HM1 (designation P-HM1). The maximum absorption and fluorescence emission were detected after size exclusion chromatography.

Lyase1	Lyase 2	Lyase 3	Phycobilin biosynthesized	Apo-protein	A _{max} /Em _{max}
CpeS	SS120CpeT	FdCpeZ	PEB	CpeB	555 nm/ 567 nm
		SS120CpeZ	PEB	CpeB	555 nm/ 567 nm
		MpeX	PEB	CpeB	555 nm/ 567 nm
		Pro1634	PEB	CpeB	555 nm/ 567 nm
	P-HM1CpeT	FdCpeZ	PEB	CpeB	555 nm/ 567 nm
		SS120CpeZ	PEB	CpeB	555 nm/ 567 nm
		MpeX	PEB	CpeB	555 nm/ 567 nm
		Pro1634	PEB	CpeB	555 nm/ 567 nm
	MpeX	Pro1634	PEB	CpeB	555 nm/ 567 nm

Table S3. Overview of three lyase involved in Duet system. Different lyases from *P. marinus* SS120, Cyanophage P-HM1 (designation P-HM1) and cyanobacteria *Fremyella diplosiphon* (designation Fd). The maximum absorption and fluorescence emission were detected after size exclusion chromatography.

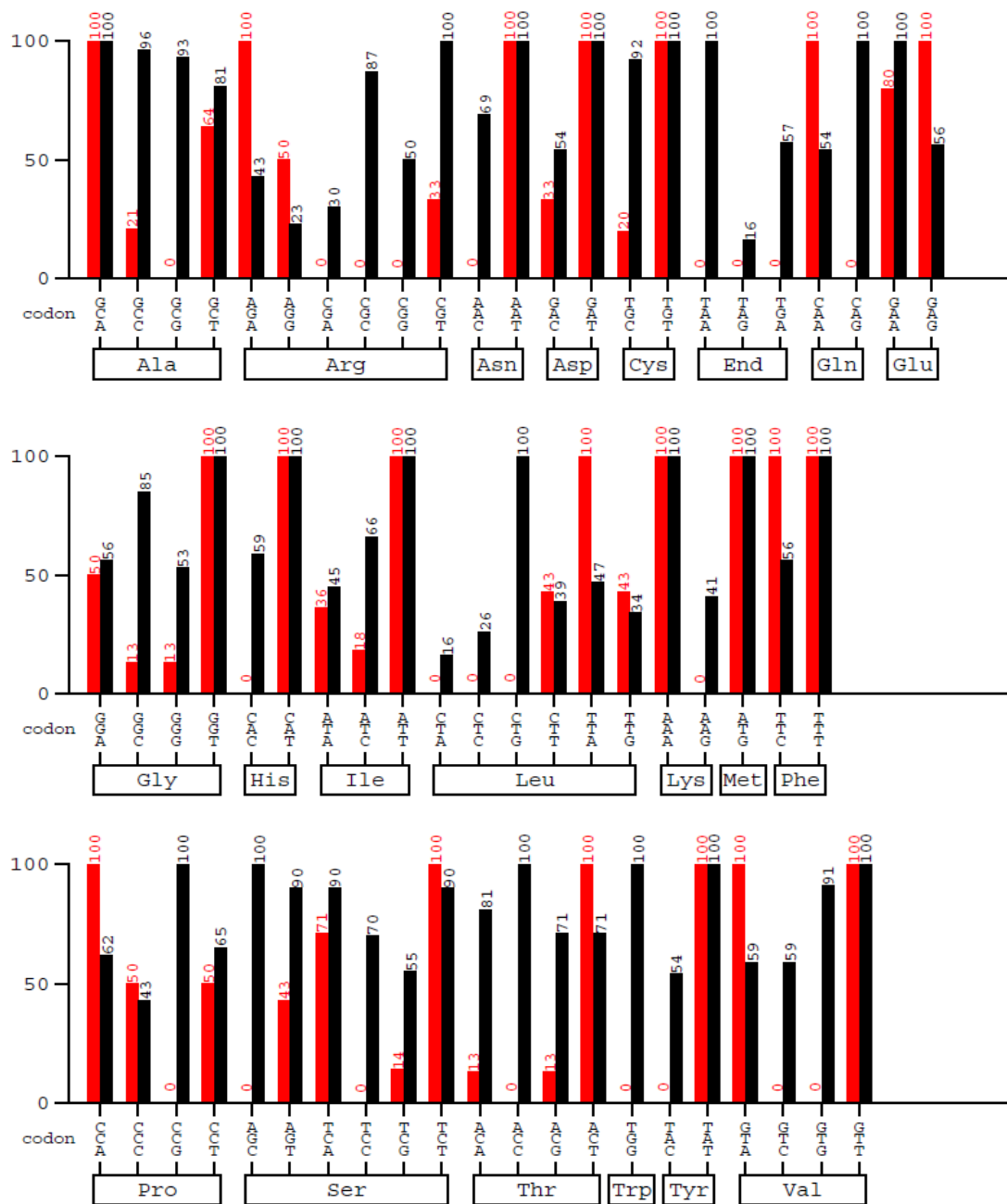


Figure. S5 Codon usage analysis between *P. marinus* SS120 and *E. coli*. Red is present in *P. marinus* SS120 and black color present in *E. coli*. Ordinate (y-axis): relative adaptiveness. The figure was analyzed by graphical codon usage analyser (www.guca.de)

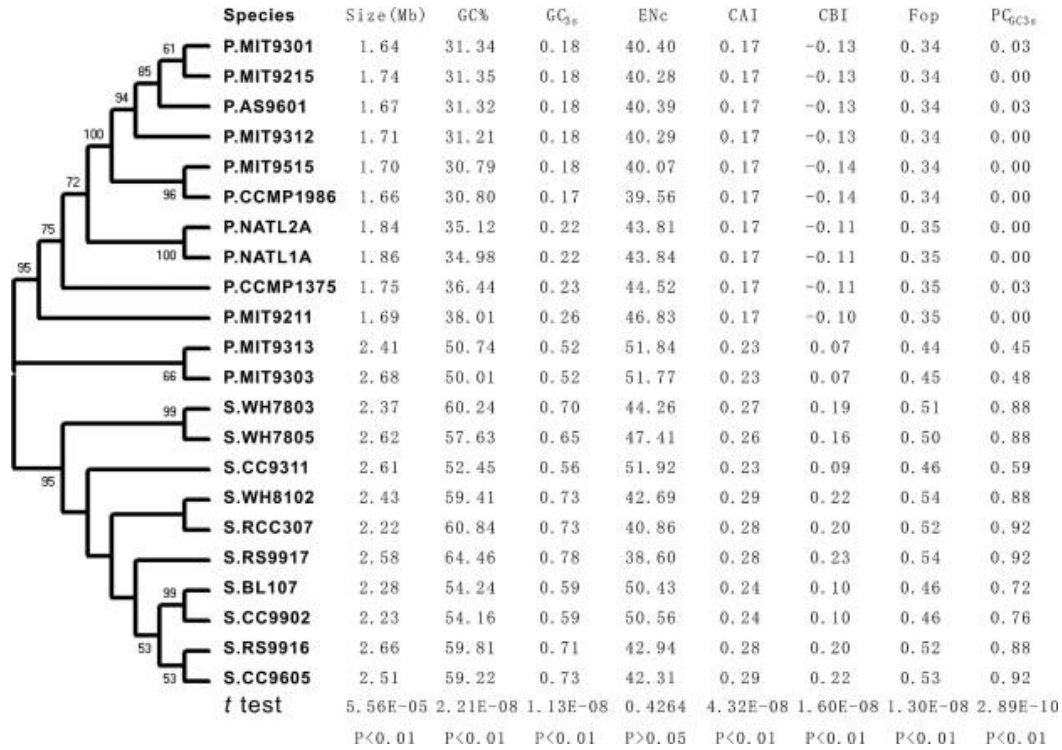


Figure. S6. Genomic characteristics and codon usage patterns in marine *Synechococcus* and *Prochlorococcus*. The organism tree was constructed based on the 16S RNA sequences of 22 *Synechococcus* and *Prochlorococcus* organisms. We choose the representative tree constructed by NJ methods. Bootstrap support values above 50 % are shown on the nodes (figure adapted from Yu *et al.* (2012)).

Acknowledgement

First and foremost, I would like to express my heartfelt gratitude to my doctoral supervisor, Prof. Dr. Nicole Frankenberg-Dinkel, for allowing me to join her research group and for providing me with scientific guidance and unwavering support throughout my Ph.D. studies. I am truly grateful for the scientific freedom that she afforded me, as well as her continuous support and readiness for discussion. I would also like to extend my sincere thanks for the assistance she provided during my time overseas.

I am also deeply appreciative of Prof. Dr. Michael Schroda for serving as my second supervisor for my doctoral thesis. His valuable input and guidance were instrumental in the successful completion of my research.

Furthermore, I would like to express my gratitude to Prof. Dr. Thorsten Stoeck for agreeing to serve as the chair of my doctoral committee.

I would like to thank Wendy Schluchter (University of New Orleans) for kindly providing the necessary constructs and LC-MS support. I am also grateful to Dr. Frederik Sommer for analyzing the mass spectra, and to Dr. Claudia Steglich (University of Freiburg) for providing the cyanobacteria material support.

My sincere thanks also go out to my current and former colleagues in our research group, particularly the graduate students and post-docs who have worked or are currently working on this topic. Their friendly and collaborative approach, as well as their contribution to creating a pleasant working atmosphere, have been invaluable. I would like to extend special thanks to Susanne, Michelle, Federica, Nora, Helen, Steffen, Thomas, Christina, and Anna for the wonderful memories we shared. I am also deeply appreciative of Dr. Eugenio Pérez Patallo and master student Jacqueline Hackh for their excellent communication of ideas and generous assistance. Many thanks also to Jonas and Alba (Ruhr-Universität Bochum) for the AlphaFold support.

My biggest thanks go to my parents, whose unwavering support and encouragement have been instrumental in my success. Although they may not fully understand my research work, their constant motivation has been a driving force in my academic journey. Without them, my studies and this work would not have been possible.

Last but not least, I would like to acknowledge the Chinese Scholarship Council and DFG for providing me with a doctoral scholarship.

Curriculum Vitae

Personal data

Family name	Gu
First name	Bin
Date of birth	
Place of birth	Henan, P.R. China

Education

10/2017 - now	Post-graduate study in the Technische Universität Kaiserslautern, Department of Microbiology, Kaiserslautern, Germany
09/2013 - 06/2016	Master study in Nanjing Agriculture University, Department of Food Science and Technology, Nanjing, P.R. China
06/2015 - 11/2015	Exchange program in John Innes Centre, Department of Biochemistry, Norwich, UK
09/2009 - 06/2013	Bachelor of food quality and safety, Hunan Agriculture University, Changsha, P.R. China
09/2011- 06/2012	Minor program of law, Hunan Agriculture University, Changsha, P.R. China

Publication

Tomazic, N., Overkamp, K. E., Wegner, H., **Gu, B.**, Mahler, F., Aras, M. & Frankenberg-Dinkel, N. (2021). Exchange of a single amino acid residue in the cryptophyte phycobiliprotein lyase GtCPES expands its substrate specificity. *BBA*.

Eidesstattliche Erklärung

Ich erkläre hiermit an Eides statt, dass ich die vorliegende Dissertation selbstständig und ohne Benutzung anderer als der angegebenen Hilfsmittel angefertigt habe. Die aus fremden Quellen übernommenen Gedanken sind ausnahmslos als solche kenntlich gemacht. Die Promotionsordnung des Fachbereichs Biologie der Rheinland-Pfälzische Technische Universität Kaiserslautern-Landau ist mir in der derzeit gültigen Fassung bekannt. Die Ergebnisse anderer Mitarbeiter sowie anderer Autoren wurden klar gekennzeichnet. Die Dissertation oder Teile daraus wurden in keinem anderen Fachbereich oder keiner anderen Fakultät als Prüfungsarbeit eingereicht. Ich habe zu keinem früheren Zeitpunkt an einer anderen Universität ein Promotionsverfahren beantragt.

Kaiserslautern, 06.03.2023

Bin Gu